Spring 2021

Regulation of MEK Signaling and Inhibitor Sensitivity in Melanoma

Eunice Cho
Yale University Graduate School of Arts and Sciences, eunice.y.cho@gmail.com

Abstract

Regulation of MEK Signaling and Inhibitor Sensitivity in Melanoma

Eunice Cho

2021

Melanoma, the deadliest form of skin cancer, is characterized by aberrant hyperactivation of the ERK mitogen-activated protein kinase signaling pathway. Genetic lesions in the core components of the RAS-RAF-MEK-ERK protein kinase cascade as well as its upstream regulators are key features of melanoma progression and drug resistance. MEK, the central kinase within the cascade, is constitutively activated by many upstream oncogenic events and is an important drug target. MEK inhibition in combination with BRAF inhibition is the standard of care for treating $BRAF^{V600E}$ melanoma. However, not all $BRAF^{V600E}$ melanomas respond to these inhibitors, and those that do respond eventually acquire resistance. To better understand mechanisms of MEK inhibitor susceptibility and MEK regulation in $BRAF^{V600E}$ melanoma, I performed a loss-of-function screen to identify kinases and phosphatases that modulate sensitivity to two clinical MEK1/2 inhibitors. In this screen, I identified PPP6C, the catalytic subunit of protein phosphatase 6 (PP6), as a factor promoting sensitivity to MEK inhibition. I established PPP6C as a major MEK phosphatase in cells exhibiting oncogenic ERK pathway activation. Recruitment of MEK to PPP6C occurs through an interaction with its associated regulatory subunits. Loss of PPP6C causes hyperphosphorylation of MEK at both activating and crosstalk phosphorylation sites, promoting signaling through the ERK pathway and decreasing sensitivity to the growth inhibitory effects of MEK inhibitors.

Consistent with its role in regulating ERK signaling, PPP6C is frequently mutated in melanoma, as is MEK1. I found that recurrent melanoma-associated PPP6C mutations cause MEK hyperphosphorylation and ERK signaling hyperactivation when expressed in cells. Recurrent MEK1 mutations all promote MEK1 kinase activity but are activated by different mechanisms of action. The elevated MEK activity associated with PPP6C mutations or MEK1 mutations suggests that they promote disease by a common mechanism: activating the core oncogenic pathway driving melanoma.

Collectively, our studies identify novel modulators of susceptibility to ERK pathway

targeted cancer therapies, including PPP6C, a key negative regulator of ERK signaling, and cancer-associated mutations that influence ERK signaling activation.

Regulation of MEK Signaling and Inhibitor Sensitivity in Melanoma

A Dissertation
Presented to the Faculty of the Graduate School
Of
Yale University
In Candidacy for the Degree of
Doctor of Philosophy

By
Eunice Cho

Dissertation Director: Dr. Benjamin Turk Ph.D.

June 2021

TABLE OF CONTENTS

TABLE OF FIGURES

GLOSSARY OF TERMS

ANKRD	Ankrin repeat domain
ATP	Adenosine triphosphate
BRAFi	BRAF inhibitor
Cas	CRISPR-associated protein
CDK	Cyclin-dependent kinase
CFC	Cardio-facio-cutaneous
CHEK1	Checkpoint kinase 1
CRISPR	Clustered regularly interspaced short palindromic repeats
DGKE	Diacylglycerol kinase Epsilon
DMSO	Dimethyl sulfoxide
DSB	Double-strand break
DSTYK	Dual serine/threonine and tyrosine protein kinase
DUSPS	Dual-specificity MAPK phosphatases
EGFR	Epidermal growth factor receptor
ERK	Extracellular signal-related kinase
ERKi	ERK inhibitor
GAP	GTPase activating protein
GFP	Green fluorescent protein
GPCR	G-protein coupled receptor
HDR	Homology directed repair
IC50	Half-maximal inhibitory concentration
IKK	IκB kinase
IL-1β	interleukin-1β
INPP4A	Inositol polyphosphate-4-phosphatase type 1A
ITK	Interleukin-2-inducible T-cell kinase
JAK	Janus kinase
KD	Kinase dead
KSR	Kinase suppressor of Ras
LPPR3	Phospholipid phosphatase related 3
MAP2K	MAPK Kinase
MAPK	Mitogen-activated protein kinase
MAPKi	MAPK pathway inhibitor
MEK	MAPK/ERK Kinase
MEKi	MEK inhibitor
MITF	Melanocyte inducing transcription factor
MYPT1	Myosin phosphatase targeting subunit 1 (PPP1R12A)

NF1	Neurofibromin 1
NHEJ	Non-homologous end joining
NRBP1	Nuclear receptor binding protein 1
NRR	Negative regulatory resion
OA	Okadaic acid
ORF	Open reading frame
PAK	p21-activated kinase
PCR	Polymerase chain reaction
PD	Phosphatase dead
PI3K	Phosphoinositide 3-kinase
PP1	Protein phosphatase 1
PP2A	Protein phosphatase 2A
PP6	Protein phosphatase 6
PPP2CA	Protein phosphatase 2 A catalytic subunit A
PPP6C	protein phosphatase 6 catalytic subunit
PPP6R	Protein phosphatase 6 regulatory subunit
PTPN9	Protein tyrosine phosphatase non-receptor type 9
RIGER	RNAi gene enrichment ranking
RNAi	RNA interference
RTK	Receptor tyrosine kinase
SFK	Src family of protein tyrosine kinases
sgRNA	Single guide RNA
SHP2	Src homology 2 domain containing phosphatase 2
shRNA	Small interfering RNA
siRNA	Short hairpin RNA
SOS1	Son of sevenless homolog 1
STAT	Signal transducers and activators of transcription
TAK1	TGF-β-activated kinase 1
TCGA	The Cancer Genome Atlas
TCR	T-cell receptor
TNF-α	Tumor necrosis factor-α
UVR	Ultraviolet radiation
WCL	Whole cell lysate
WT	Wild-type

ACKNOWLEDGEMENTS

To all my friends and family. Thank you.

CHAPTER 1: INTRODUCTION

1.1 ERK MAPK Signaling

The extracellular signal-regulated kinase (ERK) mitogen activated protein kinase (MAPK) signaling cascade regulates essential cellular functions in response to growth factors and cytokines in many cell types[1-3]. This pathway is canonically activated through receptor tyrosine kinases (RTK) activation of RAS GTPases (NRAS, KRAS, and HRAS), which directly bind and activate RAF kinases (BRAF, CRAF, and ARAF) (Figure 1.1A). Activated RAF kinases dimerize to phosphorylate and activate MEK1/2, which phosphorylate and activate ERK1/2. ERK1/2 phosphorylate substrates that act as effectors mediating the functional output of the pathway. With hundreds of target phosphorylation sites on cytoplasmic and nuclear substrates, ERK signaling mediates a diverse range of responses which includes cell differentiation, survival, proliferation, growth, migration, and metabolism. Specific cellular responses are determined by tightly regulated mechanisms: signal duration and intensity, cell-type specific substrate expression, scaffold proteins, and localization of cascade components. Further regulation is provided by the greater complex signaling network surrounding the ERK signaling cascade which includes feedback regulation mechanisms and crosstalk with peripheral pathways such as the PI3K-AKT pathway[3-5] (Figure 1.1A). Deregulation of the pathway, primarily through mutations or amplification of genes, leads to various disease states, namely cancer.

1.1.1 Oncogenic ERK MAPK Signaling

Because the ERK signaling pathway has the highest frequency of alterations across all cancer types, the ERK pathway is one of the most extensively studied signaling pathways[6,7]. Constitutive activation of ERK signaling in these cancers not only can lead to uncontrolled cell proliferation and survival, but also tumor invasion, metastasis, and angiogenesis. Activating genetic mutations in RAS and RAF are the most prevalent. RAS

mutations occur in 19% of all cancers, primarily at codons 12, 13, or 61 and favor the GTP-bound, active state of RAS[8]. The V600E mutation in BRAF is by far the dominant BRAF mutation, making up 95% of all BRAF mutations[9,10]. V600K, V600D and V600R mutations occur but at a much lower frequencies[11]. The substitution of a larger charged residue for V600 on the BRAF activation loop, destabilizes V600 interactions that maintain the DFG motif in an inactive conformation and presumably mimics conformational changes promoted by activation loop phosphorylation at T599[12]. Recurrent non-V600 BRAF mutations, though not as common, occur at higher frequencies in some cancer types such as lung cancers where ~50% of BRAF mutations are non-V600 mutations[13,14]. Non-V600 BRAF mutations are activated by different mechanisms and consequently exhibit different drug sensitivities[15,16]. More recently, loss-of-function mutations in Neurofibromin 1 (NF1), a GTPase activating protein (GAP) that downregulates RAS activity, have been appreciated as driver mutations in lung adenocarcinoma, melanoma, and glioma[17-19]. NF1-mutations in melanoma commonly co-occur with mutations in pathway-related genes like RASA2, another GAP that downregulates RAS activity, and SOS1, a guanine nucleotide exchange factor (GEF) that promotes RAS activation[18]. Activating mutations in MEK and ERK occur at low frequencies in head and neck cancer, lung squamous cell carcinoma, cervical carcinoma, colorectal cancer, and melanoma[7,18,19]. Many of the less common ERK pathway mutations are acquired resistance mechanisms that emerge as secondary pathway mutations to overcome pathway suppression by ERK pathway inhibitors, described in detail below.

The hallmarks of cancer described by Hanahan and Weinberg are the key cellular capabilities required for tumor development and progression[20]. Constitutive activation of the ERK MAPK pathway provides signaling to support several of these hallmark capabilities. Examining the normal functions of ERK signaling provides insights into how ERK signaling contributes to tumorigenesis. For example, one key role of the ERK

pathway in cell proliferation is controlling the G1 to S phase transition in the cell cycle. Continuous or repetitive pulses of ERK pathway activation results in progression of cells from G1 to S phase, initiating the growth factor independent phase of cell cycle progression[21-23]. ERK phosphorylates the ETS family of transcription factors, including ELK1, which induce the expression of transcription factors JUN, FOS, and MYC, which regulate early G1 phase and late G1 phase genes for irreversible S phase entry. ERK pathway activation provides pro-survival signals by inhibiting pro-apoptotic factors (BIM, BAD, BIK) through direct phosphorylation by ERK or downstream kinases and also by stimulating antiapoptotic proteins[23-27] (MCL-1). Constitutive oncogenic ERK signaling, through these normally highly regulated functions, can sustain proliferative signaling and resist cell death for tumor growth. Other less defined potential mechanisms of ERK signaling in cancer include the promotion of the Warburg effect for deregulated cellular metabolism[28,29] and regulation of matrix metalloproteinases MMP-2 and MMP-9 to activate invasion and metastasis[30-32]. Many potential physiological mechanisms by which ERK signaling influences tumorigenesis have been investigated and described in great detail. The pleiotropic nature of oncogenic ERK signaling underscores why the ERK signaling pathway is the most frequently altered in melanoma.

1.1.2 Genetic Landscape of Driver Mutations in Melanoma

With the advancement of high-throughput genomic sequencing technology and large-scale initiatives in tumor characterization of melanoma patient cohorts, the full range of somatic mutations observed in melanoma have been recorded for hundreds of melanoma tumors[18,19,33-37]. These genomic landscape studies confirmed the prevalence of ERK pathway mutations in melanoma and classified the disease into 4 genomic subtypes based on the driver mutation present in the ERK pathway[7,18,19] (Figure 1.1B). The largest subtype (~50%) includes tumors harboring BRAF mutations. Three additional subtypes—NRAS mutant (~25%), NF1 mutant (~15%), and “triple wild-type”

make up the remaining 50% of melanomas (Figure 1.2). BRAF, NRAS, and NF1 mutations occur largely mutually exclusively.

While BRAF, NRAS, and NF1 are thought to be the major genes driving melanoma progression, their individual mutation alone is insufficient for malignant transformation of melanocytic nevi[38]. Additional mutations must occur in conjunction with these driver mutations to promote transformation. However, because melanoma has a high somatic mutational burden, identifying driver mutations from inconsequential passenger mutations is challenging, especially with the abundance of sequencing datasets for melanoma tumors available. Thus far, mutational frequency is the main criterion used to predict potential driver genes. This approach to driver gene discovery not only overlooks infrequently occurring driver mutations, but also does not offer insight into the functional or mechanistic consequences of mutations. Because extensive studies are required to fully understand how identified mutations drive oncogenesis, the rate at which genomic datasets are generated far exceeds their analysis for oncogene or tumor suppressor functions. For example, TP53, CDKN2A, KIT, RAC1, and PTEN are frequently mutated genes whose oncogenic functions have been well elucidated in the context of melanoma[18,33-35] (Figure 1.2). Conversely, PPP6C, ARID2, IDH1, KMT2C, and DDX3X are also significant frequently mutated genes whose contributions to melanoma progression have not been thoroughly investigated. While some of these potential clinically important therapeutic targets are implicated in known oncogenic pathways, others have yet unclear associations with oncogenic signaling. Establishing how these secondary driver mutations alter oncogenic signaling can aid in predicting disease progression and drug response, leading to the further advancement of precision medicine.

1.2 Pathway Inhibitors in Melanoma

Targeted therapeutic approaches have been a major breakthrough for treating melanoma patients and for personalized medicine. The development of ERK pathway

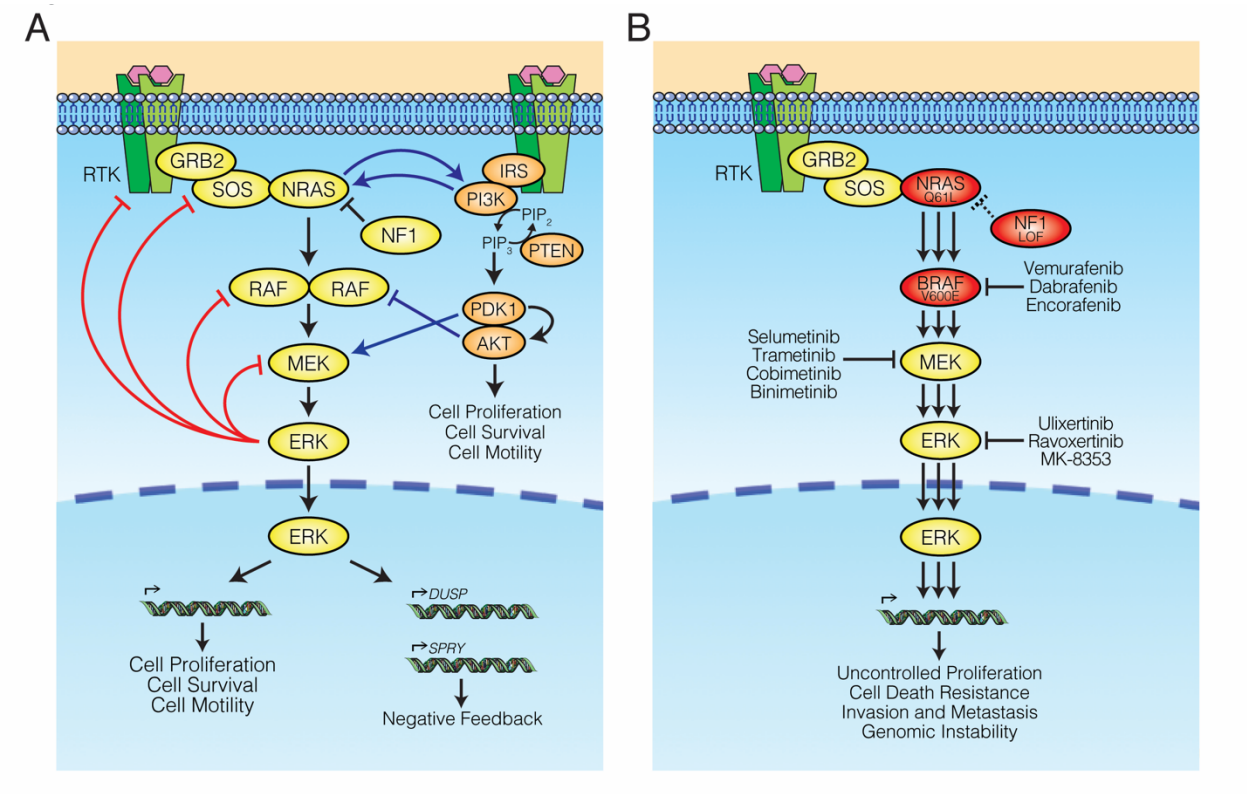

Figure 1.1 Normal and Oncogenic ERK MAP Kinase Pathway

(A) Simplified schematic of the ERK MAPK signaling pathway (yellow) and PI3K-AKT signaling pathway (orange). Blue lines indicate cross-talk between pathways. Red lines indicate negative feedback via ERK.

(B) Major oncogenic ERK MAPK pathway mutations (red) and clinical pathway inhibitors.

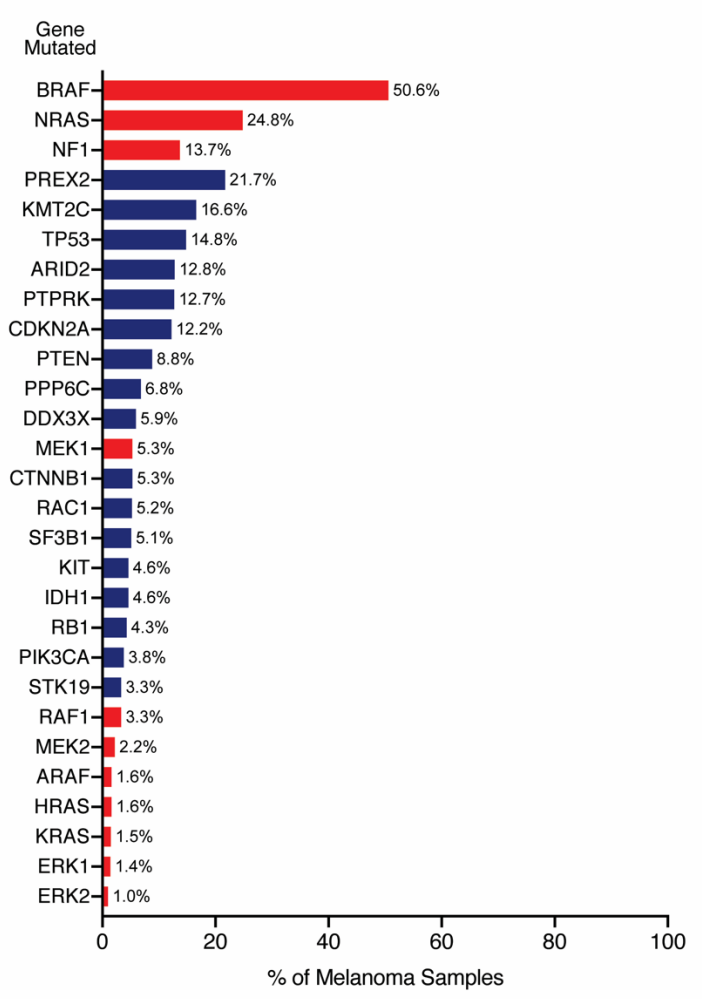

Figure 1.2 Mutational Frequencies of Genes in Melanoma

List of selected mutated genes in patient samples from non-redundant melanoma and cutaneous melanoma studies in cBioPortal[39,40]. ERK MAPK pathway genes are in red.

inhibitors (MAPKi) was motivated by the growing appreciation of oncogenic ERK signaling activation in melanoma (Figure 1.1B). In the clinic, inhibitors targeting core components of the ERK signaling pathway results in improved response rates and prolonged progression free survival. The efficacy of these inhibitors has shifted first line therapy options away from chemotherapy to targeted therapy for $BRAF^{V600E}$ melanoma. While many of the MAPKi described below have revolutionized cancer treatment, there is still much to be done for longer progression-free survival or curative responses.

1.2.1 BRAF Inhibitors (BRAFi)

The discovery of the prevalence of $BRAF^{V600E}$ mutations and the establishment of constitutive ERK signaling in the majority of melanomas identified BRAF as a key driver gene and favorable therapeutic target[9,10,41] . siRNA and shRNA knockdown of BRAF result in loss of MEK and ERK phosphorylation and the induction of cell cycle arrest and death in $BRAF^{V600E}$ melanoma cell lines and xenograft models[41-43], confirming the critical role of $BRAF^{V600E}$ in melanoma tumor growth and validating $BRAF^{V600E}$ as a drug target. Small molecule ATP competitive inhibitors for BRAF have been developed and used as research tools and investigated for clinical intervention. Sorafenib (BAY43-09006), a multitarget kinase inhibitor with a wide spectrum of cellular targets, was initially investigated in various melanoma clinical trials due to its activity against $BRAF^{V600E}$. However, its nonselective inhibition of various RTKs as well as CRAF and wild-type BRAF makes it difficult to interpret which targets promote antitumor activity. In clinical trials, sorafenib monotherapy and combination therapy have largely resulted in insufficient benefit for melanoma patients[44-49]. More selective BRAF inhibitors (BRAFi) have been successful in the clinic. Vemurafenib (PLX4032), like its precursor PLX4720, was developed using a structure guided discovery approach to preferentially inhibit the mutant form of BRAF[50,51]. This selectivity for $BRAF^{V600E}$ induces cell death in $BRAF^{V600E}$ cells and tumor regression in $BRAF^{V600E}$ tumor xenograft models[43,52,53]. Vemurafenib has

had dramatic results in $BRAF^{V600E}$ melanoma patients, producing impressive rapid response rates and progression free survival with minimal treatment-related toxicity[51,54-57]. Vemurafenib was the first FDA approved BRAFi. Dabrafenib and encorafenib are also approved BRAFi shown to have similar efficacies in melanoma patients[58-60]. Despite the rapid response and early clinical benefits to BRAFi treatment, advanced metastatic melanoma patients acquire resistance shortly after starting BRAFi treatment, with median time to disease progression of 5-7 months[55-57,61]. Mechanisms of resistance and strategies to combat resistance are discussed below.

While the described BRAFi inhibit ERK signaling in $BRAF^{V600E}$ cells, they unexpectedly enhance ERK signaling in wild-type BRAF cells, promoting cell growth and proliferation[62-64]. This paradoxical ERK activation is caused by BRAFi binding to one protomer of a BRAF/CRAF heterodimer or homodimer followed by transactivation of the drug-free RAF molecule. In the context of $BRAF^{V600E}$ cells, BRAF exists as an active monomer, minimizing transactivation of dimers. In the context of RAS mutations, increased wild-type BRAF expression, or increased upstream receptor activation, the increased signaling activity promotes RAF dimerization for transactivation upon BRAFi binding. In patients, paradoxical ERK activation can induce cutaneous squamous cell carcinoma and keratoacanthoma tumors commonly harboring RAS mutations[54,65,66]. Thus, depending on the genomic and signaling context, BRAFi can have inhibitory or activating effects on ERK signaling, underscoring the importance of genotyping or mutational profiling of tumors for patient selection.

The next generation of BRAFi, known as “paradox breakers”, have been developed to address the issue of paradoxical ERK activation[67]. PLX7904 and PLX8396 inhibit both monomeric $BRAF^{V600E}$ and dimeric wild-type BRAF, as well as non-V600E mutant forms of BRAF. PLX8396 has shown greater efficacy in inhibiting ERK signaling and inducing apoptosis in wild-type BRAF, $BRAF^{V600E}$, or BRAF splice-variant expressing melanoma cell lines, xenografts, and patient derived explant models[68]. Ongoing phase

I/IIA clinical trials thus far show promising results and a more favorable safety profile for the use of PLX8394 in patients with advanced solid tumors[69].

1.2.2 MEK Inhibitors (MEKi)

MEK inhibitors (MEKi) were the first inhibitors of the MAPK pathway developed and originally intended to be in vitro research tools for dissecting the MAPK signal transduction pathway[70,71]. The development of MEKi for the treatment of cancer was motivated by MEK's position as a bottleneck for ERK signaling, integrating upstream oncogenic signaling from overactive RAS, RAFs, and RTKs, where the majority of pathway activating mutations and mechanisms occur, to activate ERK (Figure 1.1B). Unlike most kinase inhibitors, MEKi are highly selective, allosteric, non-ATP competitive inhibitors. Improving on the poor bioavailability, potency, and tolerability of early MEKi research compounds, several newer MEKi are FDA approved or are being investigated in ongoing clinical trials[72,73]. Trametinib (GSK1120212), the first FDA approved MEKi, inhibits phosphorylation of MEK by RAF, attenuating ERK signaling and inducing cell death in $BRAF^{V600E}$ melanoma cells and xenografts[74]. Although trametinib monotherapy improved overall survival rates and progression free survival of $BRAF^{V600E}$ mutant melanoma patients compared to conventional chemotherapy[75,76], it did not show improvement over BRAFi treatment. This may partially be due to dose-limiting toxicity because MEKi target MEK in all cells and not a specific mutant form found in only cancer cells as with $BRAF^{V600E}$.

The emergence of MAPK re-activation as the primary mechanism of BRAFi resistance (described in 1.3) led to proposing MEK inhibition as a strategy to combat BRAFi resistance through targeting the immediate downstream effector of BRAF[77,78]. As anticipated, MEKi in combination with BRAFi does show improvement over BRAFi monotherapy[61,79,80]. The therapeutic effect of the combination therapy is synergistic while reducing the toxicity with either alone[81,82]. As a first line therapy, 72.3% of patients were

free of disease progression at 6 months with BRAFi and MEKi versus only 55.4% with BRAFi alone. Trametinib/dabrafenib, binimetinib/encorafenib, and cobimetinib/vemurafenib, all FDA approved MEKi/BRAFi treatment options for $BRAF^{V600E}$ melanoma, result in improved median time to progression from ~7.3 months with BRAFi monotherapy to ~11.9 months[83]. As adjuvant therapy in patients with resected stage III $BRAF^{V600E}$ melanoma, MEKi/BRAFi combination therapy prolongs survival without relapse or distant metastasis, resulting in 52% of patients without relapse at 5 years compared to 36% of patients with placebo[84]. MEKi/BRAFi combinations are the current standard of care for advanced $BRAF^{V600E}$ melanoma[85]. While the combination delays the emergence of drug resistance, as evidenced by the significantly improved progression free survival, resistance through similar mechanisms as BRAFi monotherapy resistance remains a critical obstacle in the use of targeted therapy.

MEKi are in on-going preclinical and clinical investigation for combinatorial treatment with other targeted therapies and immunotherapies[73,86]. Novel MEKi treatment combinations are expected to benefit the treatment of different melanoma genetic subtypes and other cancer types.

1.2.3 ERK inhibitors (ERKi)

The major mechanisms of resistance to MEKi/BRAFi combination and monotherapy reactivate MAPK signaling[87-89] (Figure 1.3). Inhibition downstream of the majority of these resistance mechanisms (Figure 1.2) at ERK was proposed to overcome or further delay resistance. Additionally, ERK inhibitors (ERKi) have the potential to be rational treatment options for BRAFi-resistant $BRAF^{V600E}$ melanoma and other cancers driven by MAPK activity but insensitive to BRAF and MEK inhibition.

In preclinical studies, selective ATP-competitive ERKi reduce the strong reactivation of ERK signaling in MEKi/BRAFi resistant cells and inhibit cell growth and proliferation in cells and mouse xenograft models[90-96]. These inhibitors also have

antitumor activity against some wild-type BRAF and NRAS mutant cell lines in addition to most MEKi/BRAFi sensitive $BRAF^{V600E}$ cells, suggesting potential therapeutic response in additional patient genetic subtypes. Of the numerous ERKi under investigation in early clinical trials[97,98], Ulixertinib (BVD-523) is the most promising, having shown partial responses in NRAS mutant, $BRAF^{V600E}$ and wild-type BRAF solid tumors, including melanomas[99]. Partial responses were also observed with the ERKi MK-8353 and Ravoxertinib (GDC-0994) in melanoma[96] and other $BRAF^{V600E}$ tumors[100]. The mentioned clinical studies demonstrate early efficacy as well as acceptable safety profiles but more clinical trial data is necessary for a complete assessment of the clinical benefits of ERKi as monotherapies and combination therapies. Ongoing clinical trials are investigating ERKi in combination with MEKi, chemotherapies, CDK4/6 inhibitors, and anti-PD-1 immunotherapies[97,98].

1.3 Melanoma Targeted Therapy Resistance

The use of MAPK pathway inhibitors in the clinic has significantly improved the treatment of melanoma and patient outcomes. Unfortunately, the rapid responses to BRAFi and MEKi are almost invariably short-lived due to the development of acquired resistance[80]. Of the $BRAF^{V600E}$ melanoma patient population, 10-20% of patients do not have any initial response due to intrinsic resistance. Additionally, the heterogeneity of tumor resistance mechanisms complicate how resistance is addressed. Not only is there resistance heterogeneity between patients, there are often multiple mechanisms of resistance within a patient or even a single tumor[101].

1.3.1 ERK MAPK Pathway Reactivation

Analyses of tumors with acquired resistance to BRAFi and/or MEKi have identified reactivation of the MAPK signaling pathway as the major driver of resistance[87,101-104]. Mechanisms underlying pathway reactivation are diverse but usually involve pathway

components (Figure 1.3). Resistance mechanisms involving alterations in $BRAF^{V600E}$ and NRAS are the most common. $BRAF^{V600E}$ amplification and alternative splicing are found in 8-30% and 13-29% of post-treatment progressive melanoma tumors, respectively[101-106]. Activating mutations in NRAS are found in 8-23% of progressive tumors[101-104,107,108]. Activating mutations in KRAS are less common, occurring in 2-7% of progressive tumors[101,104]. MEK mutations occur in 3-20% of progressive tumors[89,101-104,107]. The frequency of BRAF amplification and MEK2 mutations are significantly higher in MEKi/BRAFi combination therapy resistance than in BRAFi monotherapy resistance[89], suggesting these mechanisms cause the substantially greater reactivation of ERK signaling characteristic of combination therapy resistance. This is not surprising given resistance to kinase inhibitors is often associated with secondary mutations to the target gene. Upregulation of receptor tyrosine kinases, NF1 loss, CRAF overexpression, and COT (MAP3K8) upregulation are less common MAPK reactivation mechanisms observed in BRAFi and/or MEKi resistant tumors[87,88,102,108,109].

Strategies to overcome MAPK reactivation-mediated resistance such as the implementation of intrapathway dual inhibition by BRAFi and MEKi combinations have only delayed the time to acquired resistance, as detailed above. While early indications suggest ERKi will combat resistance from MAPK reactivation, ERKi resistance mechanisms have not yet been identified or thoroughly investigated. Although many ERK1 and ERK2 mutations have been identified in mutagenesis screens for drug resistance[110-114], ERK mutations are rare in cancers. The ERK2 E320K mutation, which has been observed in 27 squamous cell carcinoma patients, elevates ERK pathway activation in cells and confers resistance to BRAFi and MEKi but not ERKi[112,113]. The number and heterogeneity of MAPKi resistance mechanisms for MAPK reactivation identified thus far suggests resistance is expected to remain a major clinical challenge.

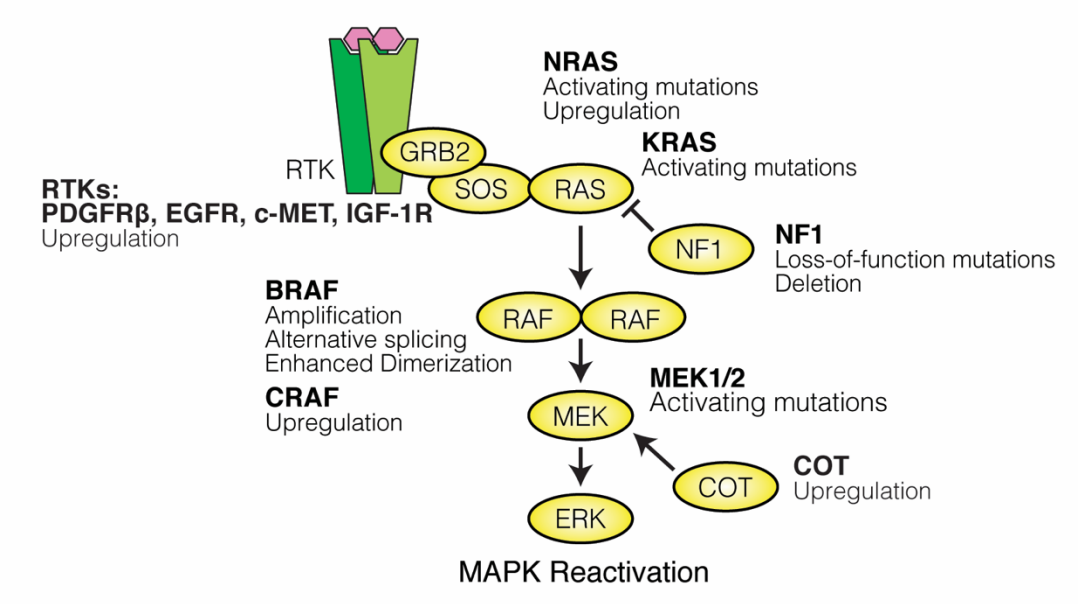

Figure 1.3 MAPK Reactivation Mechanisms for MAPKi Resistance

1.3.2 PI3K-AKT Pathway Activation

ERK MAPK signaling remains inhibited in 20-30% of BRAFi and MEKi resistant tumors indicating the activation of alternative cell growth and survival pathways for resistance[88,101,102]. While upregulation of or activating mutations in RTKs can be a MAPK reactivation mechanism, it can also activate other survival pathways peripheral to the ERK signaling pathway for resistance. The upregulated RTKs EGFR, PDGFR, MET, and IGF-1R activate both the PI3K-AKT pathway and the ERK MAPK pathway[108,115]. The PI3K-AKT pathway is the second core resistance pathway identified for BRAFi and MEKi resistance in $BRAF^{V600E}$ melanoma. The PI3K-AKT pathway, another central signaling pathway for regulating essential cellular pathways, is activated in many cancers through various genetic and epigenetic alterations[116,117]. In this pathway, activated RTKs and G protein-coupled receptors (GPCR) activate phosphatidylinositol 3'-kinase (PI3K), which phosphorylates and converts the plasma membrane lipid PIP_2 to PIP_3 (Figure 1.1A). PIP_3 recruits AKT and PDK1 to the cell membrane where PDK1 phosphorylates and activates AKT. Downstream effectors of AKT regulate cell proliferation and cell survival. In melanoma, PI3K-AKT signaling has been implicated in both intrinsic and acquired resistance[118,119]. Genetic alterations in the PI3K-AKT pathway can precede or succeed MAPKi resistance. Generally, MAPKi resistant cells either have high basal levels of activated AKT or increased AKT activation in response to MAPKi[91].

The most commonly detected PI3K-AKT pathway alterations in melanoma are copy number loss or loss-of-function mutations of PTEN, a negative regulator of the PI3K-AKT pathway and established tumor suppressor (Figure 1.1A, 1.2). PTEN loss is detected in 8-20% of melanoma tumors and often co-occur with $BRAF^{V600E}$ mutations[37,120,121]. These PTEN alterations are found in pretreatment and/or post-treatment progressive tumors. Although higher PTEN expression levels are associated with BRAFi responders, PTEN expression levels are not predictive of MAPKi response[107,119]. Mechanistically, PTEN loss mediates inhibitor resistance by suppressing

BIM-mediated apoptosis[119]. Furthermore, ERK signaling inhibition in PTEN null cells activates AKT signaling. This is all consistent with the decreased clinical benefit of BRAFi treatment for $BRAF^{V600E}$ melanoma patients with PTEN loss compared to $BRAF^{V600E}$ melanoma patients with wild-type PTEN.

Other alterations within the pathway include mutations in PIK3CA, the catalytic subunit of PI3K and an established oncogene, and AKT, which are detected in 2-6% and 1-2% of melanoma[18,33,122], respectively. Mutations in PHLPP1, PIK3R1, and PIK3R2, negative regulators of the pathway, are rare (<2%) in melanoma but have been observed in MAPKi resistant progressive tumors[101,117]. Identical pathway mutations have been observed in other cancer types and shown to activate oncogenic signaling. Although there are limited studies, PI3K-AKT mutations present in MEKi/BRAFi combination resistant tumors were present pre-treatment as well[89,123], suggesting the PI3K-AKT pathway may potentially have a more limited role in resistance to dual MAPK pathway inhibitor treatment.

PI3K-AKT pathway alterations elicit MAPKi resistance in a complex and context-dependent manner. These alterations occur independently and co-occur with MAPK activation or reactivation. Crosstalk between the two pathways likely influence how resistance is mediated (Figure 1.1A). Preclinical studies have demonstrated the added benefit and synergistic inhibition of combining PI3K inhibitors with MAPKi[124,125]. PI3K-AKT pathway inhibition can delay resistance to MEKi in $BRAF^{V600E}$ melanoma[126]. In clinical trials investigating pan-PI3K inhibitors with BRAFi or MEKi in $BRAF^{V600E}$ patients, poor tolerability was a major limitation[127-130]. Similarly, MAPKi in combination with AKT inhibitors showed poor tolerability and limited efficacy.

1.3.3 Other Pathways in MAPKi Resistance

Beyond activation of the two major oncogenic signaling pathways, MAPKi resistance can involve other known oncogenic signaling pathways. Signal transducer

and activator of transcription (STAT) proteins are a family of transcription factors that when phosphorylated dimerize and translocate to the nucleus where they activate gene transcription. STAT3 is an oncogene[131,132] constitutively activated in several cancers including melanoma[133]. STAT3 oncogenic function comes from its regulation of apoptosis inhibitors, inducers of angiogenesis, and cell cycle regulators. STAT3 is activated by interleukin-6 (IL-6) family cytokine receptor associated Janus Kinases (JAKs) as well as EGFR-activated SRC-family kinases (SFK). $BRAF^{V600E}$ melanoma cells with acquired BRAFi resistance have elevated EGFR activating phosphorylation and decreased EGFR negative regulatory phosphorylation accompanied by activating phosphorylation of its downstream effector AKT[134]. Consequently, phosphorylation of SFKs and STAT is elevated in BRAFi resistant cells, which were found to be sensitive to pan-SFK inhibitors and a STAT3 dimerization inhibitor. Alternatively, a subset of $BRAF^{V600E}$ cells with intrinsic resistance to BRAFi have increased autocrine IL-6 secretion which activates the JAK-STAT3 pathway[135] to overcome ERKi signaling inhibition. Combining JAK inhibition with MEK inhibition suppresses STAT3 phosphorylation and can overcome resistance. STAT3 silencing or inhibition also overcomes acquired resistance and can restore BRAFi sensitivity in $BRAF^{V600E}$ melanoma cells[136,137].

p12-activated kinases (PAKs) become activated in cells with acquired BRAFi and MEKi/BRAFi resistance[138]. For BRAFi monotherapy resistance, phosphorylation of CRAF and MEK by PAKs are another mechanism for ERK MAPK reactivation. For MEKi/BRAFi combination resistance, PAKs activate JNK, which activates downstream targets shared with ERK such as ELK1, JUN, and FOS. In the context of MEKi/BRAFi resistance, PAKs also regulates β-catenin phosphorylation, activates mTOR signaling, and inhibits apoptotic signaling to mediate MAPKi drug resistance.

1.3.4 Identifying Novel Resistance Mechanisms

Numerous screening strategies have been used to identify genetic dependencies

for MAPKi sensitivity and novel therapeutic targets. The advantage of these exploratory and unbiased genetic approaches is their potential to discover unexpected pathways involved in MAPKi resistance as well as synthetic lethal interactions that can be exploited in melanoma treatment. These newly identified vulnerabilities may inform biomarker-based patient selection for MAPKi treatment.

Pooled screening strategies model intratumor heterogeneity and the clonal evolution of cancer for emergence of resistance. Screens investigating MAPKi response in melanoma have confirmed known resistance pathways. For example, a high throughput functional screen expressed ~600 kinases or kinase related open reading frames (ORFs) in BRAFi sensitive $BRAF^{V600E}$ melanoma cell line to identify ORFs that confer resistance to BRAFi[139]. This systemic gain-of-function screen identified COT and CRAF as top candidate kinases that mediate BRAFi resistance. Establishing COT-dependent mechanisms of MAPK reactivation, this study proposed dual intrapathway inhibition with RAF/MEK inhibition and RAF/COT inhibition combinations, substantiating the use of BRAFi and MEKi combinations in the clinic. Elevated COT expression has been detected in BRAFi resistant tumors (Figure 1.3). A large-scale RNA interference (RNAi) screen identified functional loss of NF1 as a mediator of BRAFi resistance in $BRAF^{V600E}$ melanoma, which was confirmed by the NF1 mutations present in BRAFi resistant tumors[109]. An insertional mutagenesis screen in a $BRAF^{V600E}$ melanoma mouse model identified the PI3K-AKT signaling pathway as a mediator of BRAFi resistance[140].

With the advancement of screening techniques and enrichment analysis and the increased availability of sgRNA and shRNA libraries, recent genetic screens have identified novel vulnerabilities in MAPKi resistance. Large-scale CRISPR screens in BRAFi resistant $BRAF^{V600E}$ melanoma cells and subsequent pathway enrichment analysis discovered a novel class of cell cycle genes (CDK6, CCND1, PSMB1, and RRM2), not previously linked BRAFi resistance, enriched within the 314 genes whose depletion sensitized cells to BRAFi[141]. Further characterization established that the depletion of

CDK6 and its regulator ETV5 restores MAPKi sensitivity. Although there are ongoing clinical studies investigating MAPKi and pan CDK4/6 inhibitor combinations[142,143], the authors establish that the inhibition of CDK6, and not other CDKs, synergizes with BRAFi. Interestingly, CDK6 expression and up-regulation of genes functionally connected to CDK6 are associated with poor survival in BRAFi-treated melanoma patients.

In an epigenome-wide shRNA screen, knockdown of BOP1, HAT1, ING5, and KDM4C conferred resistance to BRAFi in a $BRAF^{V600E}$ mutant melanoma cell line[144]. The authors focused on Block of proliferation 1 (BOP1), which they propose downregulates DUSP4/6 and results in MAPK reactivation for BRAFi resistance. Analysis of paired melanoma patient samples before and after BRAFi treatment showed BOP1 down regulation in progressive tumors. Similarly, HAT1 was found to reactivate the MAPK pathway, and 63% of progressive tumors showed reduced HAT1 expression compared to patient matched MAPKi treatment naive tumors[145].

These large-scale pooled screening strategies are complicated by off-target effects, varying knockdown efficiencies, library complexity, selection of bioinformatic pipelines, and scalability for appropriate library coverage. For example, a genome-wide shRNA screen identified CUL3, a key protein in E3 ubiquitin ligase complexes, as a driver of MAPKi resistance[146]. However, 7 of the 9 candidate drivers identified in this screen did not recapitulate MAPKi resistance in validation studies. Overall, the described functional genetic screens were able to identify verifiable genes and pathways that modulate MAPKi sensitivity. Validation studies demonstrate the ability of these candidate therapeutic targets to overcome MAPKi resistance. More importantly, analysis of target gene expression in patient tumors and patient response rates underscore the clinical relevance of the findings from genetic screens.

1.4 PPP6C in Melanoma

The work in this dissertation describes the identification of PPP6C as a key

regulator of ERK signaling in melanoma. PPP6C is a conserved essential serine-threonine metallophosphatase related to the catalytic subunit of PP2A[147]. PPP6C functions within heterotrimeric PP6 holoenzymes consisting of a Sit4-associated protein (SAPS) domain regulatory subunit (PPP6R1, PPP6R2 or PPP6R3) that mediates substrate recruitment and an ankyrin repeat (ANKRD28, ANKRD44 or ANKRD52) subunit that may serve a scaffolding role[148,149] (Figure 1.4A). The presence of multiple regulatory and scaffolding subunits defines nine potential PP6 complexes that collectively participate in a variety of cellular processes.

1.4.1 Established PP6 Functions

As an essential protein ubiquitously expressed in mammalian tissues, PPP6C has roles in key cellular functions including cell cycle progression[150-152], the DNA damage response[150,153-155], autophagy[156], miRNA processing[157], inflammatory response[158,159], and antiviral immunity[160]. Despite the scope and diversity of signaling roles described, our current understanding of PPP6C functions is limited, especially when considering the number of PPP6C studies compared to that of its extensively studied close relative PP2A. Because PP2A was the first PP2A family phosphatase purified and characterized, many PP2A studies use okadaic acid, a pan-PP2A family phosphatase inhibitor, as a PP2A inhibitor and report that its biological effects are attributed to PP2A inhibition. Okadaic acid inhibits PP2A, PP4, and PP6 with nearly identical potency. These studies are reporting on the effects of collective inhibition of all three of these phosphatases and likely incorrectly assigning PP6 functions to PP2A.

PPP6C has well-established roles in cell cycle progression. PP6 regulation of chromosome segregation and spindle assembly in mitosis is highly conserved in eukaryotes, from yeast to humans[152,162,163]. PPP6C or PPP6R1/2/3 loss results in defective chromosome segregation in anaphase and fragmented nuclei in telophase. PPP6C and PPP6Rs associate with mitotic spindles along with its substrates[164]. Aurora A, an

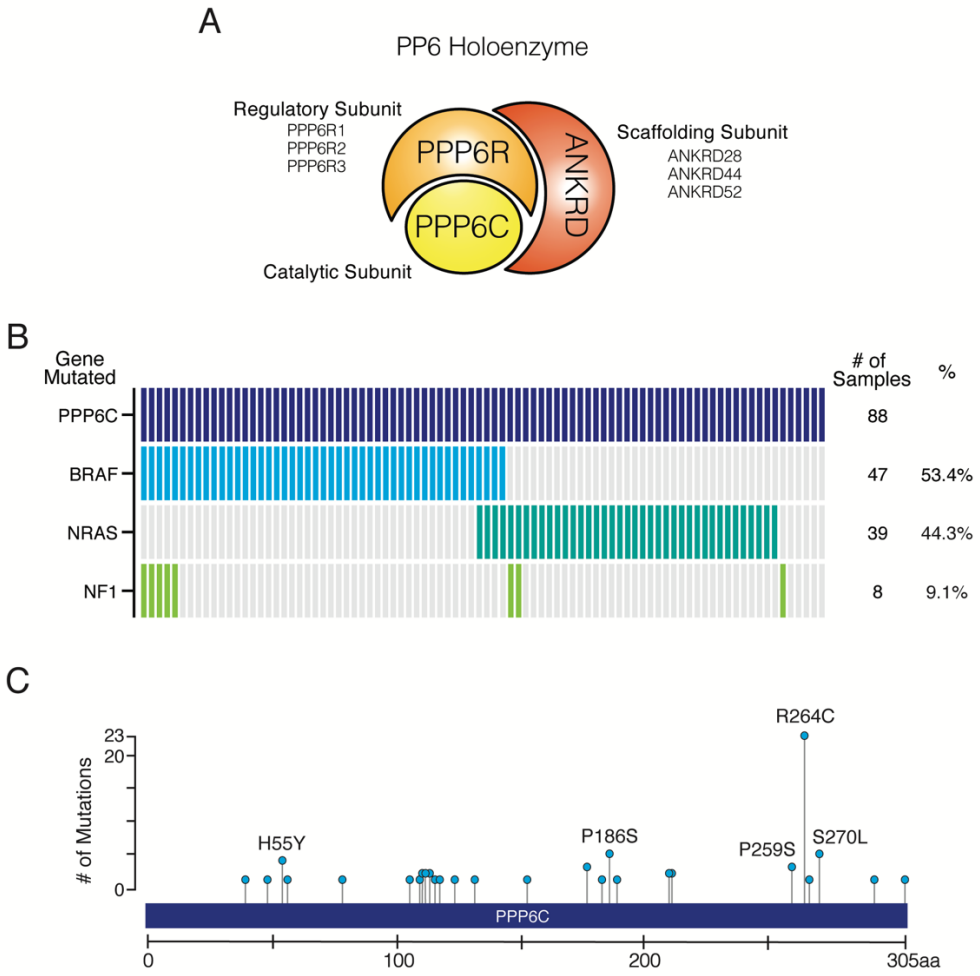

Figure 1.4 PPP6C Mutations in Melanoma

(A) PP6 heterotrimeric complexes

(B) Frequencies of mutations in BRAF, NRAS, and NF1 co-occurring with PPP6C in melanoma. Data are from nonoverlapping melanoma studies in cBioportal[39,40]

(C) Frequencies of PPP6C mutations reported in melanomas. Data are from nonoverlapping melanoma studies in cBioportal[39,40]

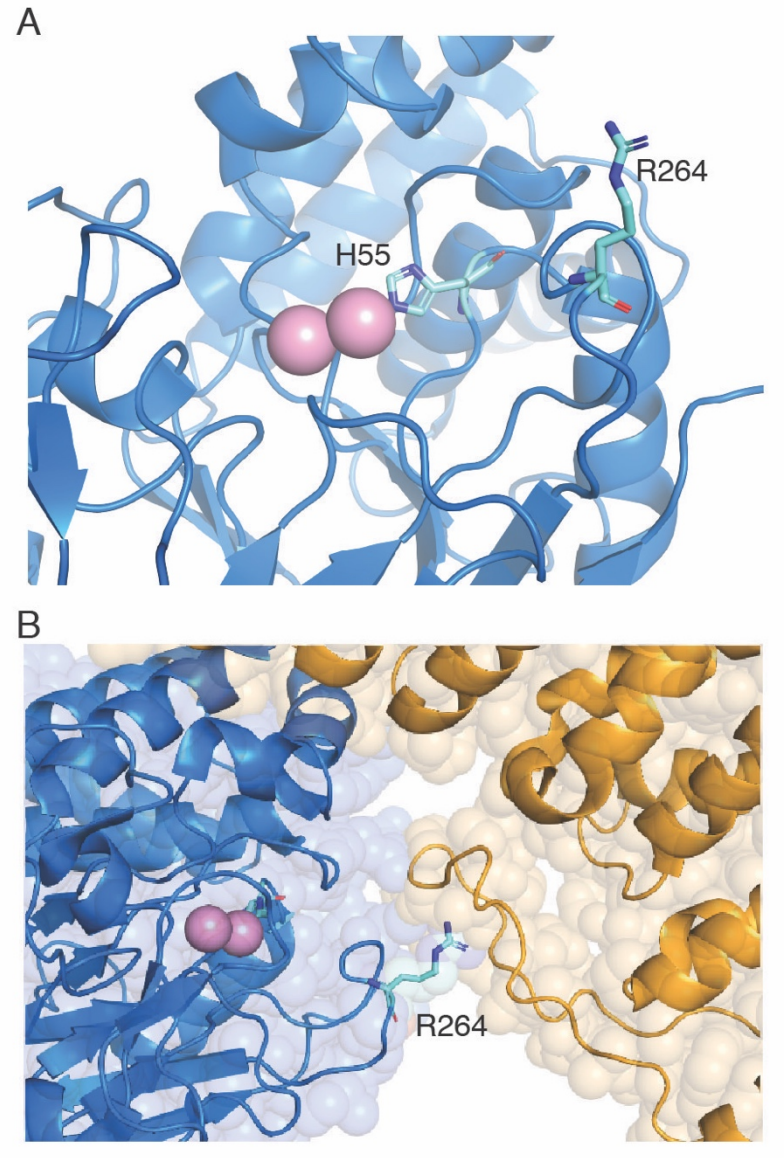

Figure 1.5 PPP6C residues mutated in melanoma mapped onto the structure of the PP2A catalytic subunit

(A) Recurrently mutated PPP6C residues His55 and Arg264 are shown in cyan in stick representation modeled onto the crystal structure of PPP2CA[161] (PDB: 2IAE). Catalytic metal ions are shown as pink spheres.

(B) Arg264 maps to the interface of the PP2A catalytic subunit (blue) and the PP2A regulatory B56γ1 subunit (orange).

essential mitotic kinase, localizes to spindle poles and centromeres during mitosis upon associating with its binding partner TPX2. PP6 recognizes and dephosphorylates Aurora A-TPX2 complexes, inactivating Aurora A[152]. DNA-PK, a regulator of mitosis and DNA damage repair, localizes to centrosomes, spindles, and the midbody during mitosis. PP6 dephosphorylation of DNA-PK during mitosis mediates mitotic exit and cytokinesis. A broad phosphoproteomics study aimed to identify PP6-regulated phosphorylation events during mitosis confirmed PP6 regulation of chromosome segregation and spindle formation in protein network and pathway analysis of increased phosphorylation events upon PPP6C depletion[165]. PP6 was also found to mediate chromosome condensation, in part through direct dephosphorylation of the condensin 1 subunit NCAPG to activate condensin-1[151,165]. Other than in mitosis, PP6 has been reported to have roles in other phases of the cell cycle including the G1/S transition[166,167] and S phase progression[168,169] as well as meiosis[170,171].

In DNA damage response signaling, PP6 is involved in both non-homologous end joining repair (NHEJ) and homology-directed repair (HDR), the two processes that fix DNA double-strand breaks (DSBs). Ionizing radiation (IR), which causes DSBs, induces the expression of PP6 subunits in cells[172,173]. Conversely, PP6 depletion sensitizes cells to IR, marked by increased phosphorylation of γ-H2AX[164,174,175]. PPP6R1 targets PP6 to DNA-PK for dephosphorylation and activation of DNA-PK in NHEJ[150,153,164,174,175]. There is also evidence for DNA-PK recruitment of PP6 for dephosphorylation of γ-H2AX to repair DSBs resulting from IR via NHEJ[164]. Similarly, PPP6C is recruited to DSB sites to dephosphorylate γ-H2AX to repair DSB resulting from replication blockage via HDR[155].

PP6 negatively regulates the canonical nuclear factor-κB (NF-κB) pathway, which is essential for immune and inflammatory responses. Proinflammatory cytokines like tumor necrosis factor-α (TNF-α) and interleukin-1β (IL-1β) stimulate TGF-β-activated kinase 1 (TAK1) autophosphorylation and activation, which activates IκB kinase (IKK) for

phosphorylation of IκBε and activation of NF-κB signaling[176]. PP6 associates with and dephosphorylates TAK1, inhibiting its activity and therefore negatively regulating its downstream pathways, the NF-κB pathway and MAPK signaling pathways[158,177]. PPP6C and PP6 regulatory subunits also associate with IκBε, which binds and inhibits NF-κB by trapping it in the cytoplasm[149,178]. PPP6R1 targets PPP6C to IκBε to dephosphorylate and protect IκBε from degradation, limiting NF-κB activity. Loss of PP6 subunits results in enhanced NF-κB pathway activation by TNF-α or IL-1β[149,158,159,179]. Other roles of PP6 in immune signaling include involvement in lymphocyte development and homeostasis[159,180,181]. PP6 loss impairs the development of CD4+, CD8+, and CD4+/CD8+ T cell populations and results in T cells more prone to differentiation and production of cytokines[159]. This likely occurs through PP6 dephosphorylation and regulation of the transcription factor Bcl11b, an essential factor for T-cell development[181]. In antiviral immune signaling, PPP6C in complex with WHIP and TRIM14 to dephosphorylate RIG-1 to promote production of type 1 interferons (IFN-1)[160].

Many large-scale proteomics studies and screens have implicated PP6 in other signaling pathways and cellular functions. In some cases, the relevant PP6 substrates have been identified, such as Argonaute 2 (AGO-2) in miRNA-mediated silencing pathway[157] or ASK3 in osmotic stress response[182]. However, the precise roles or mechanisms of PP6 involvement in other signaling pathways are largely unknown or poorly understood, for example, its regulation of pre-mRNA splicing[183] or the Hippo pathway[184]. The diversity of PP6 substrates and functions is unsurprising, given the hundreds of known substrates for PP2A. PP6 involvement in many pathways is consistent with its ubiquitous expression and its categorization as a “common essential” gene, or gene that is essential to cell growth and survival across a large panel of cell lines (739), in the Cancer Dependency Map Project[185-187].

1.4.2 PPP6C Mutations in Melanoma

PPP6C mutations are found across multiple cancer types but are most common in melanoma and other skin cancers, where they are thought to contribute to tumor development[18,33,37,188]. Somatic PPP6C mutations have been detected in 6-9% of malignant melanomas (Figure 1.2), generally co-occurring with BRAF and NRAS mutations[18,19,33] (Figure 1.4B). The majority of these melanoma-associated mutations are missense mutations and often occur with loss of heterozygosity[33,34,189]. Of melanoma patient tumors with both mutational and copy number profiling data, 33 of 54 (61%) mutations occurred with shallow or heterozygous deletions[39,40]. PPP6C mutations are distributed throughout the primary sequence but recurrently cluster to highly conserved regions in or near the catalytic cleft, with R264C being the most common mutation[189] (Figure 1.4C). The clustering of PP6C mutations, and specifically the high recurrence of the PPP6C R264C point mutation, are suggestive of activating mutations, as seen with classical oncogenes. However, prior analysis of recurrent and non-recurrent PPP6C mutations indicate that all of them, to varying degrees, reduce catalytic activity[189,190]. Copy number loss and loss-of-function mutations indicate PPP6C likely functions as a tumor suppressor. Potential signaling mechanisms for known oncogenic mutations in melanoma have been explored and are detailed below.

Based on where recurrent mutations map to on the structure of the PP2A catalytic subunit, the mutations likely have varying consequences on PP6 activity and signaling. The His55 residue coordinates a critical catalytic metal ion (Figure 1.5A). Loss of this coordination from the recurrent H55Y mutation would be expected to render PPP6C catalytically inactive. Arg264 is located at an interface of the PP2A catalytic subunit and one of its regulatory subunits (Figure 1.5B) Instead of causing the loss of intrinsic phosphatase activity of the catalytic subunit, the R264C mutation may disrupt PP6 holoenzyme assembly, possibly altering the composition of PP6 heterotrimers in cells. By promoting or disrupting the association of PPP6C with specific regulatory subunits,

mutations can alter substrate specificity and shift signaling outputs. This is the case with a recurrent cancer-associated mutation in a PP2A scaffolding subunit, which has been found to disrupt interactions with some regulatory B subunits and not others to activate the ERK signaling pathway[191]. Because PPP6C is an essential gene, complete loss of PPP6C function would not be tolerated by most cells. Some melanoma-associated mutations may spare essential functions of PP6 for survival and only disrupt tumor suppressive functions.

One of the major environmental risk factors for melanoma development is ultraviolet radiation (UVR) from sun exposure[192]. Cytosine to thymidine (guanine to adenosine) mutations (C > T), especially in dipyrimidine contexts, are signature of UVR-radiation-induced genetic changes. PPP6C mutations predominantly occur in sun-exposed tumors[34]. The overwhelming majority of PPP6C missense mutations including all recurrent mutations are C > T transitions, likely attributed to mismatch repair of UV-induced DNA damage. The R264C mutation is a cytosine to thymidine transition at a dipyrimidine site. While the majority of established activating MAPK pathway mutations (e.g., $BRAF^{V600E}$, $NRAS^{Q61L/R}$) in melanoma do not appear to be due to direct UV-induced damage, PPP6C mutations are presumably generated by UVR mutagenesis and contribute to UVR-induced melanomagenesis. This is consistent with the belief that PPP6C mutations are early events in the development of melanoma[189]. Mutations in tumors before BRAFi therapy harbor a predominance of C > T transitions compared to mutations in progressive tumors, which have a relative reduction in C >T transitions and increase in other transitions[101]. UVR-damage-induced PPP6C mutations potentially contribute to the transformation of melanocytic nevi with BRAF and NRAS mutations into melanoma.

1.4.3 A Tumor Suppressor Role for PPP6C in Melanoma

PPP6C is thought to be a tumor suppressor in melanoma[18,19,33,37,188], yet our

understanding of how it modulates cancer relevant pathways is limited. Partly due to the lack of overtly cancer-relevant known PP6 substrates, it is unclear which substrates or pathways provide the molecular basis for the occurrence of melanoma-associated PPP6C mutations. Biochemical studies characterizing melanoma-associated PPP6C mutants found some mutations disrupt holoenzyme assembly and decrease PPP6C stability[156,189,190]. However, this was not the case for all mutants investigated, suggesting heterogeneity in functional and signaling consequences of PPP6C mutations.

Most studies of PPP6C in melanoma have focused on its regulation of Aurora A in mitotic spindle assembly and chromosome segregation[152,190]. Melanoma-associated PPP6C mutations impair its ability to dephosphorylate and inactivate Aurora A, resulting in genomic instability, DNA damage, and micronucleation are early events contributing to cancer progression[189,190]. Expression of the PPP6C H114Y mutant, which has been observed twice in melanoma, in cells increases Aurora-A activity and disrupts chromatin and mitotic spindle organization[190]. The resultant mitotic spindle defects lead to chromosome instability and therefore DNA-damage and micronucleation. This chromosome instability, a hallmark and driver of cancer, suggests a role for PPP6C driver mutations in melanoma. Characterization of 12 other PPP6C mutants found 5 mutations increase Aurora A activation, 4 of which disrupts binding to the PPP6R3 subunit[189]. A subset of PPP6C mutations sensitize cells to Aurora A inhibitors independently of their effect on Aurora A activation.

Work characterizing melanoma-associated PPP6C mutations is limited and inconsistent. Aside from the described studies of PPP6C mutants, PPP6C loss has been investigated for roles in tumorigenesis. Loss of PPP6C promotes oncogenic RAS driven tumors in mouse keratinocytes[179,193] and in drosophila[194]. Further work is required for better understanding of the molecular mechanisms underlying the role of PPP6C mutations in melanoma. As studies point to distinct consequences of different PPP6C

mutations, the progress in identifying diverse functions of PP6 suggest the involvement of several mechanisms.

1.5 Statement of Purpose

The incidence of malignant melanoma has been rapidly increasing worldwide with a 270% increase over the past 30 years in the United States[195]. Despite important advances in understanding the aberrant signaling pathways driving melanoma tumorigenesis, current treatment options, including targeted therapies and immunotherapies, rarely yield complete responses. With increasing knowledge of tumor heterogeneity and drug resistance mechanisms, it is clear that the oncogenic signaling network in melanoma is highly complex and has yet to be comprehensively understood. A more complete understanding of these signaling networks is necessary to develop more efficacious and durable therapeutic strategies.

Broadly, the purpose of this dissertation is to further advance our understanding of ERK MAPK signaling regulation and its deregulation in melanoma. The work described within this dissertation primarily focuses on MEK1/2, examining MEK regulation, response to MEK inhibition, and melanoma-associated mutations that alter MEK activity. PPP6C is identified in shRNA screens designed to identify novel modulators of MEKi response in $BRAF^{V600E}$ melanoma. Through comprehensive biochemical and cellular studies investigating the mechanism of PPP6C regulation of ERK signaling, PPP6C is established as a MEK phosphatase and therefore influences sensitivity to MAPKi. These findings support previous predictions of a tumor suppressor role for PPP6C in melanoma. Beyond the identification of a novel MEK phosphatase, melanoma-associated PPP6C and MEK1 mutations are characterized to better understand how these mutations alter oncogenic signaling and potentially contribute to melanoma progression and MAPKi response.

This dissertation further sheds light onto the complex regulatory mechanisms of

the ERK signaling network in melanoma involved in MEK and BRAF inhibitor response and identifies a novel role for PPP6C in a key oncogenic signaling pathway. By contributing to a more comprehensive understanding of the molecular mechanisms underlying MEK and BRAF inhibitor response, this work provides insight into the therapeutic limitations of targeted therapies.

CHAPTER 2: POOLED SHRNA SCREENS TO IDENTIFY GENES MEDIATING MEK INHIBITOR RESPONSE

2.1 Introduction

The RAF-MEK-ERK mitogen-activated protein kinase (MAPK) signaling cascade regulates essential cellular processes including cell proliferation, differentiation, and survival[23]. Deregulation of ERK signaling, typically through mutations in core pathway components or upstream regulators, is among the most frequent driver events in human cancer[196]. Malignant melanoma in particular is dependent upon hyperactivated ERK signaling. The dependence of melanomas on the ERK pathway fueled the development and approval of selective BRAF inhibitors (BRAFi) and MEK inhibitors (MEKi) with clinical efficacy in treating tumors harboring $BRAF^{V600E}$ mutations[197]. Unfortunately, responses to BRAFi and MEKi are almost invariably short-lived due to the development of acquired resistance[80]. While resistance to these agents can involve activation of alternative cell growth and survival pathways, it most commonly occurs through reactivation of the ERK pathway despite the continued presence of inhibitor[198]. Mechanisms underlying ERK pathway reactivation include acquisition of RAS or MEK mutations, BRAF amplification or alternative splicing, disruption of negative feedback regulation, and induction of receptor tyrosine kinases[101-104]. Understanding how tumor cells become resistant to BRAFi and MEKi can suggest additional therapeutic targets and thus contribute to the development of durable and more generally applicable cancer treatments. In addition, investigations into mechanisms of inhibitor resistance have provided insight into the basic wiring of the ERK pathway and how it participates in larger signaling networks.

Functional genetic screening strategies have been effective discovery tools for identifying new drug targets and biomarkers for drug response. The two technologies used in pooled loss-of-function screens, CRISPR and RNAi, yield robust and reliable results assessing large numbers of genes, even at genome-wide scale, simultaneously. shRNA screens were initially limited by noise due to off-target effects and inefficient gene

silencing. With the rapid development of CRISPR/Cas9 technology, which has a very low-incidence of off-target effects[199,200], CRISPR-based screening has quickly gained popularity and become the dominant genomic screening technology, seeming to outperform RNAi-based screening in terms of noise and consistency[201]. Increasing redundancy in shRNA libraries and use of validated shRNA for efficient knockdown has improved the reproducibility of shRNA screens. Parallel comparison of CRISPR and shRNA screens have demonstrated similar precision in detecting essential genes depending on the sgRNA and shRNA libraries used[201,202].

The choice of CRISPR or shRNA systems for a functional screen should depend on the research question or intended application of screen results with careful consideration of the limitations of each technology. For example, in the case of drug target discovery, knockdown in shRNA screens better mimics the inhibition of a target by a drug. shRNA screen results are representative of hypomorphic phenotypes. The knockdown of genes by shRNA demonstrates the phenotypic effects of partial losses-of-gene function depending on the knockdown efficiency of the specific shRNA hairpin. Another complicating factor is slow protein degradation or the discrepancy between mRNA transcript levels and protein levels, which would prevent loss-of-function phenotypes. CRISPR screen results are representative of true null phenotypes. The phenotypes resulting from complete knockout are not obscured by the effects from low levels of remaining protein expression from incomplete knockdown. This allows for high sensitivity from stronger phenotypes in CRISPR screens. However, this also makes it difficult to study the complexity of essential genes. The lethality of the knockout of these genes overpowers any non-survival-related functions.

These differences in shRNA and CRISPR screens likely contribute to their ability to detect distinct groups of genes related to specific cellular processes[202]. For example, gene sets related to RNA polymerase and the Mediator complex, which functions as a transcriptional co-activator, are found in shRNA screens but not CRISPR screens,

presumably because shRNA knockdown depends on continued transcription of the shRNA unlike with sgRNAs. In the case of some other gene sets unique to one type of screen, the cellular functions or signaling mechanisms governing this exclusivity are unclear.

Cell viability-based loss-of-function genetic screens can yield information on negative genetic selection and/or positive genetic selection in response to a given selection pressure such as an inhibitor. Negatively selected genes identify genes that when silenced gives cells a disadvantage in the conditions being studied. When interpreting screen results, the shRNA or sgRNA sequences targeting these genes are depleted from the cell population over the course of the screen. Negative selection is used to identify genes essential for survival or proliferation in the context of a given selection pressure, providing insight into synthetic lethal dependencies and context-specific genetic vulnerabilities. Genes identified under negative selection from drug treatment represent potential drug targets for combinatorial therapeutic strategies. Because negatively selected genes also include essential genes, understanding which genes are specific to the added selection pressure requires comparison to appropriate control conditions. Positively selected genes identify genes that when silenced gives cells a growth or survival advantage. The shRNA or sgRNA sequences targeting these genes are enriched in the cell population over the course of the screen These genes confer sensitivity to the selection pressure when expressed and therefore provide insight into potential mechanisms of drug resistance.

The emergence of BRAFi resistance in melanoma has prompted several genetic screens investigating BRAFi susceptibility. When comparing results from similar screens, whether they use the same inhibitor or the same cell line, there is often a divergence in genes-of-interest outside of essential genes due to the many variables involved in these large-scale screens, including context dependency of genetic interactions, library size and complexity, and inhibitor treatment conditions, just to name

a few[202]. COT, CDK6, BOP1, HAT1, and CUL3 have all been identified as mediators of BRAFi resistance in $BRAF^{V600E}$ melanoma in different screens[139,141,144,146], demonstrating that similar screens are able to identify unique physiologically relevant hits and produce non-redundant information.

BRAFi and MEKi combinations are the current standard of care for $BRAF^{V600E}$ melanoma but are limited by the onset of inhibitor resistance. While both BRAFi and MEKi block the same pathway, mechanisms involved in BRAFi and MEKi response and resistance in cells may differ as suggested by the longer progression-free survival with combination therapy and the additional increase in response rate to BRAFi upon acquiring MEKi resistance in BRAF melanoma patients in studies investigating treatment schedules[203]. MEK and $BRAF^{V600E}$ are individually regulated and exhibit different susceptibility to ERK pathway negative feedback and therefore can be limited by target-specific resistance in addition to pathway-specific resistance.

Functional genetic screens with MEKi have focused on RAS-driven cancers because of the limited efficacy of MAPKi in RAS mutant cancers[204-207]. Finding synthetic lethal interactions in the context of inhibited RAS effector pathways, such as the ERK signaling pathway, for combination therapeutic development is the major approach to treat the MAPKi-resistant majority population of RAS mutant cancers. With the FDA-approved use of MEKi in $BRAF^{V600E}$ melanoma, genetic screens investigating MEKi response in $BRAF^{V600E}$ melanoma can provide a better understanding of the specific genetic vulnerabilities of $BRAF^{V600E}$ melanoma in MEKi response.

2.1.1 MEKi Sensitivity Screen Design

To identify genes involved in modulating the response to MEKi, we performed a pooled shRNA screen in two $BRAF^{V600E}$ melanoma cell lines (Figure 2.1). We used a custom-made lentiviral library of 7,649 shRNAs targeting 817 genes encoding annotated protein and lipid kinases and phosphatases. This library targets genes encoding

theoretically druggable proteins. These proteins are able to bind drug-like molecules and in the case of many kinases have specific chemical inhibitors readily available for studies exploring combinatorial effects with MEKi. After transduction with the shRNA library, we harvested a portion of the cells for a start time reference sample (T_0) and divided the remaining cells into 5 populations, which were subsequently treated with either vehicle control or one of two concentrations of the clinical MEKi trametinib and selumetinib. MEKi concentrations were chosen to flank the approximate IC_{50} for inhibition of cell growth. Cells were propagated through 10 population doublings (T_1-T_{10}). The change in abundance of each shRNA under each growth condition was then determined by next-generation sequencing (Illumina HiSeq) following PCR amplification from genomic DNA preparations of cells collected at T_0 and T_{10}. We used RNAi gene enrichment ranking (RIGER) analysis[208] to rank genes based on the depletion or enrichment of their shRNAs in the screen.

"Depleted genes", which are genes whose hairpins are depleted from MEKi-treated cell populations over the course of the screen, will also be referred to as "drop-out hits". These negatively selected genes sensitize cells to MEK inhibition when knocked down. Not only do these drop-out hits offer insight into the signaling involved in MEKi response, they also represent potential drug targets for combinatorial therapy with MEKi. "Enriched genes", which are genes whose hairpins are enriched in MEKi-treated cell populations, will also be referred to as "drop-in hits". Downregulation or loss of these positively selected genes render the cells less sensitive to MEK inhibition. Similar to drop-out hits, these genes provide insight into MEKi response signaling but can also suggest potential drug resistance mechanisms and biomarkers for patient selection.

2.2 Results

2.2.1 501mel screens

Studies have described a largely cytostatic effect or growth delay with MEKi in

melanoma, both in cell culture and xenografts[199,209-211]. Tumor growth inhibition but not tumor regression in mouse xenograft models[199,211] translates to mostly stable disease and some partial responses to trametinib monotherapy in patients for improved progression-free and overall survival[76,212]. We selected 501mel cells, a $BRAF^{V600E}$ melanoma cell line that exhibits cytostatic responses to MEKi, hoping to gain insight into the signaling limiting MEK inhibition to cytostatic effects as opposed to cytotoxic effects in melanoma. High and low MEKi concentrations were selected to flank the IC_{50} for inhibition of cell growth (1 nM trametinib, 3.3 nM trametinib, 33 nM selumetinib, and 100 nM selumetinib). To assess the performance of both screen replicates, we evaluated the mean coverage of mapped reads per each shRNA which was 12,551 in the first replicate and 15,364 in the second replicate. This is well above the recommended read depth of 1,000 reads per shRNA for accurate hit identification. As expected for a $BRAF^{V600E}$ cell line, all 6 hairpins targeting BRAF in the shRNA library are depleted from all populations over time, providing an internal control for the screen (Figure 2.2).

To identify enriched genes of interest, I selected the top 50 ranking genes (top 6.1%) from RIGER analysis of each MEKi condition and removed overlapping top-ranking genes from the no drug condition. The overlap of enriched genes between MEKi conditions for each screen replicate was used to generate a list of drop-in genes of interest (Figure 2.3). Of these MEKi specific hits, Protein Phosphatase 6 Catalytic subunit (PPP6C), is the top ranked gene in 5 of 8 MEKi conditions across the two screen replicates and scored within the top 20 genes in all drug conditions (Figure 2.4). The hairpins targeting PPP6C are the most consistently enriched in the presence of MEKi and are generally depleted from the untreated culture (Figure 2.3, 2.5). These results suggest that PPP6C is required both for optimal cell growth and for a maximal cytostatic response to MEKi. Other potential drop-in genes of interest include Protein Phosphatase 1 Regulatory Subunit 12A (PPP1R12A or MYPT1), Phospholipid Phosphatase Related 3 (LPPR3), and Inositol Polyphosphate-4-Phosphatase Type 1A (INPP4A), all of which are

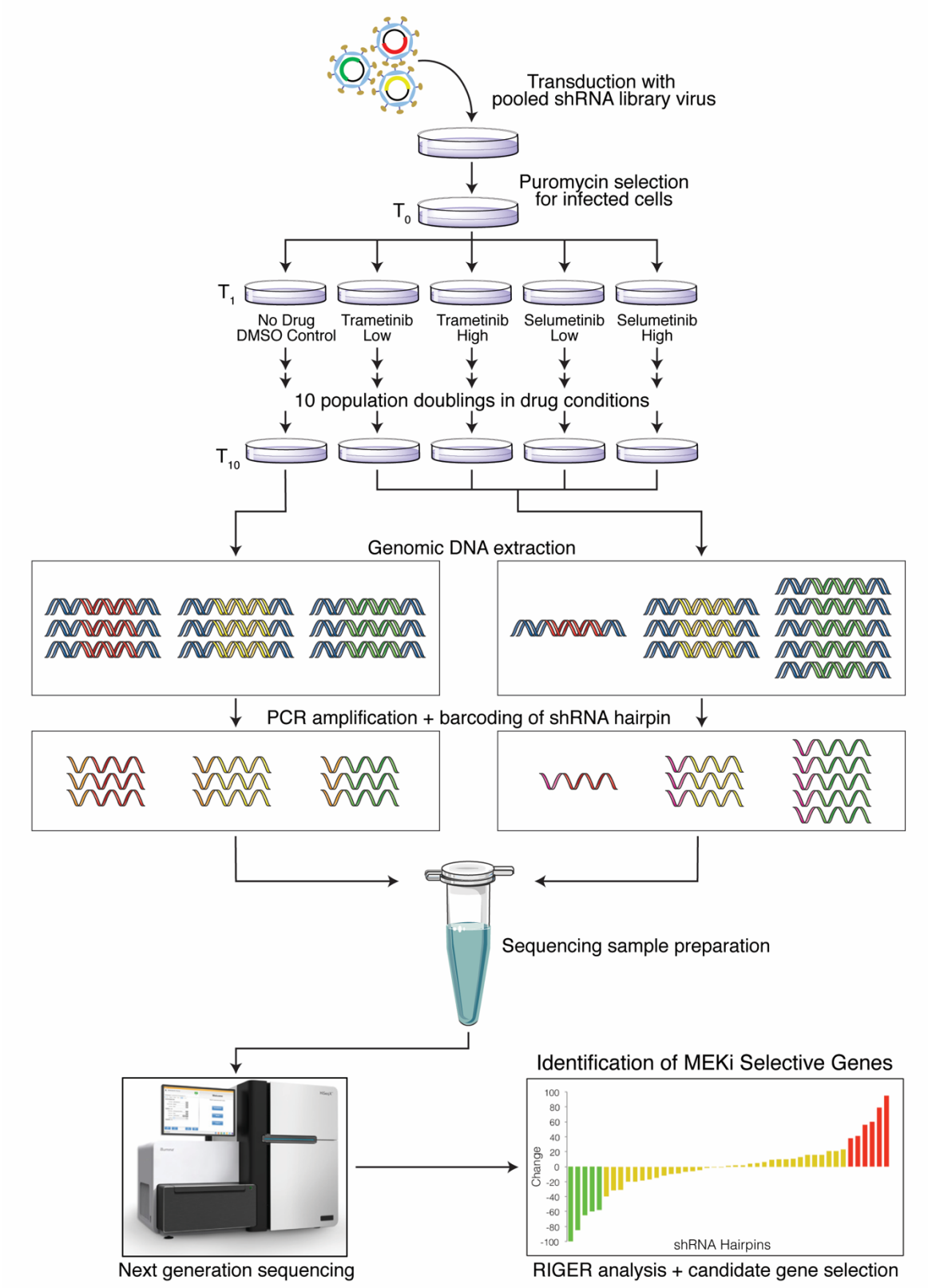

Figure 2.1 Schematic of the pooled shRNA MEKi sensitivity screen.

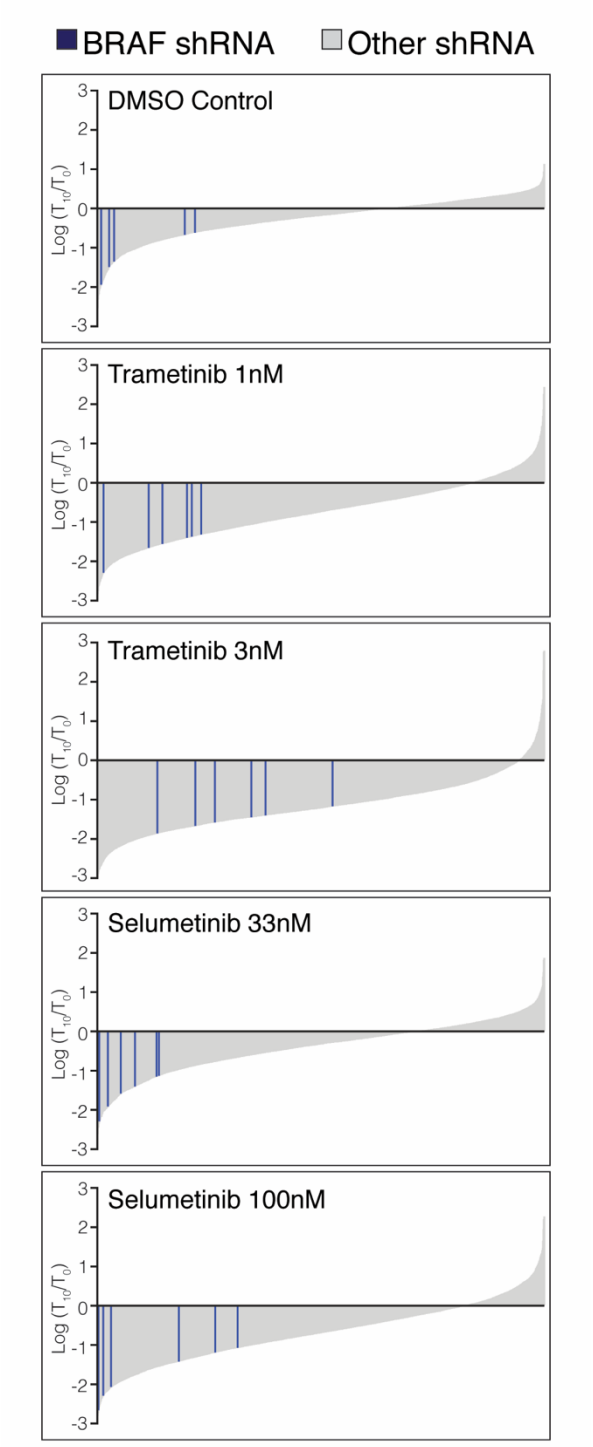

Figure 2.2 BRAF shRNA hairpins are depleted from all cell populations

Changes in all shRNA hairpins shown as $\log_2(T_{10}/T_0)$ from most depleted to most enriched for each drug condition. Bars representing shRNA hairpins targeting BRAF are shown in blue. All others are shown in grey.

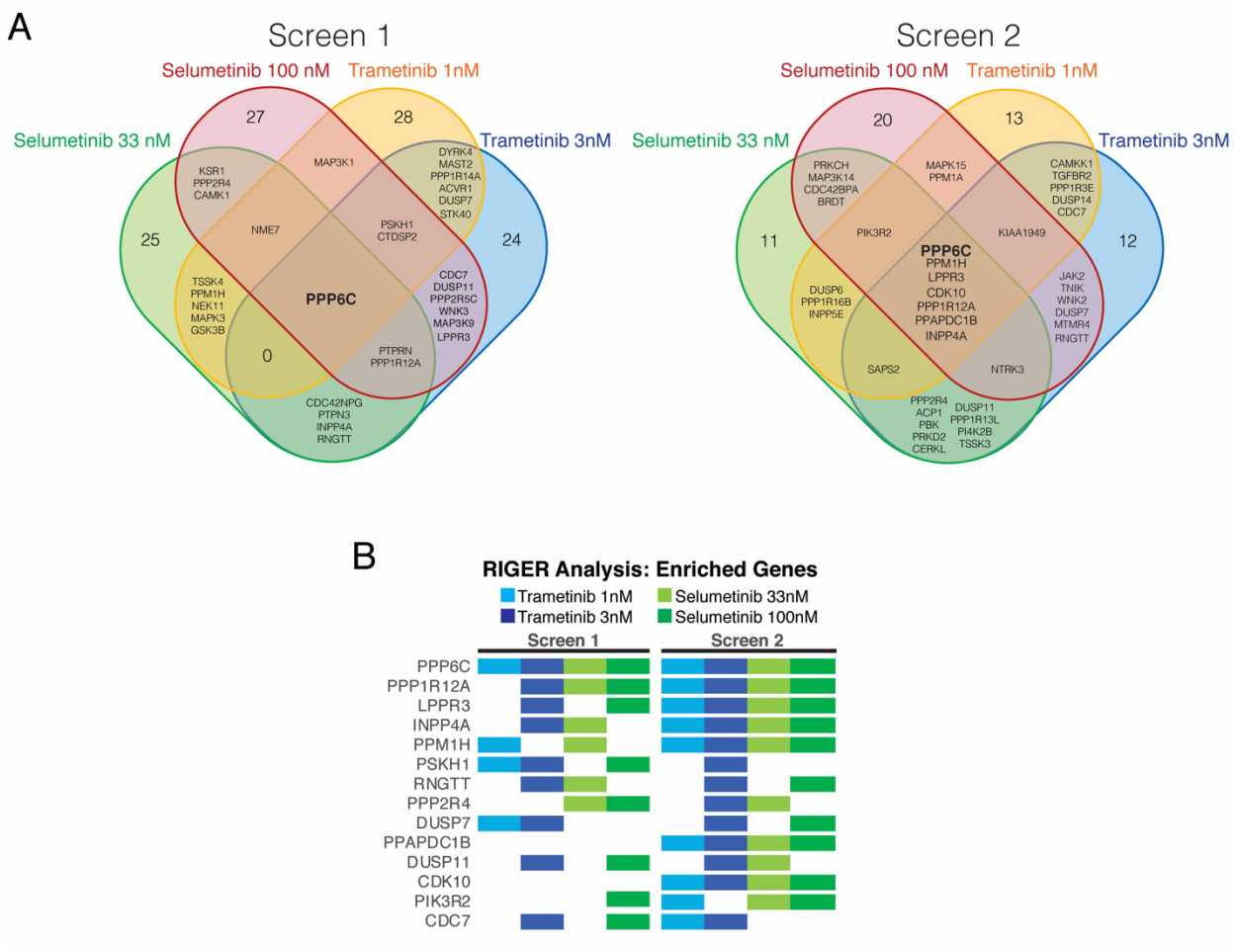

Figure 2.3 Top enriched genes for each drug condition from two replicates of the 501mel screen.

(A) Venn diagrams of top 50 enriched genes for each drug condition.

(B) The most consistently enriched genes across MEKi conditions. Colored boxes indicate the genes ranked in the top 50 enriched genes by RIGER for that drug condition not found in the DMSO control condition.

Screen 1

Rank	No Drug	Selumetinib		Trametintib	
		33nM	100nM	1nM	3nM
1	MAST4	PPP6C	PPP6C	PPAPDC2	PPP6C
2	PPP3R2	PPM1H	EGFR	PPM1H	TSSK3
3	CDK3	INPPL1	PPP1R12A	PPTC7	PTPRN
4	WNK4	TSSK3	TSSK3	MAP3K2	MAST2
5	TNK2	PPP1R3C	DUSP2	RPAP2	PPP3R1
6	PKMYT1	PPTC7	LPPR3	MST1R	CSK
7	CLK1	INPP4A	CDC7	NEK11	SCYL1
8	SAPS2	PPP1R12A	CDK10	MAP3K1	CAMK2A
9	PPP1R9B	CDC42BPA	PRKCZ	GSK3B	SMG1
10	CDK15	PPP2R4	NME1	SBF2	MLKL
11	RIPK3	PTPN4	DCLK3	SNRK	CDC7
12	FGFR2	PTPRF	PAK1	EPHA1	CABC1
13	SRPK3	MAP3K1	ADRBK1	RIPK3	WNK3
14	PLK3	CSNK1A1L	PPP2R4	PPP1R3E	PSKH1
15	PPTC7	CDK10	NTRK3	DUPD1	PBK
16	ACVR2A	CDK7	WNK3	PRKD1	C7orf16
17	PTPN12	FLT1	PBK	PPP6C	PTPN3
18	PRKD2	PRKX	PIK3R2	WNK1	PPP1R12A
19	PBK	TSSK4	PSKH1	ACVR1	EPHB6
20	CDK10	MAPK11	TESK1	BTK	PIK3C3

Screen 2

Rank	No Drug	Selumetinib		Trametintib	
		33nM	100nM	1nM	3nM
1	INPP5J	LPPR3	PPP6C	PPP6C	CDC7
2	PTPRN	PRKCH	PPP1R12A	PTPN2	PPP2R4
3	MAP3K11	PPP1R12A	PPM1H	INPP5J	PPP6C
4	PIK3C2G	PPP6C	SGPP2	SAPS2	LPPR3
5	PPM1E	INPP5J	INPP4A	PPP1R16B	ACP1
6	CDC14B	MAP3K14	LPPR3	INPP5E	PPAPDC1B
7	PTPN12	CERK	MAST1	CDK3	PPP4C
8	MTMR2	INPP4A	DUSP7	DUSP14	RPS6KA4
9	LPPR4	CDK10	PPAPDC1B	PTP4A3	RNGTT
10	RPAP2	PIK3R2	RNGTT	MTMR7	DUSP11
11	PPTC7	PPP2R4	PIK3R2	MAST1	PI4K2B
12	CERK	MAST1	JAK2	LPPR3	JAK2
13	RIPK3	CDC42BPA	PPM1A	DUSP6	MAST2
14	PTP4A3	PI4K2A	STK40	PPTC7	PPP1R12A
15	PTPRK	KDR	PRKY	PTK2B	PPP1R9B
16	MTMR10	GSK3A	PPP2R5C	PTPN20A	DUSP7
17	PPP1R7	RPAP2	PRKCH	PTPRF	NTRK3
18	PI4KB	DAPK2	INPP5D	PPM1B	MAST4
19	PTPN2	PI4K2B	MAP3K14	TAOK3	CDK10
20	TNK2	CERKL	CDK10	RPAP2	MTMR7

Figure 2.4 501mel Screen Rankings of Drop-in hits

The top 20 ranked enriched genes for each condition for 501mel screen replicates. PPP6C rankings are highlighted.

A

Screen 1 PPP6C Hairpin Rankings					
PPP6C Hairpin	No Drug	Trametinib		Selumetinib	
		1 nM	3 nM	33 nM	100 nM
TRCN0000002764	5971	182	63	19	14
TRCN0000002765	4721	949	26	16	123
TRCN0000002766	142	284	455	381	508
TRCN0000002767	6110	231	58	88	41
TRCN0000379835	5212	445	1416	25	38
TRCN0000379918	4223	646	395	884	22

Screen 2 PPP6C Hairpin Rankings					
PPP6C Hairpin	No Drug	Trametinib		Selumetinib	
		1 nM	3 nM	33 nM	100 nM
TRCN0000002764	5647	5	110	617	10
TRCN0000002765	3975	3	297	72	95
TRCN0000002766	302	24	79	69	108
TRCN0000002767	6140	745	61	560	2
TRCN0000379835	5423	2	3722	1217	1
TRCN0000379918	2810	1	3188	95	248

B

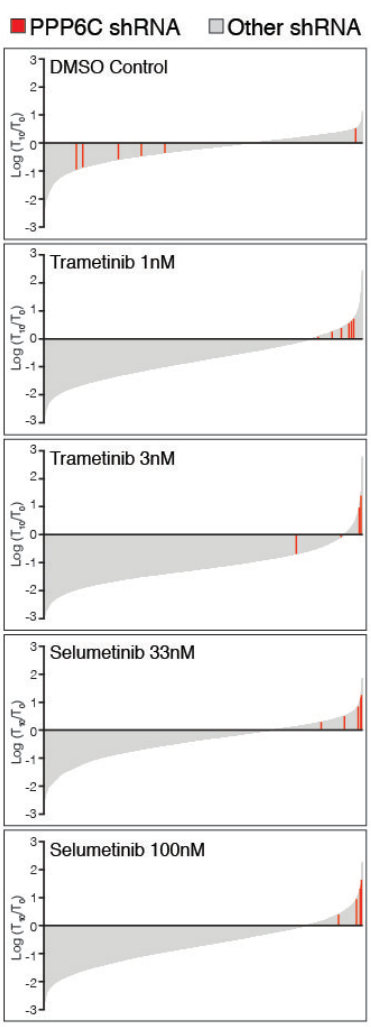

Figure 2.5 PPP6C shRNA hairpins are enriched in MEKi conditions

(A) Rankings for each of the 6 PPP6C hairpins out of the 7,649 shRNAs in the library are listed for each drug condition.

(B) Changes in all shRNA hairpins shown as $\log_2(T_{10}/T_0)$ from most depleted to most enriched for each drug condition. Bars representing shRNA hairpins targeting PPP6C are shown in red. All others are shown in grey.

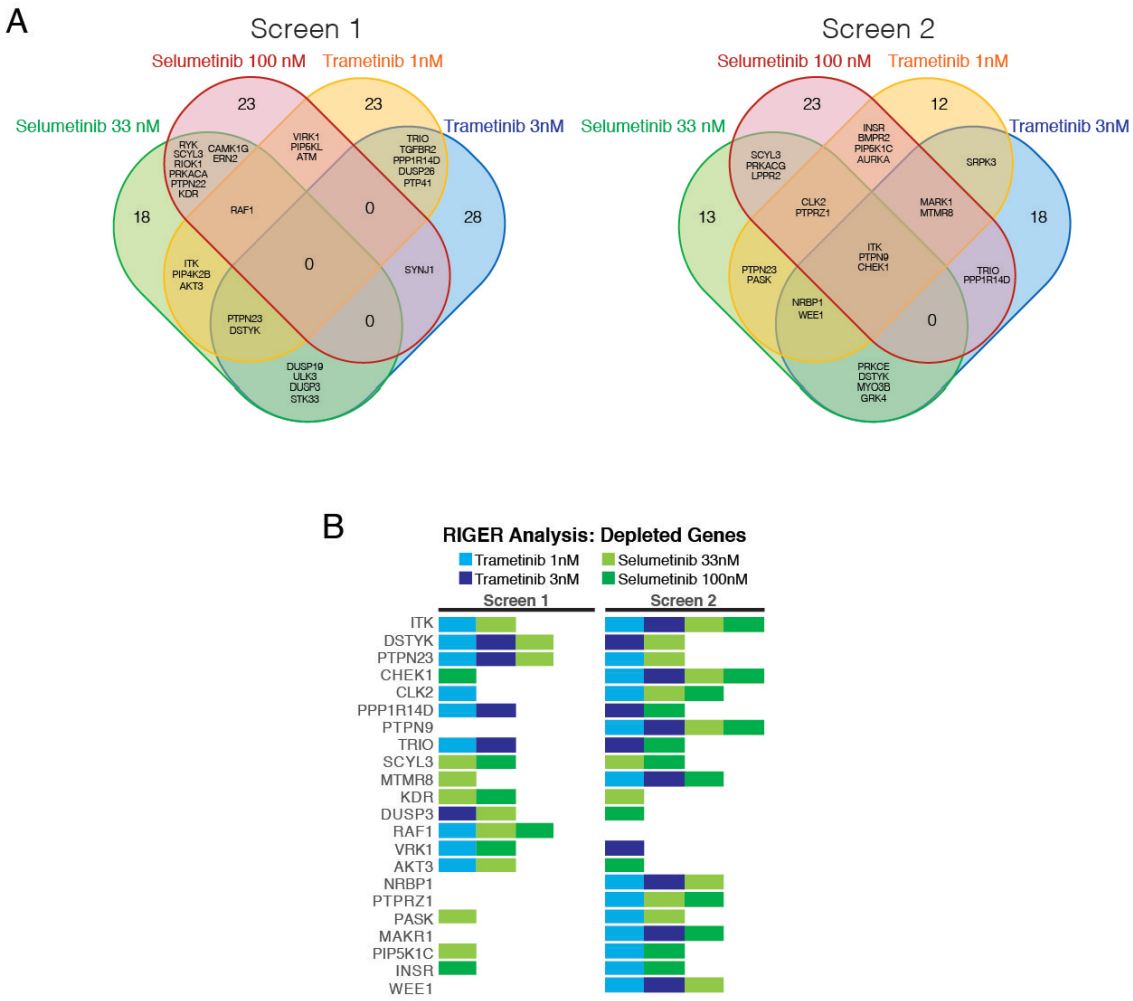

Figure 2.6 Top depleted genes for each drug condition from two replicates of the 501mel screen.

(A) Venn diagrams of top 50 depleted genes for each drug condition.

(B) The most consistently depleted genes across MEKi conditions. Colored boxes indicate the genes ranked in the top 50 depleted genes by RIGER for that drug condition not found in the DMSO control condition.

ranked as top drop-in hits in ≥ 5 of the 8 MEKi conditions (Figure 2.3, 2.4).

No genes are top drop-out hits in all 8 MEKi conditions across both screen replicates (Figure 2.6A). Of note, CRAF (RAF1) is ranked as a top gene in 3 MEKi conditions (Figure 2.6B). This is consistent with its role activating the ERK signaling pathway through the phosphorylation of MEK. CRAF upregulation is a known MAPKi resistance mechanism (Figure 1.3). ITK, DSTYK, PTPN9, and CHEK1 are top drop-out hits in ≥ 5 of the 8 MEKi conditions (Figure 2.6B). ITK, interleukin-2-inducible T-cell kinase, is a top ranked gene in the 2 low MEKi concentrations (1nM trametinib and 33nM selumetinib) of the first screen replicate and all 4 MEKi conditions of the second screen replicate.

2.2.2 Yugen8 Screens

We selected a patient derived $BRAF^{V600E}$ melanoma cell line, Yugen8, for our next set of MEKi screens. Compared to 501mel cells, Yugen8 cells are more sensitive to MEKi and exhibit cytotoxic responses. The MEKi IC_{50} flanking concentrations selected for these screens were 0.03 nM trametinib, 0.1 nM trametinib, 8 nM selumetinib, and 25 nM selumetinib. The mean coverage of mapped reads per each shRNA was 11,376 in the first replicate and 21,405 in the second replicate.

The top ranked genes in the Yugen8 screens were not as consistent between the two screen replicates as they were in the 501mel screens (Figures 2.7, 2.8). Of the drop-in hits, Kinase Suppressor of Ras1 (KSR1) was the most consistent, ranking in the top 50 genes in all 4 MEKi conditions of one screen replicate (Figure 2.7B). However, it is not ranked in any MEKi conditions in the other replicate. Other drop-in hits only rank in 3 or fewer of the 8 MEKi conditions. Of the drop-out hits, Diacylglycerol Kinase Epsilon (DGKE) and Nuclear Receptor Binding Protein 1 (NRBP1) are both ranked as top drop-in hits in 5 of the 8 MEKi conditions (Figure 2.8B). Six other genes are top ranked in 4 of the 8 MEKi conditions.

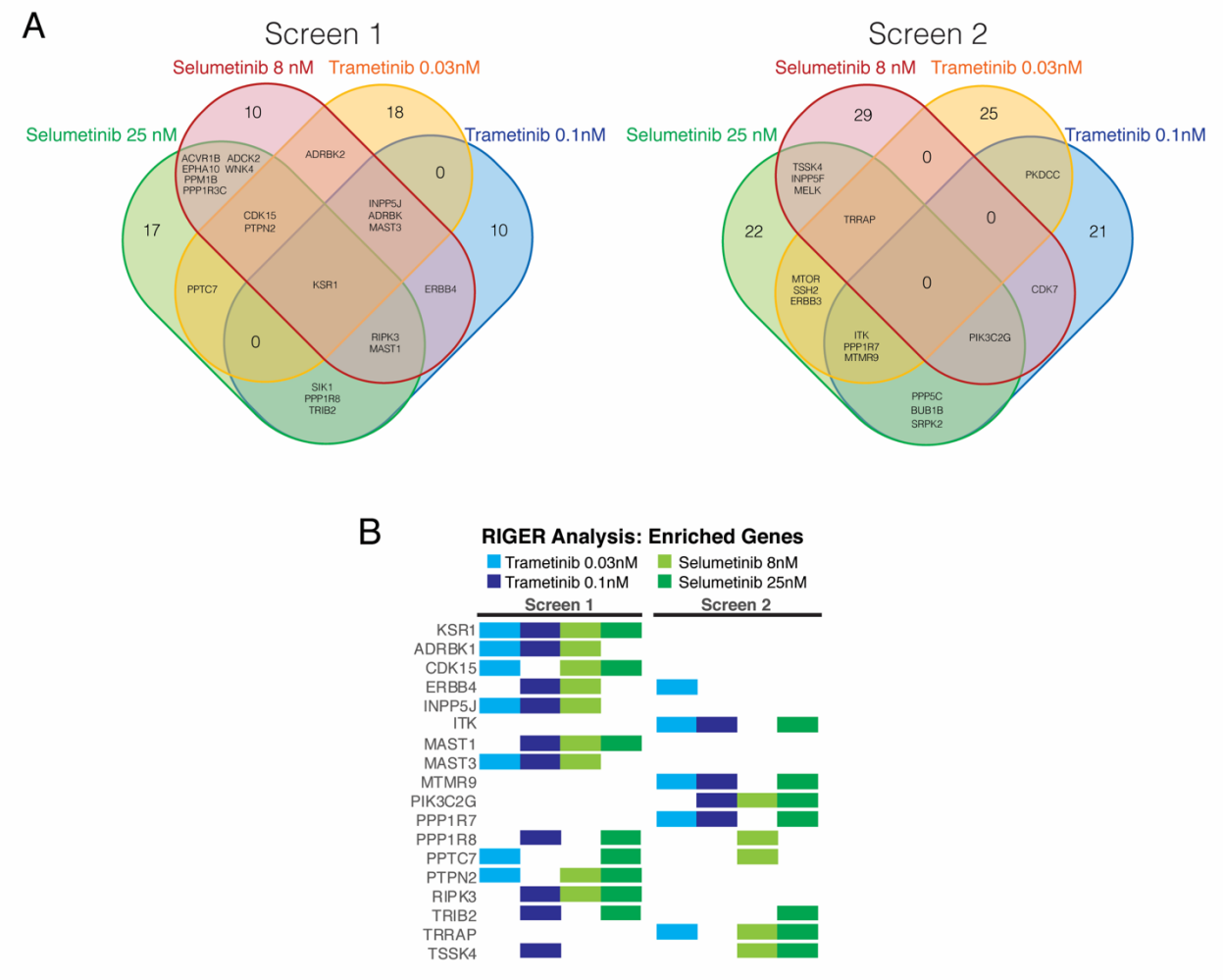

Figure 2.7 Top enriched genes for each drug condition from two replicates of the Yugen8 screen.

(A) Venn diagrams of top 50 enriched genes for each drug condition.

(B) The most consistently enriched genes across MEKi conditions. Colored boxes indicate the genes ranked in the top 50 enriched genes by RIGER for that drug condition not found in the DMSO control condition.

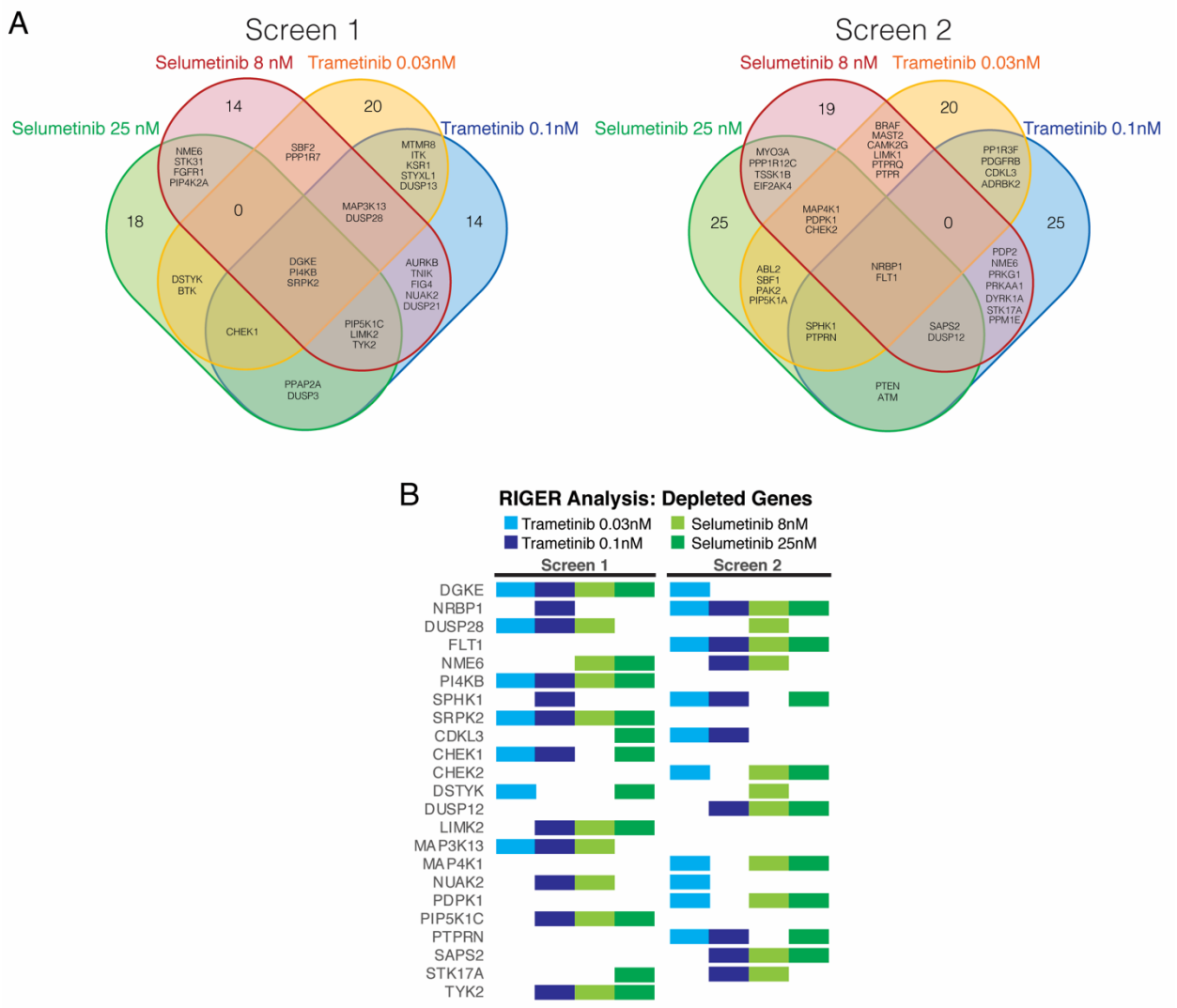

Figure 2.8 Top depleted genes for each drug condition from two replicates of the Yugen8 screen.

(A) Venn diagrams of top 50 depleted genes for each drug condition.

(B) The most consistently depleted genes across MEKi conditions. Colored boxes indicate the genes ranked in the top 50 depleted genes by RIGER for that drug condition not found in the DMSO control condition.

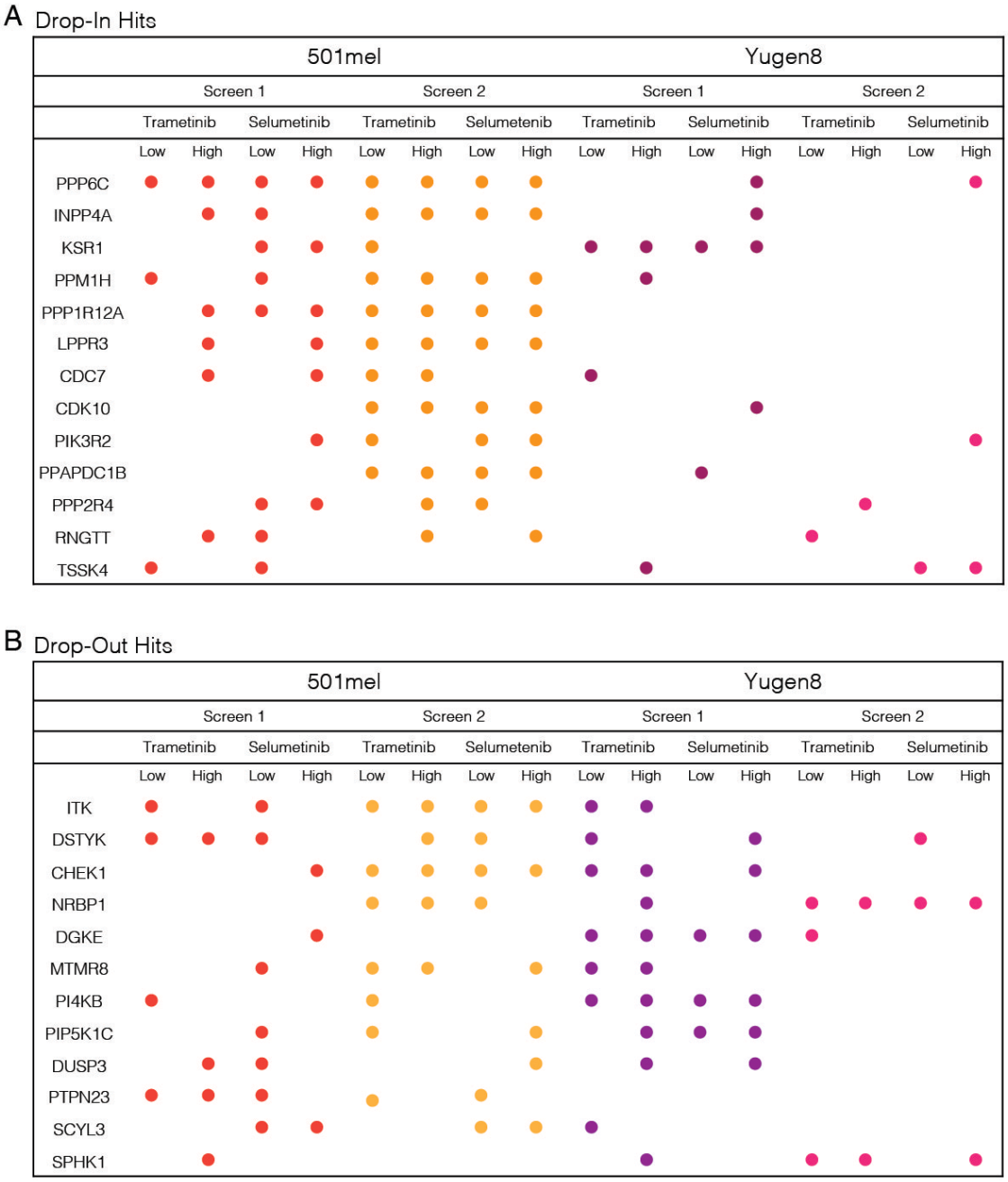

Figure 2.9 Top ranked genes from all screens.

(A) The most consistent drop-in genes across MEKi conditions. Colored circles indicate the genes ranked in the top 50 enriched genes by RIGER for that drug condition not found in the DMSO control condition.

(B) The most consistent drop-out genes across MEKi conditions. Colored circles indicate the genes ranked in the top 50 depleted genes by RIGER for that drug condition not found in the DMSO control condition.

2.2.3 Validation of Screen Hits

PPP6C Validation

The most consistent hit among shRNA screens with the 501mel cell line and the patient-derived Yugen8 cell line is PPP6C (Figure 2.9A). PPP6C ranks as a top gene in 10 MEKi conditions of 16 total MEKi conditions across both replicate screens of both cell lines.

To confirm a role for PPP6C as a factor modulating sensitivity to MEKi, 501mel cells were transduced with non-targeting control shRNA (shCTRL) or one of two independent shRNAs (shPPP6C-1, shPPP6C-2) that efficiently decrease PPP6C expression. PPP6C knockdown caused modest but consistent rightward shifts to MEKi dose responses curves, increasing IC_{50} values for growth inhibition by trametinib and selumetinib (Figure 2.10A). In clonogenic assays, cells transduced with control shRNA exhibited dose-dependent growth inhibition by both MEKi as anticipated (Figure 2.10B). PPP6C knockdown alone substantially decreased cell growth, yet this growth defect was partially reversed in the presence of low concentrations of MEKi. To further verify that PPP6C regulates ERK signaling, we generated clonal PPP6C knockout 501mel lines by CRISPR/Cas9-mediated gene disruption (Figure 2.11). Notably, we were unable to expand $PPP6C^{-/-}$ clones unless we supplemented the growth media with a low concentration of the MEKi trametinib. PPP6C knockout clones also exhibited decreased sensitivity to MEKi but with more pronounced rightward shifts to MEKi dose responses curves (Figure 2.12A). Also consistent with PPP6C knockdown, PPP6C knockout decreased cell growth in clonogenic assays which is reversible with similar as well as higher concentrations of trametinib (Figure 2.12B). These observations verify that PPP6C silencing renders 501mel cells less sensitive to the cytostatic effects of MEKi.

The results in these validation studies are consistent with the behavior of PPP6C shRNA hairpins in the 501mel screens, demonstrating the capability of these shRNA screens to identify a verifiable positive modulator of MEKi response. Additional work

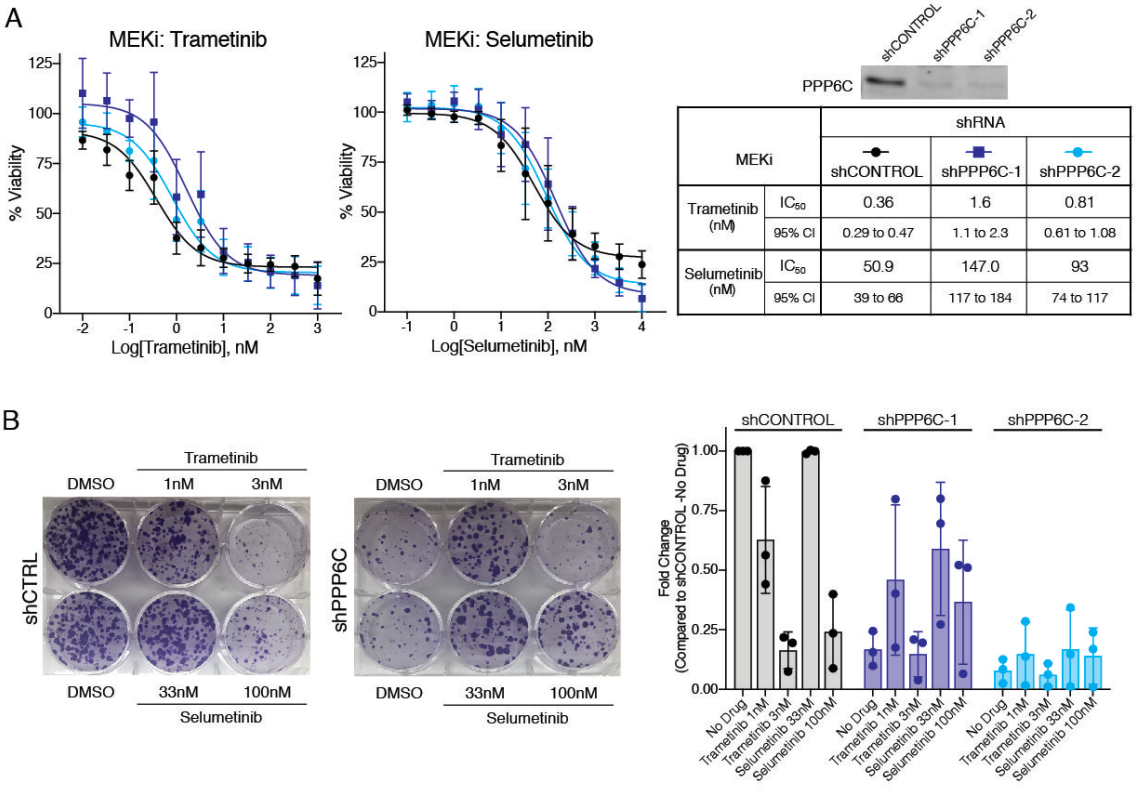

MEKi		shRNA shCONTROL	shPPP6C-1	shPPP6C-2
Trametinib (nM)	IC_{50}	0.36	1.6	0.81
	95% CI	0.29 to 0.47	1.1 to 2.3	0.61 to 1.08
Selumetinib (nM)	IC_{50}	50.9	147.0	93
	95% CI	39 to 66	117 to 184	74 to 117

Figure 2.10 shRNA knockdown of PPP6C reduces cell growth and MEKi sensitivity

(A) 501mel cell lines stably expressing control shRNA (shCTRL) or PPP6C-targeting shRNA (shPPP6C-1, shPPP6C-2) were treated for 72 hours with increasing concentrations of trametinib or selumetinib. Cell viability was detected by alamarBlue reagent and normalized to a no drug control for each cell line. Dose response curves for shCTRL (black), shPPP6C-1 (dark blue), and shPPP6C-2 (light blue) are shown. MEKi IC_{50} values and 95% confidence intervals are listed in the table.

(B) shCTRL, shPPP6C-1, and shPPP6C-2 expressing 501mel cells were cultured in DMSO or the indicated concentration of trametinib or selumetinib for 2 weeks in colony forming assays. Colonies were stained with crystal violet. Clonogenic growth was analyzed by ColonyArea in ImageJ. Quantification was normalized to $PPP6C^{+/+}$, no drug. Mean values ± SD are shown, $n = 3$.

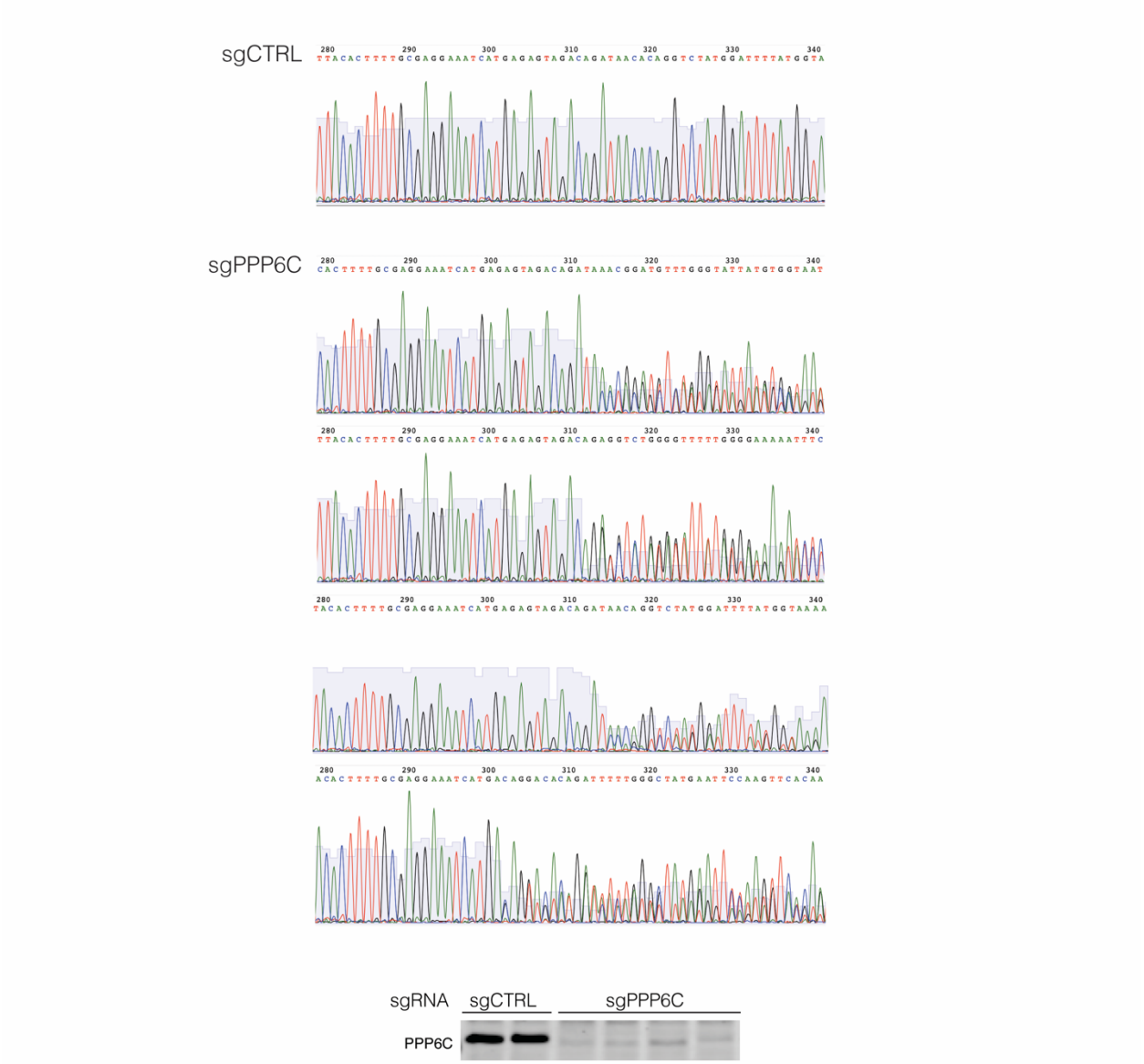

Figure 2.11 PPP6C CRISPR/Cas9 knockout cell lines

Sanger sequencing chromatograms for PPP6C$^{+/+}$ and PPP6C$^{-/-}$ clonal 501mel cell lines generated by CRISPR/Cas9. Immunoblot confirming PPP6C loss in PPP6C$^{-/-}$ 501mel cell lines is shown.

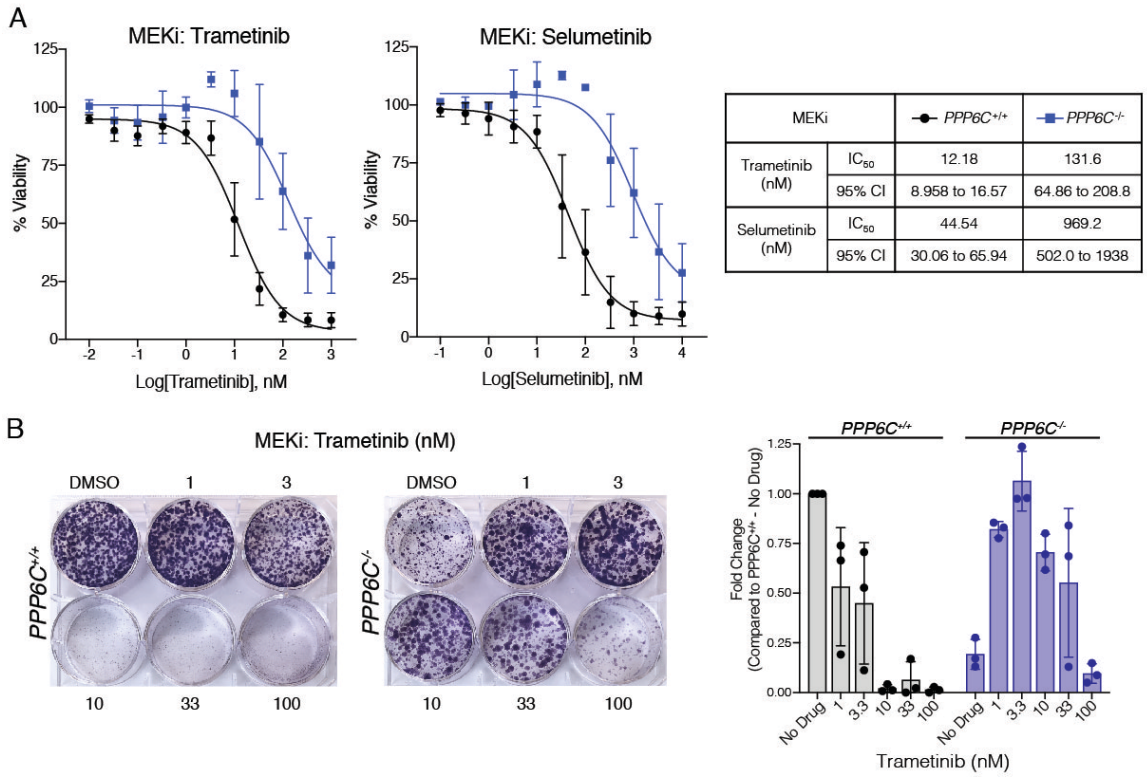

MEKi		PPP6C+/+	PPP6C-/-
Trametinib (nM)	IC_{50}	12.18	131.6
	95% CI	8.958 to 16.57	64.86 to 208.8
Selumetinib (nM)	IC_{50}	44.54	969.2
	95% CI	30.06 to 65.94	502.0 to 1938

Figure 2.12 CRISPR/Cas-9 mediated knockout of PPP6C reduces cell growth and MEKi sensitivity

(A) $PPP6C^{+/+}$ and $PPP6C^{-/-}$ 501mel cells were treated for 72 hours with increasing concentrations of trametinib or selumetinib. Cell viability was detected by alamarBlue reagent and normalized to a no drug control for each cell line. MEKi IC_{50} values and 95% confidence intervals are listed in the table.

(B) $PPP6C^{+/+}$ and $PPP6C^{-/-}$ 501mel cells were cultured in media containing DMSO or the indicated concentration of trametinib for 2 weeks in colony forming assays. Colonies were stained with crystal violet. Clonogenic growth was analyzed by ColonyArea in ImageJ and normalized to $PPP6C^{+/+}$, no drug. Mean values ± SD are shown, n = 3.

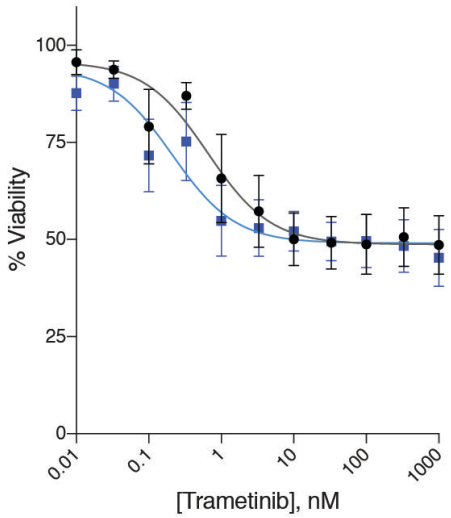

Inhibitors	IC_{50}	95% CI
Trametinib (nM)	0.65	0.45 to 0.94
Trametinib (nM) + 1μM Ibrutinib	0.21	0.18 to 0.32

Figure 2.13 ITK inhibition sensitizes cells to MEKi

501mel cells were treated for 72 hours with increasing concentrations of trametinib with (blue) or without (black) 1uM ibrutinib. Cell viability was detected by alamarBlue reagent and normalized to a no drug control for each cell line. IC_{50} values and 95% confidence intervals are listed in the table, $n = 2$.

describing a role for PPP6C in ERK signaling and MAPKi response is reported in Chapter 3 of this dissertation.

ITK Validation

ITK is one of 3 genes that are top enriched genes in 8 MEKi conditions across all four screens (Figure 2.9B). ITK is normally considered an immune cell-specific protein but has been found to be aberrantly expressed in metastatic melanoma[213]. In T-cell receptor (TCR) signaling, ITK is a downstream effector of TCR stimulation and mediates the activation of ERK[214,215]. The identification of ITK as a drop-out hit suggests inhibition of ITK may potentiate the cytostatic or cytotoxic effects of MEK inhibition in cells. Ibrutinib is a clinical inhibitor of BTK, but also potently inhibits ITK and other tyrosine kinases. To investigate ITK as a sensitizer to MEK inhibition, 501mel cells were treated with Ibrutinib in combination with trametinib in pilot assays. The addition of 1uM ibrutinib shifts trametinib dose response curves to the left, decreasing the IC_{50} value by 3-fold for growth inhibition by trametinib (Figure 2.13). Ibrutinib made cells more sensitive to the cytostatic effects of trametinib, but it did not sensitize them to potential cytotoxic effects in 501mel cells. The sensitization to MEK inhibition may be mediated by the inhibition of Ibrutinib's many targets Additional work is necessary to investigate and optimize MEKi and ITK inhibitor concentrations for use in combination as well as to elucidate a specific mechanism for this effect. These preliminary experiments confirm ITK loss or inhibition promotes MEKi response as seen in our screens.

2.3 Discussion

We demonstrate the identification of modulators of MEKi sensitivity using a loss-of-function screening strategy in $BRAF^{V600E}$ melanoma cells. Our screens generated an abundance of information including insight into potential drug targets, previously unappreciated signaling factors regulating the ERK signaling pathway, and candidate

genes identified in similar functional genetic screens investigating MAPKi response.

The use of the top 50 ranked genes to select hits only considers the top 6.1% of genes targeted by our shRNA library. This cutoff is stringent and likely results in the exclusion or lower ranking of relevant genes. Although a less conservative cutoff may allow for the identification of more candidate genes, we were able to validate the top drop-in and drop-out genes identified in our screens.

PPP6C is a clear gene of interest, given its top rankings in the majority of MEKi concentrations. In validation studies, PPP6C knockdown with shRNA and knockout with CRISPR/Cas9-mediated gene disruption decreased sensitivity of 501mel cells to MEKi. PPP6C knockdown and knockout cells exhibit impaired growth and proliferation compared to control cells which is partially reversed with MEKi treatment. This behavior mirrors what we observed in our screens where PPP6C hairpins were depleted from drug free cell populations but enriched in MEKi-treated cell populations. Our comprehensive investigation of PPP6C in ERK signaling in melanoma is described in the next chapter.

ITK, the top drop-out hit, is known to activate the ERK signaling pathway specifically in TCR signaling but has not been investigated in other signaling contexts. The expression of ITK in benign melanocytic lineage cells is low as expected but is unexpectedly highly elevated in metastatic melanoma tissue samples[213]. ITK inhibition in a $BRAF^{V600E}$ melanoma mouse model and a panel of melanoma cell lines, decreases cell proliferation and migration. In a T lymphocyte cell line, treatment with several ITK inhibitors inhibit MEK phosphorylation to varying degrees[216]. We demonstrate combining a ITK inhibitor with a MEKi has a stronger cytostatic effect in $BRAF^{V600E}$ melanoma cells compared to MEKi alone. Our findings in combination with other indications of ITK involvement in ERK signaling or melanoma progression support the additional exploration of ITK in these roles.

Cursory review of other top ranked genes suggests potentially interesting involvement of these candidate genes in MAPKi response or melanoma signaling. KSR1,

the top enriched gene in the Yugen8 screens (Figure 2.7B), is an interesting hit considering its role as a scaffold for the ERK signaling pathway. KSR1 enhances ERK1/2 signaling activation by binding ERK pathway components and regulating the efficiency of their interactions[217]. Recently solved crystal structures and functional studies show trametinib binds MEK-KSR complexes promoting MEK engagement of KSR1/2 and disrupting MEK activating interactions with RAFs[218]. This unexpected involvement of KSR in the mechanism of action for MEKi is supported by our identification of KSR1 as a drop-in hit. The loss of KSR1-MEK complexes with KSR1 knockdown likely hampers the ability of MEKi to bind and inhibit MEK.

A mutation in DSTYK, a top drop-out hit in our screens (Figure 2.9B), has been shown to activate ERK signaling to promote cell migration and invasion, which is inhibited with MEKi treatment[219]. DSTYK is upregulated in metastatic melanoma cell lines[220] and metastatic colorectal cancer tumor samples[221]. DSTYK loss inhibits FGF-stimulated ERK phosphorylation in human embryonic kidney cells (HEK)[222]. This is all in line with a potential role for DSTYK in positively regulating ERK signaling or inhibiting MAPKi response.

INPP4B, a top ranked drop-in gene (Figure 2.9A), has been described to have tumor suppressor functions in breast cancer and melanoma through its role as a negative regulator of PI3K-AKT signaling[223-225]. INPP4B expression is reduced in melanoma tumor samples compared to nevi and expression levels are only moderately correlate with AKT activation. The impact of INPP4B on the ERK signaling pathway or MAPKi response has not been explored, but a role for INPP4B in regulating both PI3K-AKT signaling and ERK signaling is possible either independently or through crosstalk between the pathways.

These speculations for possible roles for these genes-of-interest in modulating MAPKi sensitivity or melanoma progression are premature given the need for additional studies to validate their identification in our screens. The identification of these genes

may be due to off-target effects of shRNAs or other variables effecting the accuracy of these screens. However, our follow-up investigation into PPP6C and its involvement in ERK signaling establish PPP6C as a previously unknown MEK phosphatase (Chapter 3).

CHAPTER 3: PPP6C REGULATION OF ERK SIGNALING IN MELANOMA

3.1 Introduction

Because proper control of the ERK pathway is important to normal physiology, the core cascade is positioned within a complex network involving extensive feedback and crosstalk regulation[23]. By counteracting regulatory phosphorylation events, protein phosphatases play key roles in controlling the magnitude and duration of ERK signaling, and their dysregulation can contribute to disease and influence inhibitor sensitivity. For example, ERK signaling induces expression of dual-specificity MAPK phosphatases (DUSPs), which dephosphorylate and inactivate ERK[226]. Disruption of this negative feedback loop through deletion or downregulation of ERK-selective DUSPs has been reported in some tumors and is associated with more advanced disease and poor patient prognosis[227-230]. Protein phosphatases also have important roles in positively regulating ERK signaling. For example, the tyrosine phosphatase SHP2 is important for relaying signals from receptor tyrosine kinases to RAS GTPases, and SHP2 inhibitors are currently in development as cancer therapeutics[231]. In addition, the MRAS-SHOC2-PP1 complex dephosphorylates an inhibitory site on RAF and mediates ERK pathway reactivation induced by MEKi in KRAS mutant pancreatic and lung cancers[206,232]. Germline gain-of-function mutations in SHP2, MRAS and SHOC2 are a cause of developmental disorders termed RASopathies that are characterized by hyperactive ERK signaling[233]. Protein phosphatase 2A (PP2A) can promote ERK signaling by dephosphorylating inhibitory feedback phosphorylation sites on RAF and the ERK pathway scaffold KSR1[234]. While these phosphatases regulating RAS, RAF and ERK have established roles in normal and pathological signaling, less is known about phosphatases regulating MEK, the central component of the cascade. PP2A was initially identified as a MEK phosphatase in vitro and in non-transformed monkey kidney CV-1 cells[235,236]. However, other studies have suggested that PP2A restrains oncogenic MAPK signaling primarily through direct dephosphorylation of ERK[237].

We identified PPP6C as a gene modulating the response of $BRAF^{V600E}$ melanoma cell lines to MEKi in shRNA screens investigating MEKi sensitivity (Chapter 2, Figure 2.9A). Loss of PPP6C appears to decrease sensitivity to the MEKi trametinib and selumetinib. Presumptive loss-of-function melanoma-associated mutations in PPP6C has piqued interest in PPP6C potentially having a key role in melanoma. However, the specific substrates of PPP6C that contribute to melanoma have not been fully elucidated, although hyperphosphorylation of Aurora A due to PPP6C loss been proposed as an early event in melanoma formation[189,190]. Interestingly, PPP6C has not previously been identified as a regulator of ERK signaling. In this chapter, we establish PPP6C as a MEK phosphatase and negative regulator of ERK signaling. We explore the involvement of PPP6C in melanoma signaling and MAPKi response and how melanoma-associated mutations may disrupt these functions.

3.2 Results

3.2.1 PPP6C negatively regulates ERK signaling

In our validation studies (Chapter 2.2.3), PPP6C knockdown and knockout not only decreases sensitivity to the MEKi, but also decreases overall cell growth in the absence of MEKi (Figure 2.10B, 2.12B). We suspected that loss of PPP6C led to ERK pathway hyperactivation, as this phenomenon can underlie inhibitor resistance and cause growth suppression[238,239]. Indeed, we observed that silencing of PPP6C in 501mel cells elevated the levels of activating phosphorylation of ERK1/2 and MEK1/2 (Figure 3.1A). Cells expressing shPPP6C required higher concentrations of inhibitor to reduce MEK and ERK phosphorylation to levels seen in control cells (Figure 3.1B), likely explaining why PPP6C knockdown decreases sensitivity to MEKi. Likewise, low concentrations of MEKi attenuated hyperactivation of ERK signaling that is presumably toxic to these cells, explaining why decreasing PPP6C expression reduces growth. Furthermore, the ability of low concentrations of MEKi to rescue growth suggests that PPP6C is required for optimal growth of 501mel cells largely because it restrains ERK

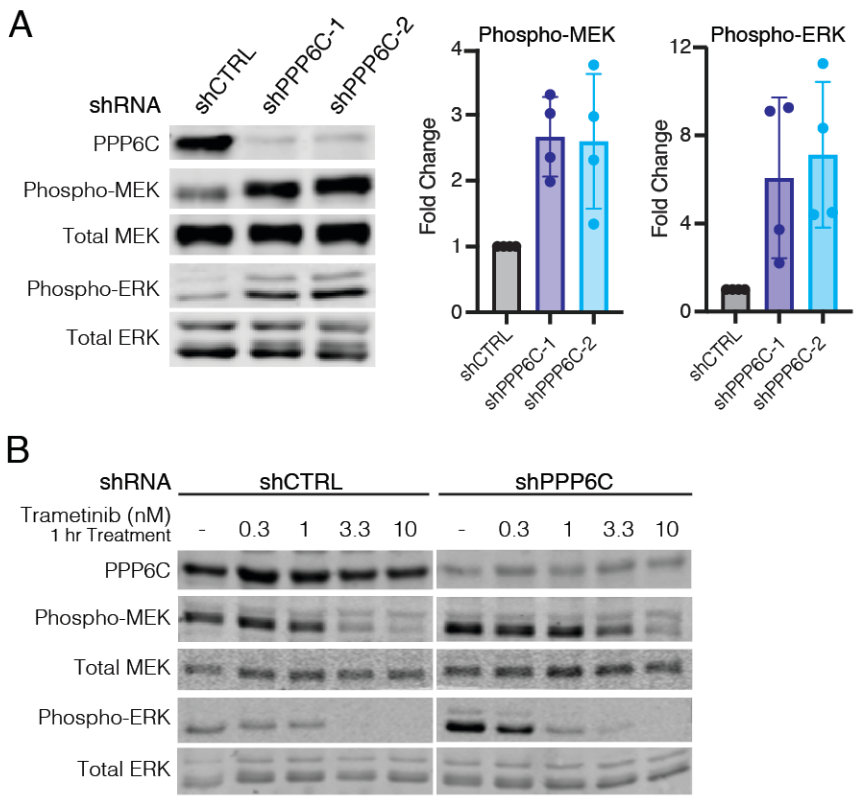

Figure 3.1 PPP6C negatively regulates ERK signaling and promotes MEKi response

(A) 501mel cells stably expressing shCTRL, shPPP6C-1, and shPPP6C-2 were lysed and assessed by immunoblot for levels of phosphorylated and total MEK and ERK. Quantification of Phospho/Total MEK and ERK was normalized to shCTRL. Data are represented as mean ± SD, n = 4.

(B) shCTRL and shPPP6C expressing 501mel cells were treated with the indicated concentrations of trametinib for 1 hour and lysed. Phosphorylated and total levels of MEK and ERK were detected by immunoblot.

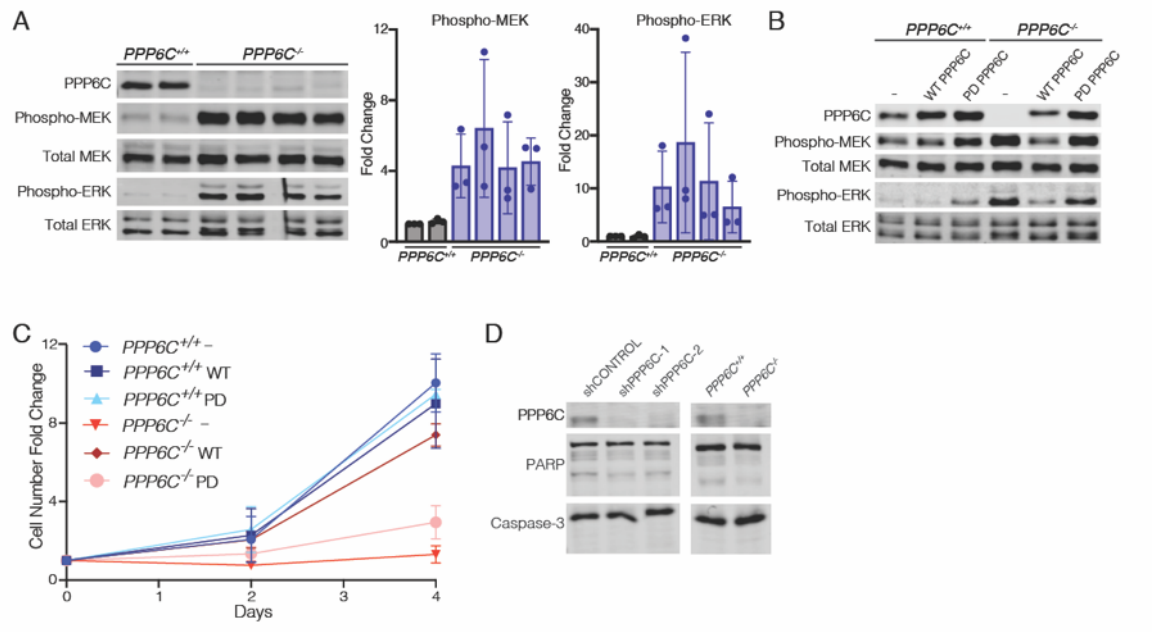

Figure 3.2 PPP6C negatively regulates ERK signaling and promotes cell proliferation

(A) PPP6C$^{-/-}$ 501mel cell lines were established by CRISPR/Cas9. PPP6C$^{+/+}$ and PPP6C$^{-/-}$ cell lines were lysed and assessed by immunoblot for levels of phosphorylated and total MEK and ERK. Quantification of Phospho/Total MEK and ERK was normalized to PPP6C$^{+/+}$. Data are represented as mean ± SD, n = 3.

(B) PPP6C$^{+/+}$ and PPP6C$^{-/-}$ 501mel cells stably expressing WT PPP6C, phosphatase inactive PPP6C^{D84N} (PD), or GFP (-) as a control were lysed and assessed by immunoblot for phosphorylated and total MEK and ERK.

(C) Cell proliferation was measured by cell counting for PPP6C$^{+/+}$ and PPP6C$^{-/-}$ cells expressing GFP, WT PPP6C, or PD PPP6C. Mean values ± SD are shown, n = 2.

(D) shCTRL, shPPP6C-1, and shPPP6C-2 expressing 501mel cells and PPP6C$^{+/+}$ and PPP6C$^{-/-}$ 501mel cells were lysed and assessed by immunoblot for full length and cleaved Caspase-3 and PARP. Representative blots shown, n = 3

signaling. The complete loss of PPP6C in the PPP6C$^{-/-}$ clonal cell lines described in 2.2.3 (Figure 2.11) resulted in an even more pronounced increase in MEK and ERK phosphorylation than seen with partial loss of PPP6C via shRNA (Figure 3.2A). Re-expression of wild-type (WT) PPP6C, but not a phosphatase inactive mutant (D84N, PD) in these cells reversed ERK hyperactivation (Figure 3.2B), indicating that negative regulation of ERK signaling requires PPP6C phosphatase activity. Consistent with this observation, re-expression of WT, but not PD, PPP6C rescued the growth defect seen in PPP6C knockout cells (Figure 3.2C). PPP6C loss did not appear to induce apoptosis in 501mel cell lines as judged by levels of caspase-3 and PARP cleavage, suggesting that it causes slow growth rather than cell death (Fig 3.2D).

To determine whether PPP6C acts as a general regulator of ERK signaling outside of the cell line used for our screen, we examined the effect of PPP6C knockdown in a panel of cell lines of varying genotype and lineage (Figure 3.3, 3.4). We found that silencing PPP6C expression led to MEK hyperphosphorylation in each of five additional BRAF^{V600} mutant melanoma cell lines tested, including Yugen8 cells from our screens described in Chapter 2 and YURIF cells heterozygous for a PPP6C^{S270L} mutation. Among four NRAS^{Q61} mutant melanoma cell lines, all but one (YUGASP) exhibited increased MEK phosphorylation upon PPP6C knockdown. We observed the same phenomenon with MEL-ST, a non-transformed immortalized melanocyte cell line. Additionally, in three colon carcinoma cell lines with BRAF or RAS mutations, we also observed increased MEK phosphorylation with PPP6C loss. We note that the impact of PPP6C knockdown on the level of ERK phosphorylation across this panel of cell lines was more variable, suggesting that feedback mechanisms acting directly on ERK may blunt regulation by PPP6C. The osteosarcoma cell line U2OS, which does not harbor BRAF or RAS mutations, and KRAS mutant A549 lung adenocarcinoma cells did not display consistent increases in phospho-MEK levels upon PPP6C knockdown. Overall, the large majority of cell lines examined displayed PPP6C regulation of ERK signaling.

We further examined a role for PPP6C as a regulator of ERK signaling by analyzing data from the Cancer Dependency Map Project[185-187], which compiles the results of genome-wide CRISPR/Cas9 screens across a large panel (739) of cell lines. PPP6C is categorized as a common essential gene with an average CERES gene dependency score of -1.00 ± 0.28, where a more negative score indicates a larger effect on cell growth or survival[187]. Notably, in skin cancer cell lines, the mean CERES score for PPP6C is -1.16 ± 0.31, indicating these cell lines are in general more dependent on PPP6C. Among skin cancer cell lines, those with BRAF hotspot mutations were significantly more dependent on PPP6C than those that are wild-type for BRAF (Figure 3.5A). Taken together with our data in 501mel cells, these data suggest that cells characterized by hyperactive ERK signaling are more sensitive to loss of PPP6C.

We also compared the dependency of skin cancer cell lines on PPP6C and core components of the ERK signaling pathway by examining pairwise correlations between genes. In these data, co-dependency between two genes across cell lines can indicate that they participate in a common pathway[240,241]. Dependency on PPP6C significantly correlates with dependency on BRAF, MAP2K1 (encoding MEK1), and MAPK1 (encoding ERK2) (Figures 3.5B-F). Strikingly, strongest co-dependency with PPP6C was found among negative regulators of the pathway, the ERK selective dual-specificity protein phosphatases (DUSP4, DUSP5, DUSP6, and DUSP7). Consistent with a key role for PPP6C in dephosphorylating Aurora A[152,190], PPP6C dependency negatively correlated with that of AURKA among the full set of cell lines across all lineages (Pearson's correlation coefficient = -0.216, $p = 1.40 \times 10^{-9}$) (Figure 3.5G). However, this correlation was not significant in skin cancer cell lines ($p = 0.44$) (Figure 3.5H), suggesting that regulation of Aurora A is not the primary determinant of PPP6C dependency in these cells. Overall, these correlations suggest that in skin cancer cell lines, dependency on PPP6C is associated with its role as a regulator of ERK signaling.

To examine whether PPP6C might modulate ERK signaling in human melanoma, we analyzed reverse-phase protein array and RNA-seq data collected across a panel of tumors from The Cancer Genome Atlas. We observed a significant correlation between PPP6C mRNA expression and levels of both phospho-MEK and phospho-ERK among tumor specimens (Figure 3.6A, B). However, the extent of ERK pathway activation was not significantly higher in tumors harboring recurrent or truncating PPP6C mutations (Fig 3.6C, D). These data suggest that MEK phosphorylation in melanoma tumors may be more strongly influenced by PPP6C levels than by its mutation.

3.2.2 PPP6C regulates ERK signaling via MEK1/2

Hyperphosphorylation of MEK observed with PPP6C loss suggests PPP6C regulates ERK signaling either at the level of MEK or upstream of MEK. To determine which component of the ERK signaling cascade is regulated by PPP6C, we initially investigated the RAF kinases directly upstream of MEK. In $BRAF^{V600E}$ mutant melanoma, oncogenic signaling is driven primarily by mutant BRAF, with little contribution from the other RAF isoforms ARAF and CRAF[42]. However, in settings of MEKi/BRAFi resistance, ERK pathway reactivation can occur in a manner dependent on CRAF, for example by induction of upstream receptor tyrosine kinases[115,242,243] (Figure 1.3). To determine if increased MEK phosphorylation observed with PPP6C loss is due to compensation by ARAF or CRAF, we silenced each of the RAF isoforms by siRNA in combination with shRNA knockdown of PPP6C in 501mel cells (Figure 3.7A, B). In both the shCTRL and shPPP6C cells, only BRAF knockdown decreased MEK phosphorylation, while silencing ARAF and CRAF alone or in combination (Figure 3.7C) did not. Thus, in the context of PPP6C loss, BRAF remains the principal activator of MEK in 501mel cells. We note that in cells harboring RAS mutations, other RAF isoforms such as CRAF likely have a predominant role in MEK phosphorylation.

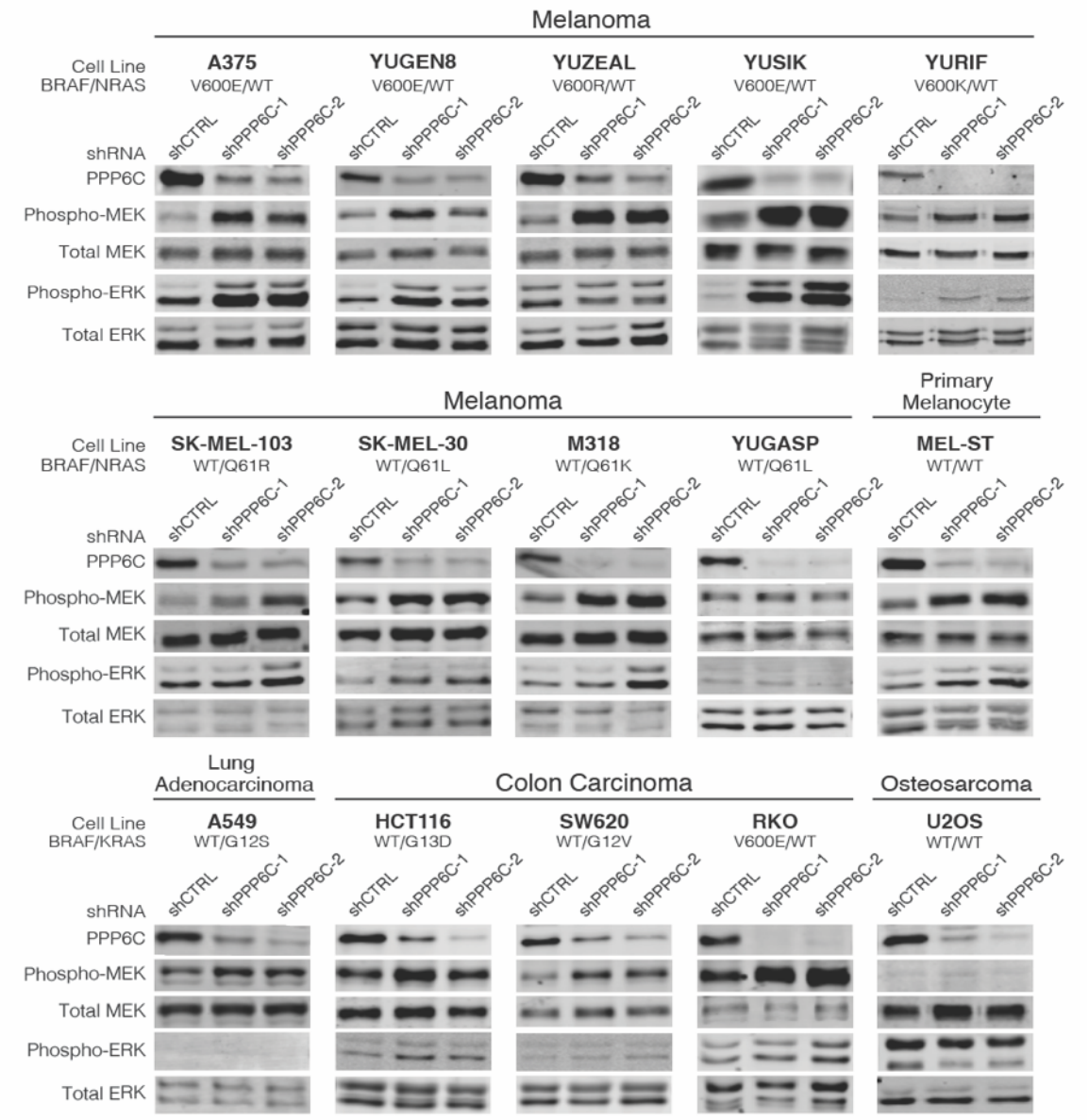

Figure 3.3 PPP6C regulation of ERK signaling is prominent in ERK pathway-driven cancer cells

The indicated cell lines were transduced to stably express control (shCTRL) or PPP6C-targeting (shPPP6C-1 or PPP6C-2) shRNAs. Cells were lysed and assessed by immunoblot for levels of phosphorylated and total MEK and ERK. Quantification is shown in Figure 3.5. $n \geq 2$.

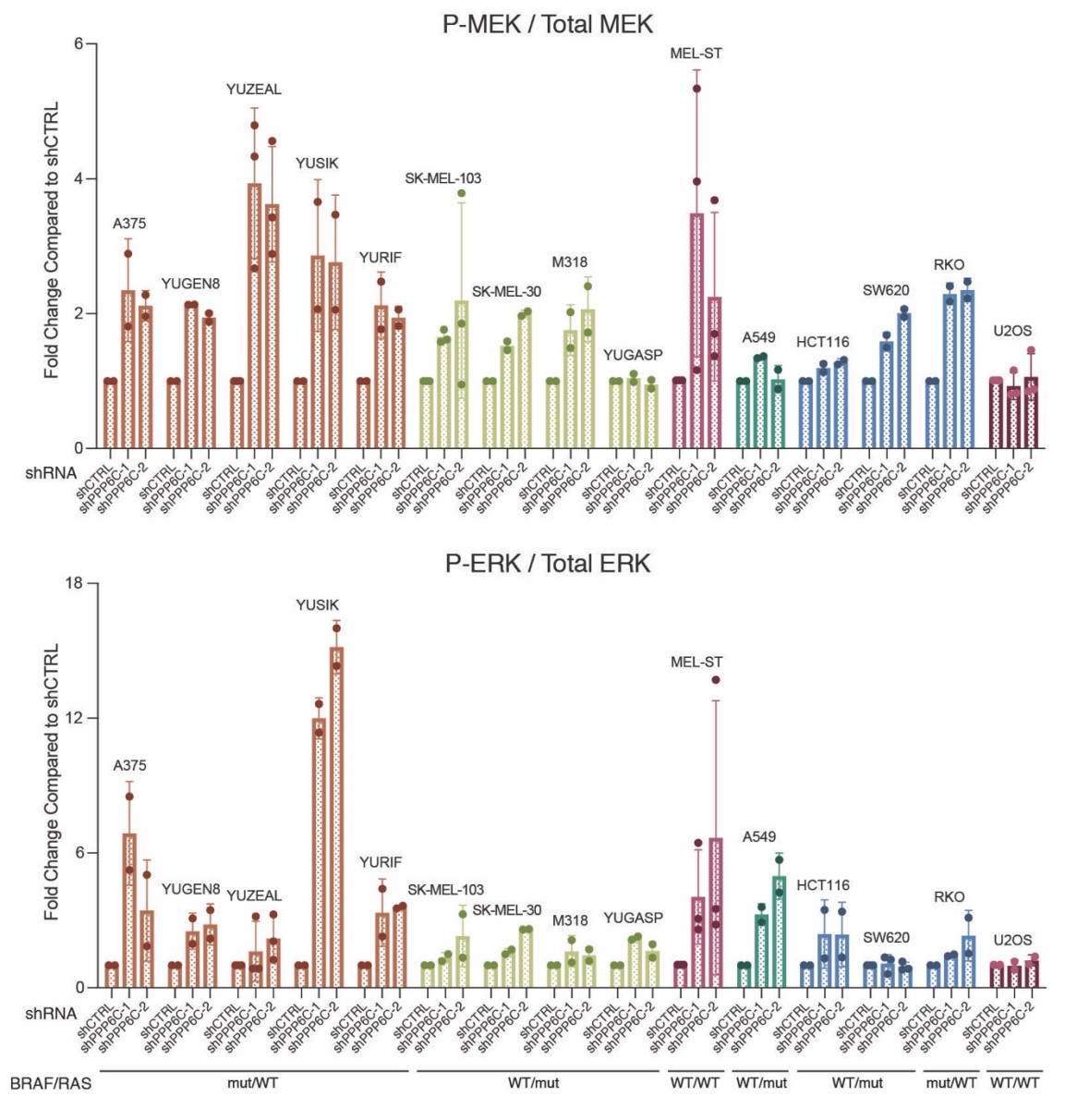

Figure 3.4 PPP6C regulation of ERK signaling in cancer cell lines

Quantification of the relative levels of Phospho/Total MEK and ERK from Figure 3.4 was normalized to shCTRL for each cell line. Data are represented as mean ± SD, n ≥ 2.

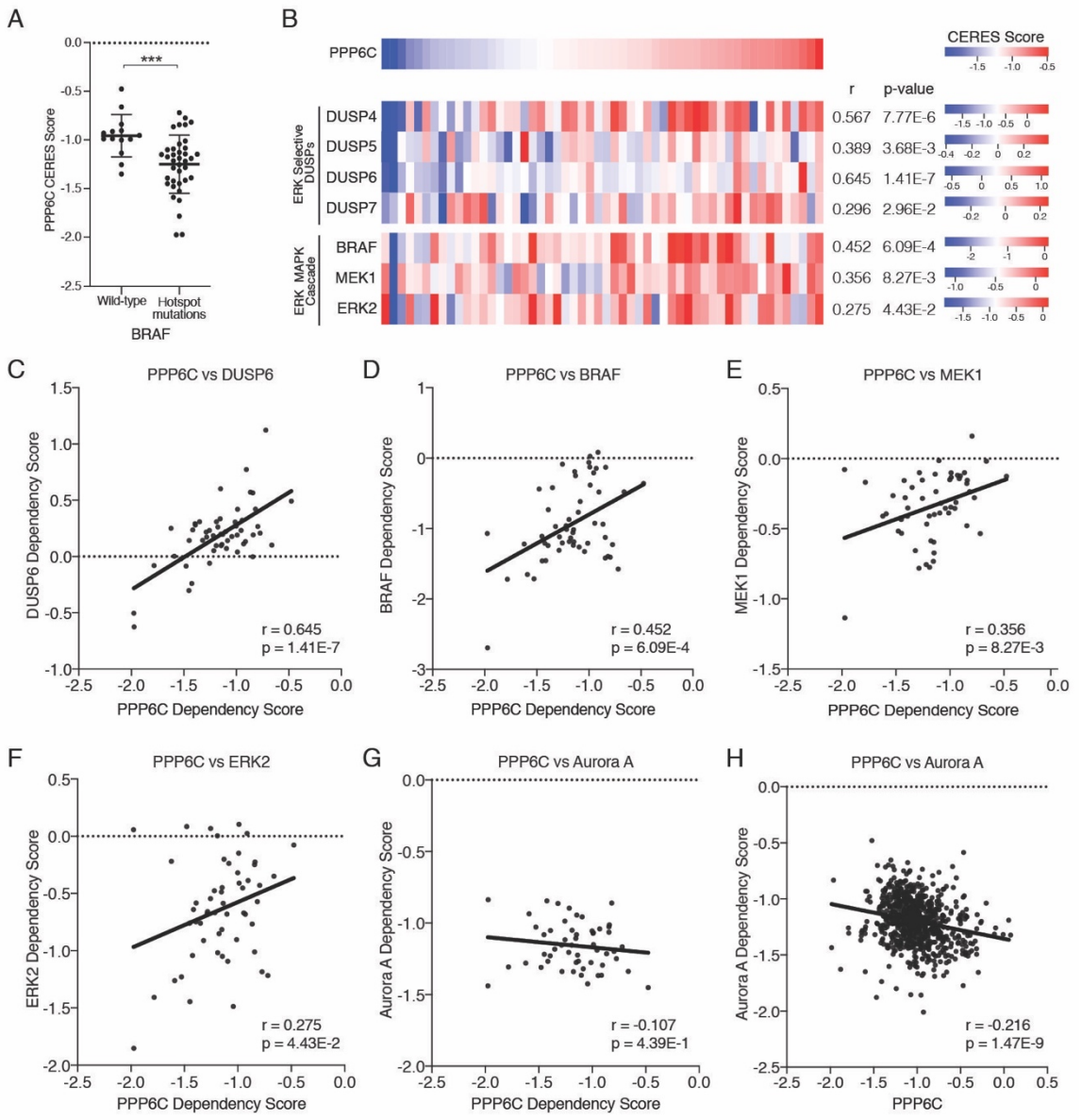

Figure 3.5 PPP6C dependency and ERK pathway dependency

(A) PPP6C CERES scores for skin cancer cell lines with WT BRAF or hotspot BRAF mutations from the Cancer Dependency Map Project. Cell lines harboring non-recurrent BRAF variants of unknown significance were excluded. Data are represented as mean ± SD. ***$p < 0.0005$, Welch's t test.

(B) Heatmaps depicting CERES scores of PPP6C, ERK selective DUSPs, and ERK MAPK cascade components in skin cancer cell lines using data from Cancer Dependency Map Project. Pearson's correlation coefficients and p-values from linear regression analysis of each gene with PPP6C in the DepMap portal are listed.

(C-G) CERES scores for PPP6C (x-axis) plotted against CERES scores for (C) DUSP6,

(D) BRAF, (E) MEK1, (F) ERK2, and (G) Aurora A (y-axis). CERES scores are for all skin cancer cell lines from the Cancer Dependency MAP Project. Pearson's correlation coefficients (r) and associated p-values from linear regression analysis are indicated.

(H) CERES scores for PPP6C (x-axis) plotted against CERES scores for Aurora A (y-axis). CERES scores are for all cancer cell lines from the Cancer Dependency MAP Project. Pearson's correlation coefficient (r) and associated p-value from linear regression analysis are indicated.

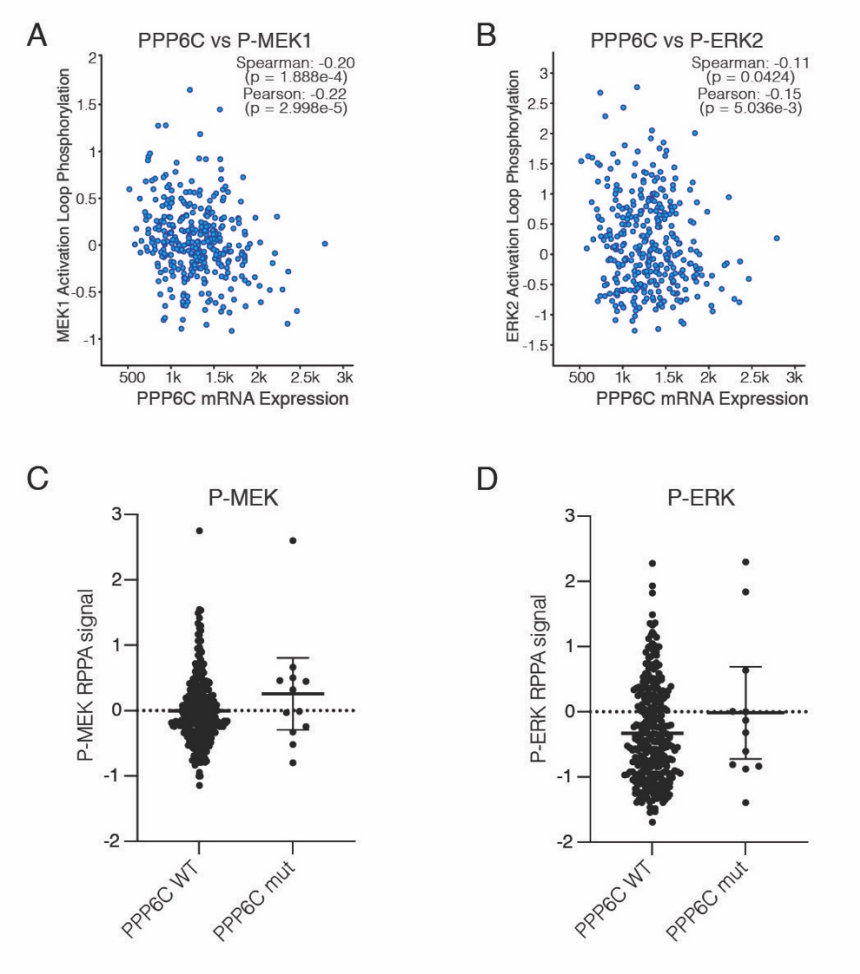

Figure 3.6 PPP6C mutational status and ERK pathway activation

(A) PPP6C RNA-seq mRNA expression level plotted against MEK1 phosphorylation levels (MEK1 pSer221, pThr217) for TCGA tumor samples in cBioPortal. Correlation coefficients and associated p-values from linear regression analyses are indicated.

(B) PPP6C mRNA levels plotted against ERK2 phosphorylation levels (ERK2 pThr202, pTyr204) for TCGA tumor samples as in (A).

(C) MEK phosphorylation levels (MEK1 pSer221, pThr217). Data were obtained from cBioPortal and are represented as mean ± SD.

(D) ERK phosphorylation levels (ERK2 pThr202, pTyr204) for TCGA tumor samples with WT PPP6C or recurrent/truncating PPP6C mutations as in (C). Data are represented as mean ± SD

We next considered whether loss of PPP6C leads to increased BRAF activity. To do so, we immunoprecipitated endogenous BRAF from shCTRL cells and shPPP6C cells and examined its vemurafenib-sensitive kinase activity on MEK1 in vitro. We found that BRAF isolated from both shCTRL and shPPP6C cells phosphorylated MEK1 at similar rates (Figure 3.8A), indicating PPP6C does not regulate BRAF activity. While we did not observe changes in RAF expression levels with PPP6C loss (Figures 3.7A), we did note upward electrophoretic mobility shifts suggestive of a change in the phosphorylation states of BRAF and CRAF that could have a regulatory role (Figure 3.8B). We found however that treatment of cells with MEKi or BRAFi caused the multiple BRAF species to collapse into a lower, presumably less phosphorylated species (Figure 3.8B, C). The increased RAF phosphorylation observed in shPPP6C cells is therefore presumably a consequence of increased negative feedback phosphorylation due to ERK hyperactivation[5,244], though we were unable to identify specific sites regulated by PPP6C (Figure 3.8C). In keeping with reports that $BRAF^{V600E}$ is insensitive to feedback phosphorylation[5], its hyperphosphorylation did not affect its activity in vitro and is thus unlikely to impact MEK phosphorylation in cells.

PPP6C regulates the level of RAF-mediated MEK activation loop phosphorylation without affecting the activity of RAF itself. MEK activation loop phosphorylation can be influenced by crosstalk regulation through phosphorylation at other sites, which could be subject to regulation by PPP6C. Indeed, we found that MEK1 phosphorylation at Ser298, which is mediated by PAK1 to promote activation loop phosphorylation[244,245], was elevated in cells lacking PPP6C (Figure 3.8D). In contrast, there was no effect on phosphorylation at Thr286, a negative regulatory site phosphorylated by CDK1 or CDK5 [246,247]. Because regulation by Ser298 phosphorylation is specific to MEK1 and not MEK2, we examined whether PPP6C selectively regulates MEK isoforms. We found that ectopically expressed MEK1 and MEK2 (upper bands), like endogenous MEK1/2 (lower bands), were both hyperphosphorylated when expressed in $PPP6C^{-/-}$ cells in comparison

to WT cells (Figure 3.8E). PPP6C therefore does not preferentially regulate one isoform of MEK but instead regulates both MEK1 and MEK2. This suggests that PPP6C regulates MEK activity by modulating activation loop phosphorylation independently of crosstalk pathway.

3.2.3 MEK1/2 is a direct substrate of PP6

As our findings above indicate PPP6C regulates MEK1/2 activation loop phosphorylation without affecting RAF activity, PPP6C likely promotes MEK1/2 dephosphorylation, possibly acting directly. To assess PPP6C dephosphorylation of MEK, we isolated PP6 complexes by affinity purification from HEK293T cells ectopically expressing FLAG epitope-tagged PPP6C with PPP6R3 and ANKRD28. Complexes containing WT PPP6C dephosphorylated the activation loop residues (pSer218 and pSer222) of MEK1 in a manner sensitive to the pan-PP2A family phosphatase inhibitor okadaic acid (Figure 3.9A). Phosphatase inactive PPP6C^{D84N} complexes had no activity against MEK1, indicating that our preparations were not contaminated with other MEK phosphatase activities. We found that PP6 also dephosphorylated pSer298 on MEK1, albeit with slower kinetics than with the activation loop sites, while it did not detectably dephosphorylate pThr286. Thus, PP6 dephosphorylates MEK1 selectively at the same sites that are elevated in cells lacking PPP6C (Figure 3.9C). Furthermore, PP6 had no activity on phospho-ERK2, consistent with PPP6C acting as a regulator of MEK (Figure 3.9B). Overall, these studies demonstrate the direct dephosphorylation of MEK1 by PP6 with substrate and phosphorylation site specificity (Figure 3.9C).

To provide additional evidence that PPP6C acts directly on MEK, we performed co-immunoprecipitation experiments to determine if PP6 can interact with MEK in cells. HEK293T cells were transfected with plasmids expressing a FLAG epitope tagged PP6 subunit (PPP6C, PPP6R1, PPP6R2, or PPP6R3) and untagged MEK1. We found that MEK1 co-immunoprecipitated with each of the PP6 regulatory subunits (Figure 3.9D),

with the amount of associated MEK1 proportional to the PPP6R expression level. Significantly less MEK1 associated with FLAG-tagged PPP6C. These results suggest that PP6 regulatory subunits serve to recruit MEK to the PP6 complex for dephosphorylation by PPP6C, consistent with a general role for non-catalytic subunits of PP6 and other PP2A family phosphatases in substrate binding[149,153,155,248,249]. In keeping with our observation that MEK binds to each of the regulatory subunits, we found that combined siRNA silencing of PPP6R1, PPP6R2 and PPP6R3, but not knockdown of individual subunits, significantly elevated MEK phosphorylation in 501mel cells (Fig 3.9E).

Our observations collectively suggest that PP6 has a general role as a MEK phosphatase across multiple cell types. Classical studies, however, had implicated PP2A as the major MEK phosphatase, suggesting that PP6 may act indirectly by regulating PP2A activity on MEK[235,236]. We therefore investigated the impact of PP6 and PP2A loss, alone and in combination, on MEK phosphorylation. We used siRNA SMARTpools to knockdown the two PP2A catalytic subunits (PPP2CA and PPP2CB) in PPP6C$^{-/-}$ and control 501mel cells (Figure 3.10A). In these cells, PPP2CA appeared to be the predominantly expressed isozyme, as PPP2CB siRNA alone did not detectably decrease total catalytic subunit levels. Knockdown of PPP2CA, but not PPP2CB, increased MEK activation loop phosphorylation levels in the control cell line. In PPP6C$^{-/-}$ cells, PP2A downregulation further increased MEK phosphorylation, with the two phosphatases having an apparently additive effect. Notably, loss of either phosphatase increased expression levels of the other, suggestive of a compensatory mechanism (Figure 3.10A, B). We further found that two other phosphorylation sites on MEK1, pThr292 and pSer298 were impacted by loss of PPP6C but not PP2A (Figure 3.10B). This experiment suggests that PP6 and PP2A act independently to dephosphorylate the activation loop of MEK, while PP6 also dephosphorylates additional sites.

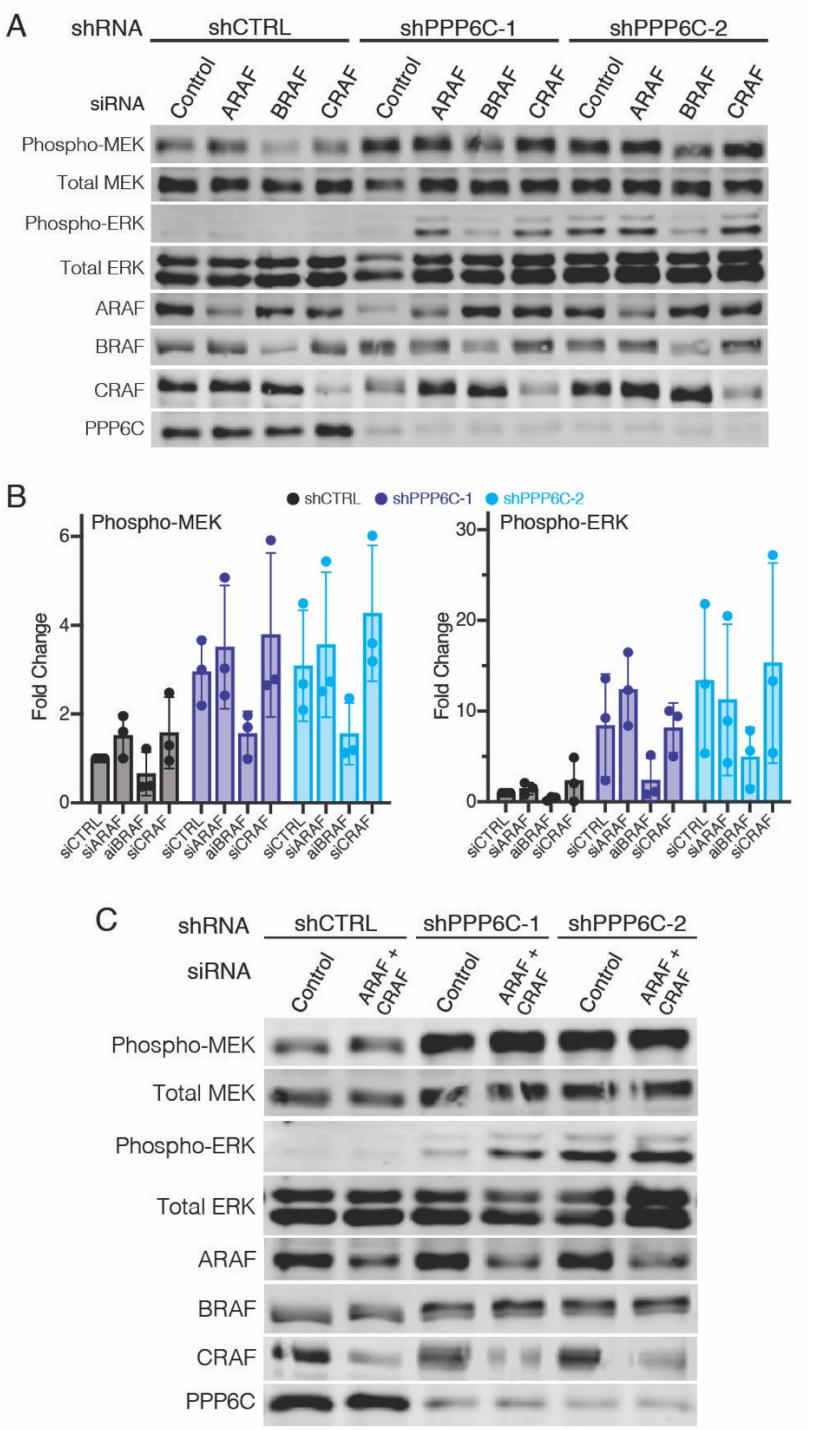

Figure 3.7 PPP6C does not regulates ERK signaling via RAFs

(A) shCTRL, shPPP6C-1, and shPPP6C-2 expressing 501mel cells were transfected with non-targeting control siRNA or siRNAs directed to ARAF, BRAF, or CRAF as indicated. Cells were lysed and assessed by immunoblot for phosphorylated and total MEK and ERK.

(B) Quantification of the relative levels of Phospho/Total MEK and ERK from (A) was normalized to shCTRL, siCONTROL. Data are represented as mean ± SD, n = 3.

(C) 501mel cells expressing shCTRL, shPPP6C-1, or shPPP6C-2 were transfected with non-targeting control siRNA or siRNA targeting both ARAF and CRAF. Cells were lysed and assessed by immunoblot for phosphorylated and total MEK and ERK. Knockdown of ARAF, CRAF, and PPP6C was also confirmed via immunoblot.

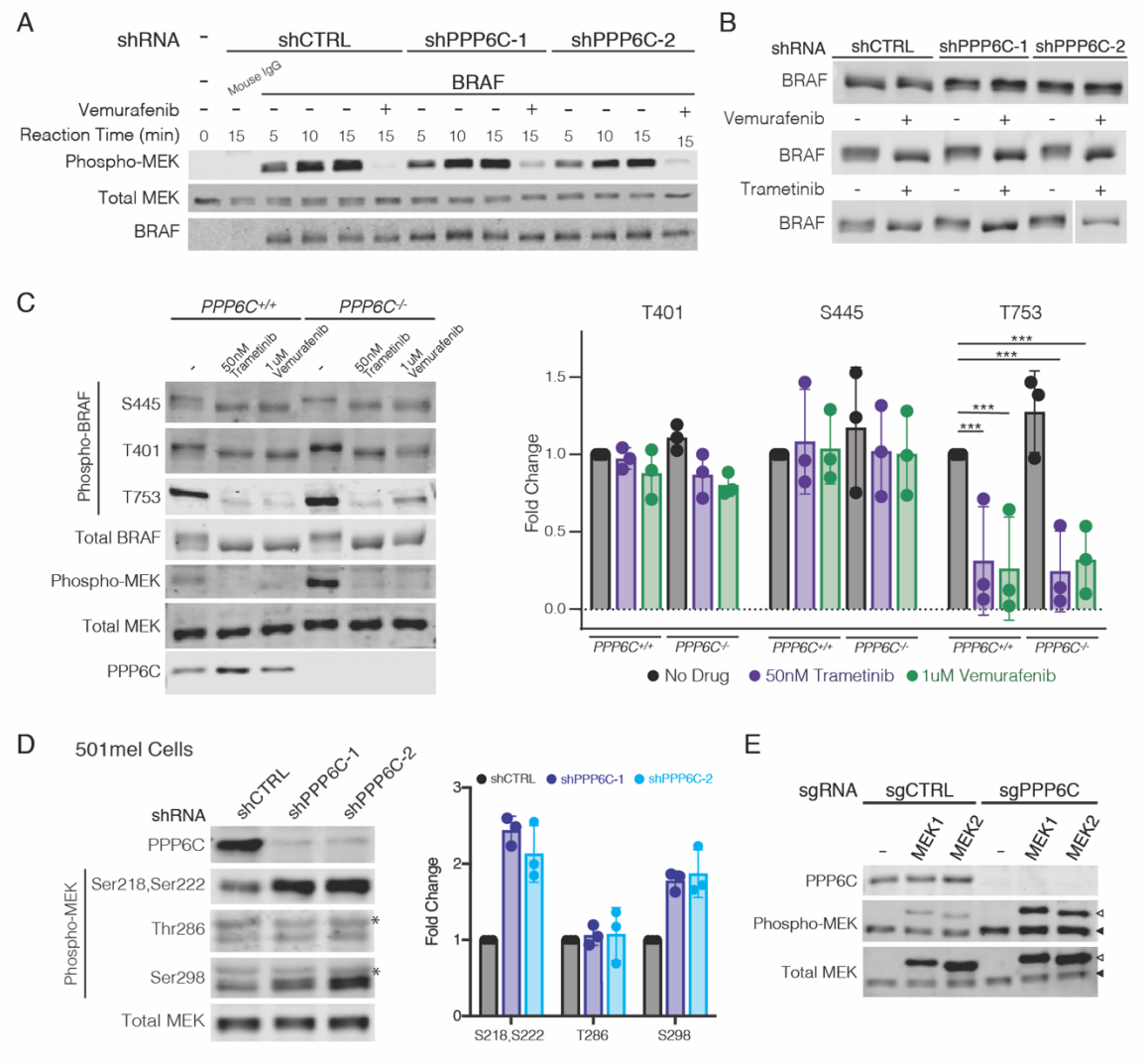

Figure 3.8 PPP6C regulates MEK and not BRAF

(A) BRAF was immunoprecipitated from 501mel cells expressing shCTRL, shPPP6C-1, or shPPP6C and evaluated in vitro in kinase assays on MEK1 over the indicated time course. Vemurafenib (1 μM) was added to negative control reactions. Reactions were evaluated by immunoblot.

(B) shCTRL, shPPP6C-1, and shPPP6C-2 501mel cells were treated with 1uM vemurafenib or 50nM trametinib for 24 hours as indicated. Cells were lysed and assessed by immunoblot for BRAF electrophoretic mobility shifts indicative of changes in phosphorylation.

(C) PPP6C$^{+/+}$ and PPP6C$^{-/-}$ 501mel cells were treated with 1uM vemurafenib or 50nM trametinib for 24 hours as indicated. Cells were lysed and assessed by immunoblot for phosphorylation at regulatory sites on BRAF. Quantification of the relative levels of Phospho/Total BRAF was normalized to PPP6C$^{+/+}$. Data are represented as mean ± SD, n = 3. ***p<0.001, unpaired t-test.

(D) 501mel cells expressing shCTRL, shPPP6C-1, and shPPP6C-2 were lysed and assessed by immunoblot for MEK phosphorylation at Ser218/Ser222, Thr286, and Ser298. Non-specific cross-reacting bands in the pThr286 and pSer298 blots are indicated with an asterisk. Quantification of the relative levels of Phospho/Total MEK was normalized to shCTRL. Data are represented as mean ± SD, n = 3.

(E) $PPP6C^{+/+}$ and $PPP6C^{-/-}$ 501mel cell lines were transiently transfected to express His epitope tagged MEK1 or MEK2. Cell lysates were analyzed by immunoblot for phosphorylated and total MEK. Upper bands (open arrows) correspond to ectopically expressed His-tagged MEK1/2, and lower bands (solid arrows) show endogenous MEK1/2.

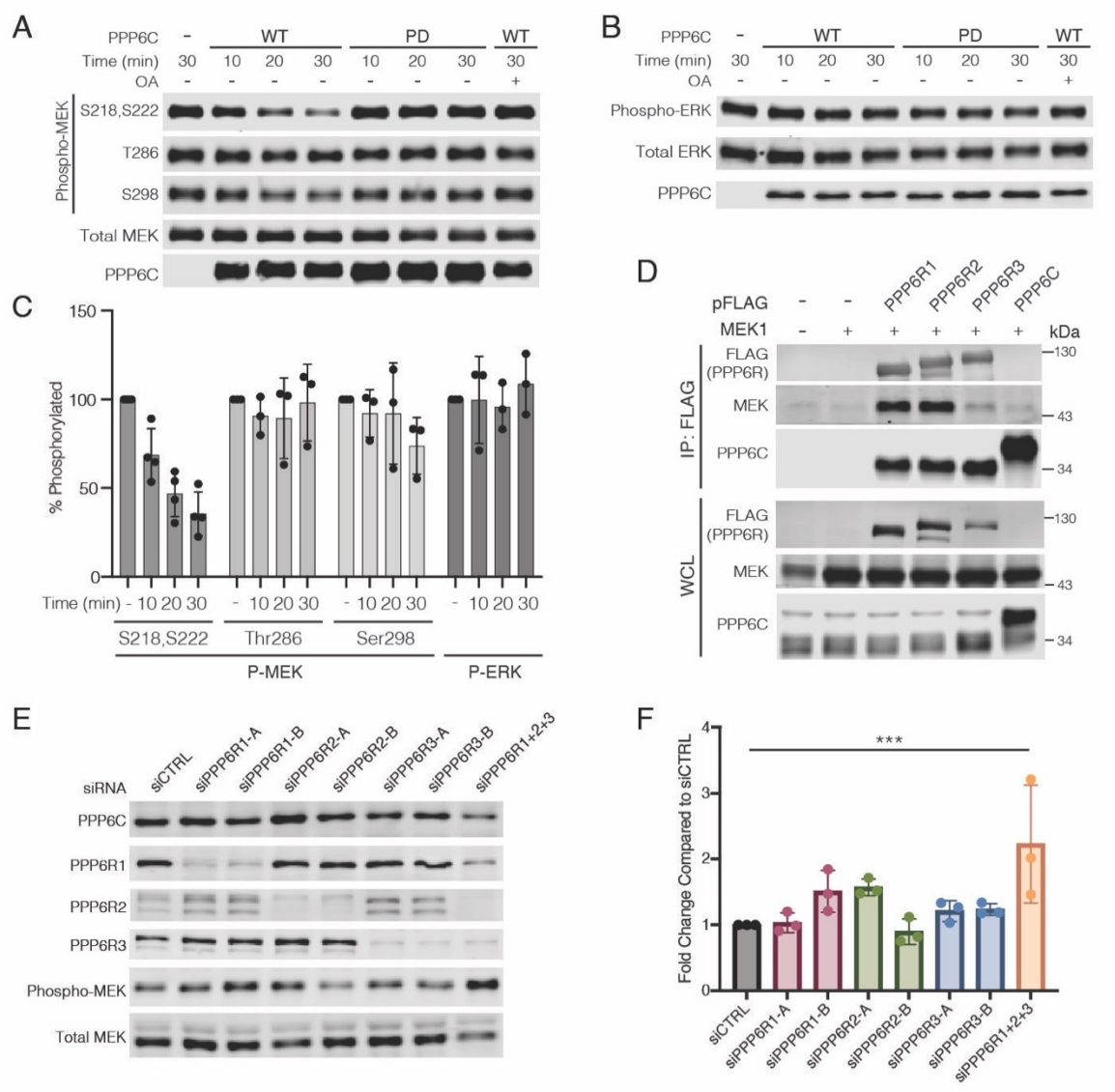

Figure 3.9 MEK1/2 is a direct substrate of PP6

(A) PP6 complexes with WT or phosphatase inactive PPP6C (PD) were partially purified from HEK293T cells and incubated with phosphorylated MEK1 in vitro for the indicated times. Okadaic acid (OA, 100nM) was added where indicated. Reactions were evaluated by immunoblot.

(B) In vitro phosphatase assays evaluating phospho-ERK2 as a PP6 substrate were carried out as in (A). Reactions were evaluated by immunoblot.

(C) Quantification of in vitro phosphatase assays in (A) and (B). Remaining phosphorylation is shown relative to the 30 min control reaction. Data are represented as mean ± SD. For MEK1 pSer218/pSer222, $n = 4$; for all other data, $n = 3$.

(D) HEK293T cells were co-transfected to express the indicated FLAG epitope tagged PP6 subunit and untagged MEK1. Anti-FLAG immunoprecipitates and whole cell lysates (WCL) were evaluated by immunoblot for MEK.

(E) 501mel cells were transfected with non-targeting control siRNA or siRNA targeting PPP6R1, PPP6R2, and/or PPP6R3. Cells were lysed and assessed by immunoblot for phosphorylated and total MEK. Knockdown of PPP6Rs was also confirmed via immunoblot.

(F) Quantification of the relative levels of Phospho/Total MEK in (E) was normalized to siCTRL. Data are represented as mean ± SD, $n = 3$. ***$p<0.001$, unpaired t-test.

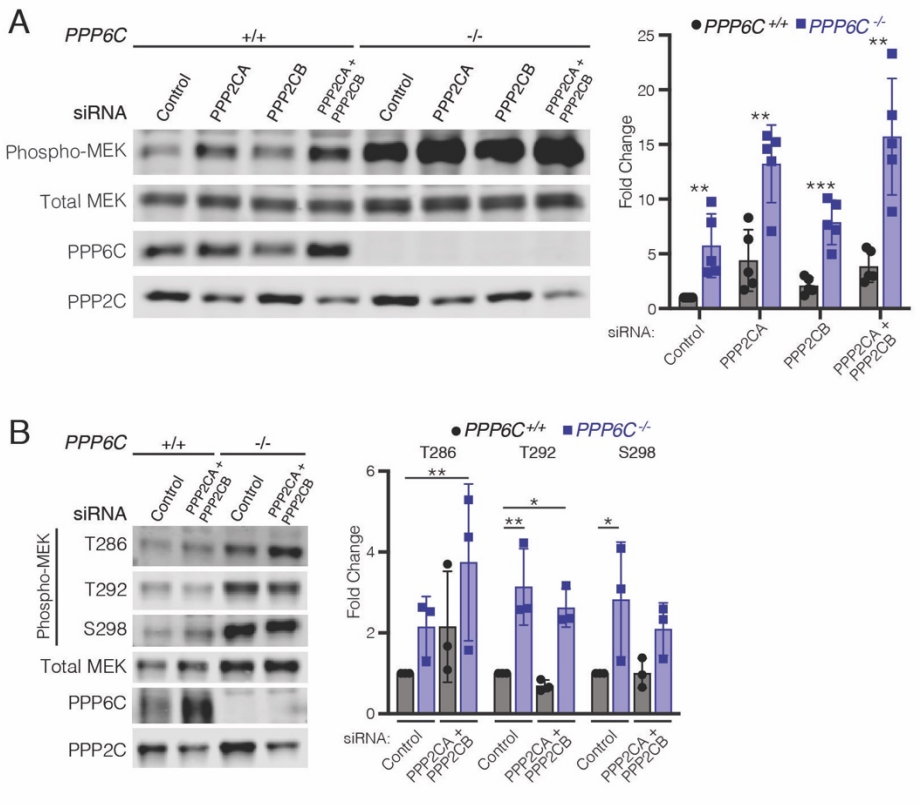

Figure 3.10 PP6 and PP2A regulate MEK independently

(A) PPP6C$^{+/+}$ and PPP6C$^{-/-}$ 501mel cells were transfected with non-targeting control siRNA or siRNA SMARTpools targeting PPP2CA and/or PPP2CB. Cells were lysed and evaluated by immunoblot for phosphorylated and total MEK. Quantification of the relative level of Phospho/Total MEK for PPP2CA/PPP2CB knockdown in PPP6C$^{+/+}$ and PPP6C$^{-/-}$ cells. MEK phosphorylation was normalized to PPP6C$^{+/+}$, siRNA Control. Data are represented as mean ± SD, $n = 5$. **p < 0.01, ***p < 0.001, unpaired t test.

(B) PPP6C$^{+/+}$ and PPP6C$^{-/-}$ 501mel cells were transfected with non-targeting control siRNA or siRNA SMARTpools targeting PPP2CA and PPP2CB. Cells were lysed and evaluated by immunoblot for phosphorylated and total MEK. Quantification of the relative levels of Phospho/Total MEK for PPP2CA/PPP2CB knockdown in PPP6C$^{+/+}$ and PPP6C$^{-/-}$ cells. MEK phosphorylation was normalized to PPP6C$^{+/+}$, siRNA Control. Data are represented as mean ± SD, $n = 5$. *p < 0.05, **p < 0.01, unpaired t test.

3.2.4 Cancer-associated PPP6C mutations abrogate PP6 phosphatase activity against MEK1/2

PPP6C mutations are found across multiple cancer types but are most common in melanoma and other skin cancers, where they are thought to contribute to tumor development[18,33,37,188,190]. Prior characterization of PPP6C mutations has focused primarily on non-recurrent mutations that cluster at the catalytic center, which reportedly reduce or eliminate phosphatase activity. Interestingly, there are several PPP6C hotspot residues that are recurrently mutated, with R264C being the most common (Figure 1.4C). When modeled onto the X-ray crystal structure of a PPP5C-peptide complex[250], sites of recurrent mutations are generally located within or proximal to the catalytic cleft (Figure 3.11A). Of these, His55 appears critical for activity as it coordinates one of the bound metal ions (Figure 1.5A).

We chose to characterize five of the most common mutations reported in melanomas (H55Y, P186S, P259S, R264C, and S270L) for their ability to regulate ERK signaling by ectopic expression in the PPP6C$^{-/-}$ 501mel cell line (Figure 3.10B). While re-expression of WT PPP6C suppressed MEK and ERK phosphorylation to levels observed in parental cells, melanoma-associated PPP6C mutants varied in their impact on MEK and ERK phosphorylation (Figure 3.11B, C). In keeping with an essential role for His55 in catalysis, cells expressing the H55Y mutant exhibited the highest level of MEK phosphorylation, similar to that seen in empty vector control cells. Cells expressing the P259S, R264C, and S270L mutants had moderate but significant increases in MEK phosphorylation compared to cells expressing WT PPP6C, suggesting partial loss of activity. We note that the S270L mutant consistently expressed to lower levels than WT PPP6C or the other mutants, likely underlying its inability to promote MEK dephosphorylation. Ser270 maps to the globular core of the PPP6C catalytic domain (Figure 3.11A), potentially explaining the instability of the S270L mutation. Unlike the other mutants, expression of PPP6C^{P186S} reduced MEK phosphorylation to a similar extent

as did the WT phosphatase. PPP6C mutants likewise impacted, to varying degrees, Aurora A phosphorylation in mitotically-arrested cells (Figure 3.11D, E). Expression of the H55Y, P259S, and S270L mutants resulted in high levels of Aurora A phosphorylation, similar to those seen in PPP6C$^{-/-}$ cells. Aurora A phosphorylation was more modest in cells expressing the PD, P186S, and R264C mutants, but still significantly higher phosphorylation than in cells expressing WT PPP6C. We also examined the impact of PPP6C mutations on the levels of several transcriptional targets of ERK (DUSP6, ETV4 and SPRY2, Figure 3.12). Elevated expression of all three targets were significantly suppressed upon re-expression of WT PPP6C in PPP6C$^{-/-}$ cells. The effect of PPP6C mutants generally correlated with their impact on MEK and ERK phosphorylation, with only levels of ETV4 being significantly affected by all mutants.

We next performed clonogenic assays to examine the impact of PPP6C mutations on cell growth and MEKi sensitivity (Figure 3.13). We found that growth of the cells in the absence of drug inversely correlated with the degree of ERK pathway activation. For example, cells expressing the PPP6C^{H55Y} mutant, which had the highest levels of MEK and ERK phosphorylation, grew equivalently to PPP6C$^{-/-}$ cells. Conversely, expression of PPP6C^{P186S}, fully rescued the growth defect of null cells, in keeping with its complete reversal of MEK hyperactivation. The other mutants, which partially impacted MEK and ERK phosphorylation, likewise grew at an intermediate rate. In all cases, treatment with low concentrations of MEKi at least partially reversed the growth impairment observed in cells expressing PPP6C mutants. Collectively, these experiments indicate that cancer-associated PPP6C mutations generally cause partial loss-of-function, impacting both dephosphorylation of substrates and sensitivity.

3.3 Discussion

Our identification of PPP6C as a MEK phosphatase suggests that it also acts as a negative regulator of the core pathway driving melanoma, likely underlying at least in

part its role as a tumor suppressor. PPP6C mutations in melanoma almost exclusively co-occur with BRAF and NRAS mutations (Figure 1.4B), suggesting that alone they do not provide oncogenic levels of ERK signaling. In this context, downregulation of PPP6C is likely to have a role in tuning flux through the ERK pathway to counteract negative feedback regulation. A similar phenomenon may drive selection for mutations in MEK1, MEK2 and ERK2 found at low frequency in melanomas that generally co-occur with other activating lesions[19,33,37,251]. We note that like loss of PPP6C, these putatively oncogenic mutants suppress growth when delivered to cultured BRAF mutant melanoma cell lines, potentially reflecting different optimal levels of ERK signaling for cells in tumors in comparison with cells in culture.

Most studies of PPP6C in melanoma have focused on its regulation of Aurora A, an essential kinase regulating mitotic spindle assembly and chromosome segregation[152,190]. Melanoma-associated PPP6C mutations impair its ability to dephosphorylate and inactivate Aurora A, resulting in genomic instability and DNA damage that may contribute to cancer progression[189,190]. Interestingly, Aurora A is reportedly a transcriptional target of oncogenic BRAF signaling in melanoma cells, suggesting that PP6 may coordinately regulate Aurora A through both direct dephosphorylation and through downregulation of ERK signaling[252]. This phenomenon may offer a therapeutic vulnerability, as melanoma cells expressing mutant PPP6C are sensitized to Aurora A inhibitors.

The observation that loss or mutation of PPP6C is deleterious to cell growth may appear at odds with its role as a tumor suppressor and a negative regulator of ERK signaling. Recent studies indicate however that in the context of activating BRAF and RAS mutations, further elevation of signaling through the ERK pathway is toxic[238,239,253,254]. This phenomenon can give rise to inhibitor addiction, in which tumor cells treated with pathway inhibitors reactivate ERK signaling to re-establish signaling within an optimal range, or “fitness zone”. Subsequent inhibitor withdrawal results in a rebound signaling,

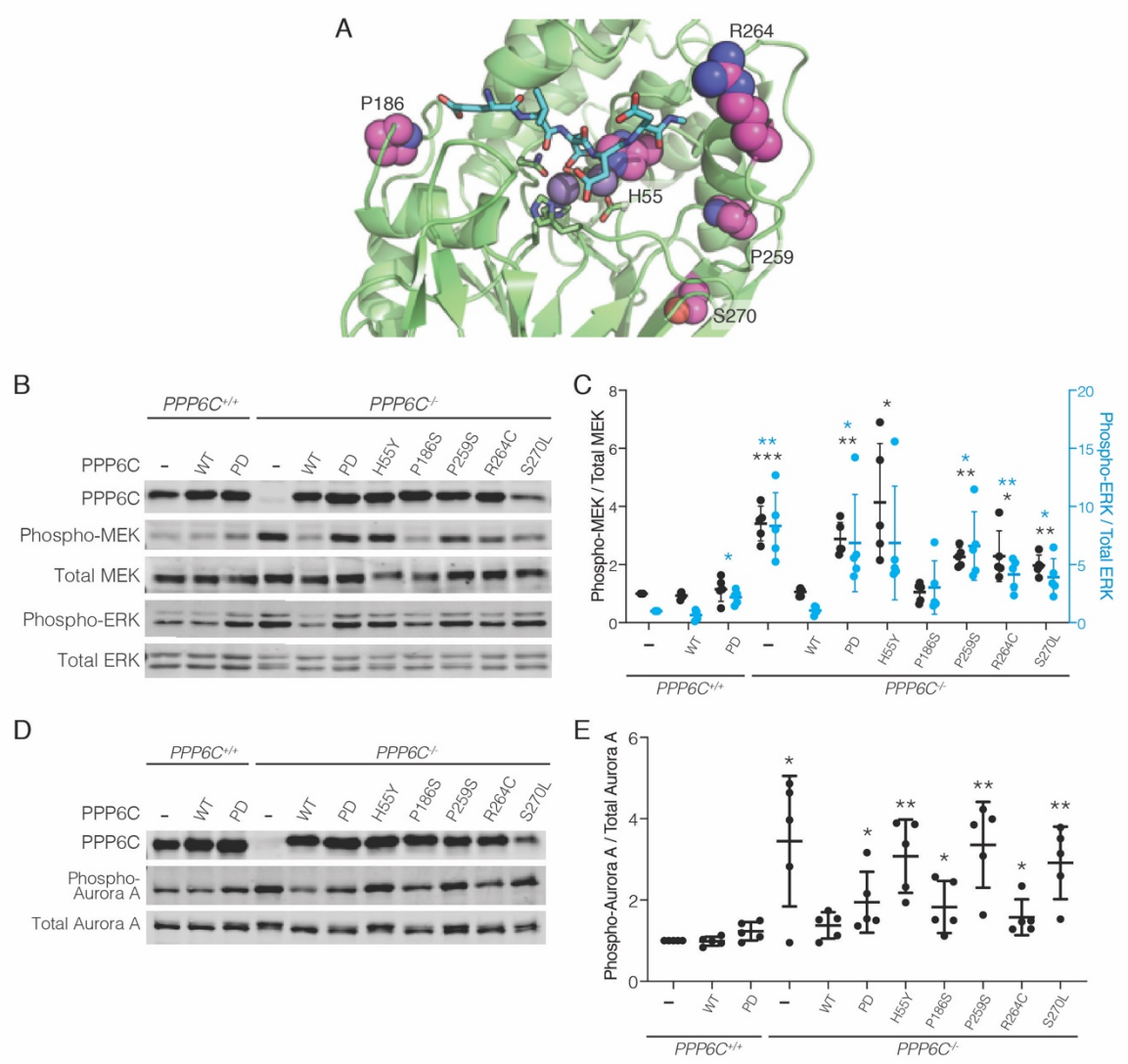

Figure 3.11 Cancer-associated PPP6C mutations abrogate PP6 phosphatase activity against MEK1/2

(A) PPP6C residues mutated in cancer are shown in spacefill representation modeled on the X-ray crystal structure of PPP5C in complex with a peptide substrate (PDB: 5HPE). The bound peptide is shown in cyan in stick representation, and the catalytic metal ions are shown as gray spheres.

(B) PPP6C$^{+/+}$ and PPP6C$^{-/-}$ 501mel cells were transduced to stably express GFP (-), WT PPP6C, or the indicated PPP6C mutants. Cells were lysed and assessed by immunoblot for phosphorylated and total MEK and ERK.

(C) Phospho/Total MEK (black) and ERK (blue) signal ratios were quantified and normalized to the GFP-expressing PPP6C$^{+/+}$ samples. Mean values ± SD are shown, n = 5. Significance is shown in comparison to PPP6C$^{+/+}$ cells expressing GFP. *p < 0.05, **p < 0.01, ***p<0.001, paired t test.

(D) Cells from (C) were treated with 100ng/mL nocodazole for 24 hours. Mitotic cells were lysed and assessed by immunoblot for phosphorylated and total Aurora A.

(E) Phospho-Aurora A/Total Aurora A signal ratios were quantified (n = 5) and significance determined as in (C). *p < 0.05, **p < 0.01, paired t test.

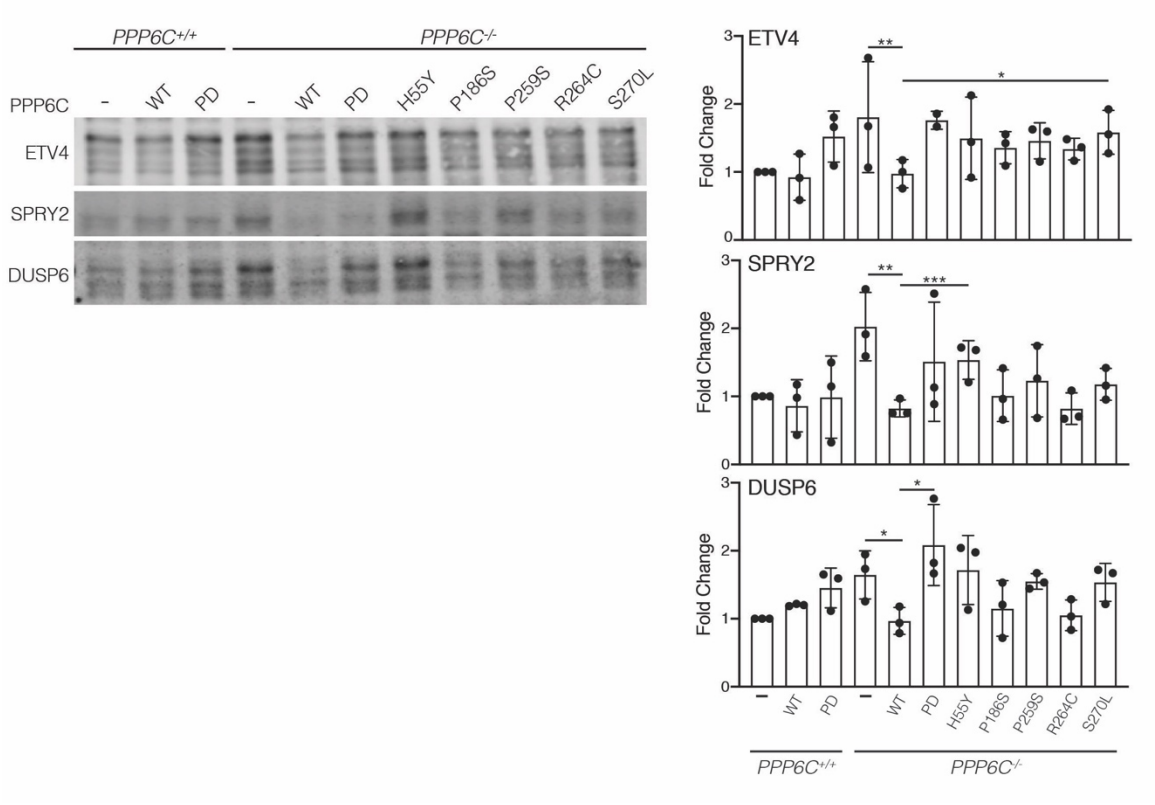

Figure 3.12 Cancer-associated PPP6C mutations upregulate ERK transcriptional targets

PPP6C$^{+/+}$ and PPP6C$^{-/-}$ 501mel cells were transduced to stably express GFP (-), WT PPP6C, or the indicated PPP6C mutants. Cells were lysed and assessed by immunoblot for ETV4, SPRY2, and DUSP6. Total protein signals were quantified and normalized to the GFP-expressing PPP6C$^{+/+}$ samples. Mean values ± SD are shown, $n = 3$. Significance is shown in comparison to PPP6C$^{+/+}$ cells expressing GFP. *p < 0.05, **p < 0.01, ***p<0.001, unpaired t test.

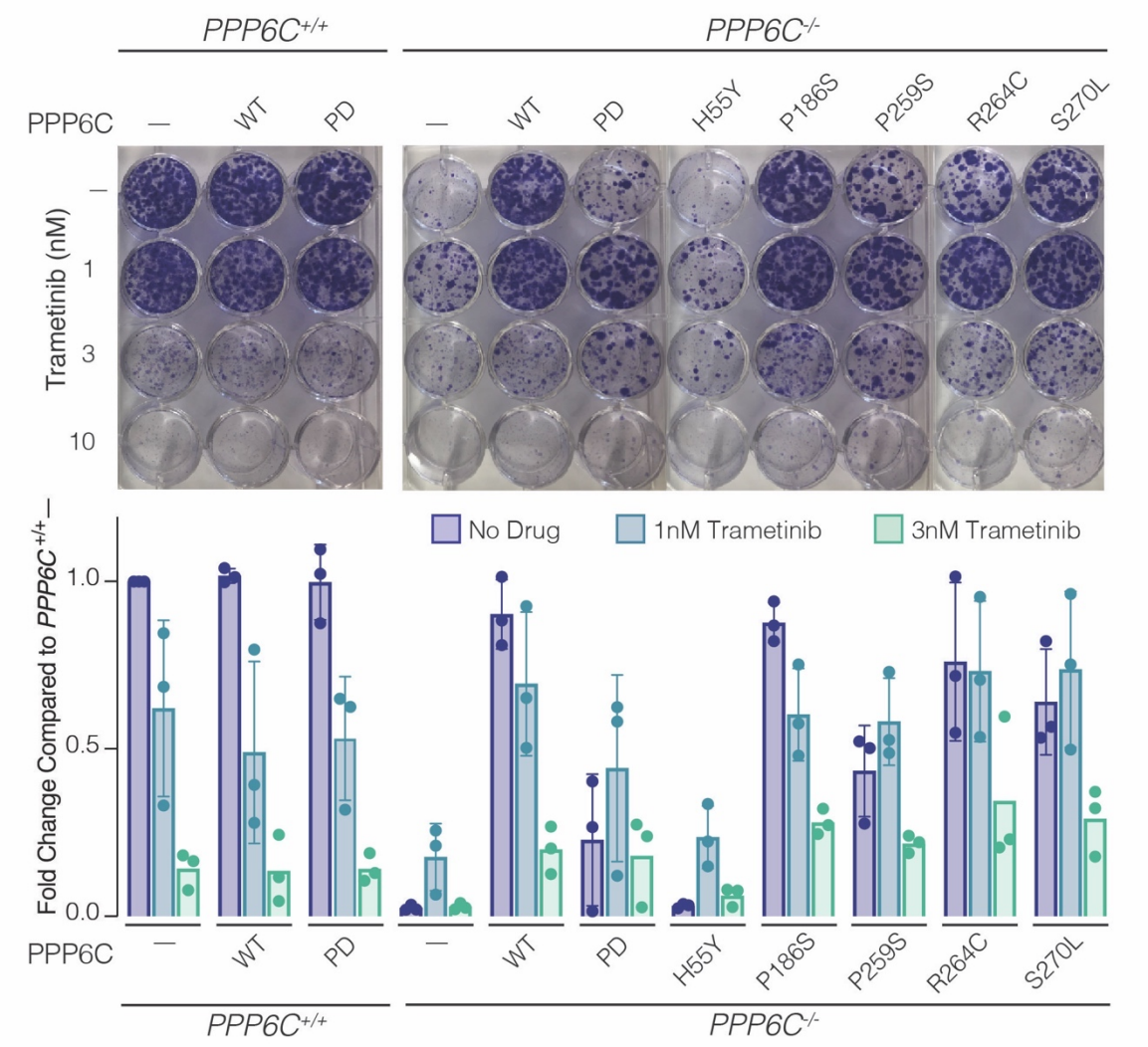

Figure 3.13 Cancer-associated PPP6C mutations decrease sensitivity to MEKi.

PPP6C$^{+/+}$ and PPP6C$^{-/-}$ 501mel cells were transduced to stably express GFP (-), WT PPP6C, or the indicated PPP6C mutants. Cells were cultured in media containing DMSO vehicle alone or the indicated trametinib concentration for 2 weeks in colony forming assays. Colonies were stained with crystal violet. Clonogenic growth was analyzed by ColonyArea in ImageJ and normalized to GFP-expressing PPP6C$^{+/+}$ samples, $n = 3$.

leading to toxic hyperactive signaling outside of the fitness zone. In this context, even modest increases in ERK phosphorylation suppress growth, while further elevation induces cell death[238]. Toxicity and growth suppression due to ERK hyperactivation has been associated with a phenotypic switch mediated in part by downregulation of the melanocyte lineage-specific transcription factor MITF and by transcriptional upregulation of genes encoding secreted cytostatic proteins[253,254]. BRAFi and/or MEKi addicted melanoma tumors grown in mice regress when treatment with inhibitors is ceased[238,253], suggesting periodic "drug holidays" could benefit patients who have progressed on BRAFi and MEKi. However, in clinical studies, cessation of BRAFi and/or MEKi therapy for several months re-sensitized to the inhibitors, though did not cause tumor regression[255,256], revealing how the diversity of resistance mechanisms, tumor heterogeneity and adaptability complicate response to drug withdrawal in patients. Our studies suggest downregulation or inactivation of PPP6C as an unappreciated mechanism influencing inhibitor sensitivity. This substantiates the identification of PPP6C in modulating sensitivity to BRAFi in an insertional mutagenesis screen in a mouse model of melanoma, and to MEKi in CRISPR/Cas9 screens conducted in NRAS and KRAS mutant cells in culture[140,143,257].

The toxicity associated with high level ERK signaling indicates that tumor cells harboring hyperactivating BRAF or RAS mutations rely on negative feedback control to maintain signaling within the fitness zone. For example, silencing expression of the ERK phosphatase DUSP6 is toxic to BRAF mutant melanoma and KRAS mutant lung cancer cells[258,259]. Indeed, in genome wide CRISPR/Cas9 screens, dependency on DUSP6 was highly correlated with dependency on PPP6C across a panel of melanoma cells lines, in keeping with PPP6C as a key negative regulator of ERK signaling. We hypothesize that through dephosphorylation of MEK, PPP6C likewise contributes to negative feedback control of the ERK pathway. While we did not observe changes in levels of PPP6C upon inhibition of BRAF-MEK-ERK signaling, we cannot rule out transcriptional control of PP6

regulatory or scaffolding subunits as a mechanism of feedback regulation. Furthermore, because phosphorylation of PP6 regulatory subunits can mediate recruitment to substrates and other interaction partners[249,260], targeting of MEK may be impacted by ERK-dependent phosphorylation or other modifications.

Atypically for a tumor suppressor, more than half of melanoma-associated PPP6C mutations occur recurrently in hotspots (Figure 1.4C). While frameshift/truncation mutations are less common, they do appear to be associated with reduced progression-free survival in melanoma[186]. Notably, non-recurrent mutations, while distributed in the primary sequence, do significantly cluster in the phosphatase catalytic center. Prior analysis of recurrent and non-recurrent PPP6C mutations indicate that all of them, to varying degrees, reduce catalytic activity[189,190]. These prior results are consistent with our observation that PPP6C mutations vary in their ability to suppress MEK phosphorylation. Given that PPP6C has been characterized as a "common essential" gene, it is possible that full loss of function is incompatible with cell proliferation. It has also been reported that PPP6C mutations weaken association with the PPP6R2 regulatory and ANKRD28 scaffolding subunits[190]. While the three-dimensional structure of a PP6 heterotrimer has not yet been determined, in the X-ray crystal structures of the PP2A-B56 holoenzyme, the residue analogous to R264 participates in interactions between catalytic and regulatory subunit[261]. In contrast, the same residue is not at the catalytic-regulatory subunit interface in structures of other PP2A holoenzymes[261,262]. This raises the possibility that PPP6C mutations might change the heterotrimer composition, favoring some regulatory subunits over others, which could favor selective dephosphorylation of substrates in a manner that preserves cell viability. By analogy, recurrent cancer-associated mutations in the PP2A scaffolding subunit PPP2R1A preferentially disrupt interactions with some regulatory B subunits rather than causing complete loss of function[191]. The capacity for specific complexes to restrain cell proliferation is key to the activity of recently developed PP2A small molecule activators,

which stabilize specific holoenzymes[263,264]. As with PP2A, at least some PP6 substrates are recruited through interaction with individual regulatory subunits[149,153,155,249], suggesting the potential for developing PP6 activators with therapeutic benefit.

While our studies implicate PP6 as a MEK phosphatase, early reports suggested that MEK is dephosphorylated by PP2A[235,236]. Indeed, downregulation of PP2A activity by loss or mutation of its scaffolding subunit PPP2R1A causes resistance to MEK inhibitors in KRAS mutated lung and colorectal cancer cell lines[191,265]. Likewise, enhancing PP2A activity through downregulation of endogenous inhibitor proteins or through small molecule activators sensitizes to MEK inhibition[265]. However, in these contexts PP2A promotes sensitivity to MEKi by restraining bypass PI3K/mTOR signaling and by direct dephosphorylation of MYC or ERK itself. Likewise, the tumor suppressor function of PP2A is suggested to involve other processes, such controlling the stability of MYC and β-catenin[266,267]. Notably, in addition to restraining ERK signaling, PP2A can also promote MEK phosphorylation through dephosphorylation of inhibitory feedback phosphorylation sites on RAF and KSR[234]. Because oncogenic mutant BRAF signals independently of KSR and is feedback-resistant[5], PP2A activity as a MEK phosphatase would not be counterbalanced by activation of upstream signaling. This phenomenon may explain our observation that like PP6, PP2A also contributes to MEK dephosphorylation in BRAF mutant 501mel cells. While we found that silencing PPP6C expression hyperactivates MEK in most cell lines we examined, this was not universally the case. The relative contributions of PP2A, PP6 and potentially other phosphatases to dephosphorylation of MEK is thus context dependent. Melanoma cells in particular are characterized by low PP2A activity, and the PP2A inhibitor protein CIP2A is an established transcriptional target of ERK signaling[268,269]. Interestingly, we observed that PP6 and PP2A catalytic subunit expression levels increase when the other is silenced (Figure 3.1A, B), suggesting compensation between the two complexes that could potentially influence dephosphorylation of any number of targets. Further work will be

necessary to understand the lineage-specific, signaling, or genetic contexts that dictate PPP6C regulation of MEK1/2.

CHAPTER 4: FUNCTIONAL CONSEQUENCES OF RECURRENT SOMATIC CANCER-ASSOCIATED MEK1 MUTATIONS AND DELETIONS

4.1 Introduction

MEK1 and MEK2 are dual specificity kinases that selectively activate ERK1/2 by phosphorylating a tyrosine and a threonine residue on its activation loop. Although MEK1 and MEK2 are structurally similar, sharing 80% sequence identity, they have non-redundant roles. MEK1 deficiency in mice is embryonic lethal whereas MEK2 deficiency in mice does not disrupt embryonic development[270,271]. It is thought that MEK1 can compensate for loss of MEK2 but not vice versa. MEK mutations observed in diseases are more commonly found in MEK1 (Figure 1.2), suggesting MEK1 has a more prominent role in development and disease. MEK1 has a core protein kinase catalytic domain with conserved features including a small N-lobe consisting of a 5-stranded β-sheet and αC-helix and a large α-helix-rich C-lobe[3,272] (Figure 4.1A). MEK1 has a proline rich insert unique to MEK1/2 in the protein kinase domain. The region N-terminal to the protein kinase domain contains a segment for ERK1/2 docking, a nuclear export sequence, and an inhibitory segment, also known as the negative regulatory region (NRR). The NRR, helix αA, stabilizes an inactive conformation of MEK1 by shifting the αC helix out of the active conformation. RAFs phosphorylate MEK1 at Ser218 and Ser222 of its activation loop, leading to conformational rearrangement into an active kinase conformation. Given the vital role of MEK1 in regulating fundamental cellular processes, MEK1 activity is highly regulated by intrapathway feedback mechanisms and cross-talk with other pathways (Figure 1.1A). Several regulatory and functional phosphorylation sites have been identified. MEK1 kinase activity is positively and negatively regulated by phosphorylation by PAK1, ERK1/2, and CDK5[3,245,273]. Many of these phosphorylation events have MEK1 activity independent consequences including cross-talk with the PI3K-AKT pathway through regulation of PTEN localization[4,274,275]. MEK1 activity is also

regulated by scaffolding proteins[276,277]. For example, KSR associates with MEK and binds RAF and ERK upon growth factor stimulation[278,279].

It was originally assumed that because of the essential roles of MEK1 in fundamental cellular processes and for viability in mice, germline mutations in MEK1 would be lethal. However, activating germline MEK1 mutations were first identified in cardio-facio-cutaneous (CFC) syndrome, a rare genetic disorder[280]. Somatic activating MEK1 mutations have been identified in various cancer types (Figure 4.1C). The first nonsynonymous MEK1 mutation associated with human cancer was discovered in an ovarian cancer cell line[281]. Since then, MEK1 mutations have been detected at low frequencies (4% or less) in lung adenocarcinoma[282-284], chronic lymphocytic leukemia[285], colorectal cancer[286-289], and gastric cancer[290,291]. MEK1 mutations are reported to have a high prevalence in rare cancers such as hairy cell leukemia and Langerhans cell histiocytosis[292-296]. In melanoma, MEK1 mutations have been found to occur at an overall frequency of less than 8% in tumors[18,19,287,297] (Figure 1.2), and identified in association with BRAF and MEK inhibitor resistant tumors[87,101-103,298,299] suggesting MEK1 mutations as resistance mechanisms to targeted therapies. However, there is also evidence suggesting MEK1 mutations preexist in treatment-naïve tumors and do not correlate with inhibitor resistance[300,301]. MEK1 mutations in cancers overlap with those in CFC. The major mutational hotspot is the NRR (Figure 4.1B, C). Several recurrent mutations within the catalytic domain are in residues proximal to the N-terminal end of the NRR in the three-dimensional structure of MEK1. Of these mutations, P124S/L is the most frequent MEK1 mutation in melanoma. A recurrent in-frame deletion, ΔE102-I103, is located on the loop between N-lobe β3 strand and the αC helix (Figure 4.1A). Several other in-frame deletions at the β3-αC loop region presumably share similar mechanisms of activation with ΔE102-I103. Despite most mutations clustering to a similar spatial region, these mutations exhibit differing activities in overexpression studies and MEK inhibitor

sensitivity profiles[297,302]. It is therefore likely that distinct MEK1 mutations have differing mechanisms of activation.

Elucidating the specific functional consequences of common somatic cancer-associated MEK1 mutations is important for understanding how MEK1 mutations contribute to or drive tumorigenesis and drug resistance. We selected 8 recurrent MEK1 mutations and in-frame deletions to investigate how MEK1 mutations alters activity (Figure 4.1B). Since we have completed these studies, other groups have published work with comprehensive biochemical and cellular characterization of tumor-associated MEK1 mutants, including our chosen mutants[251,303]. Our work presented here is consistent with the Rosen group's findings.

4.2 Results

4.2.1 MEK1 mutations increase MEK1 kinase activity

Cancer and CFC-associated MEK1 mutations have been widely characterized as gain-of-function mutations. To confirm our selected mutations as activating mutations and determine the level of kinase activity, MEK1 mutants, expressed and purified from HEK293T cells, were evaluated in *in vitro* kinase assays detecting MEK phosphorylation of ERK2. ERK2 phosphorylation by each mutant was compared to ERK2 phosphorylation by wild-type MEK1 (Figure 4.2). All MEK mutants we investigated have enhanced kinase activity against ERK2 compared to wild-type MEK1. The degree to which each mutation Is activating is highly variable. The activity of ΔE102-I103 deletion mutant is strikingly high (Figure 4.2B). The signal intensity for phosphorylated ERK2 was well above the linear dynamic range of signal detection to accurately determine the fold increase in activity compared to that of wild-type MEK1 or any of the other mutants. The other deletion mutant, ΔQ58-E62, has an 8.9-fold increase in activity compared to wild-type MEK1. The D67N mutant and the P124S mutant have modest increases in activity of < 3-fold. The remaining mutants are 4-7-fold more active than wild-type. The different

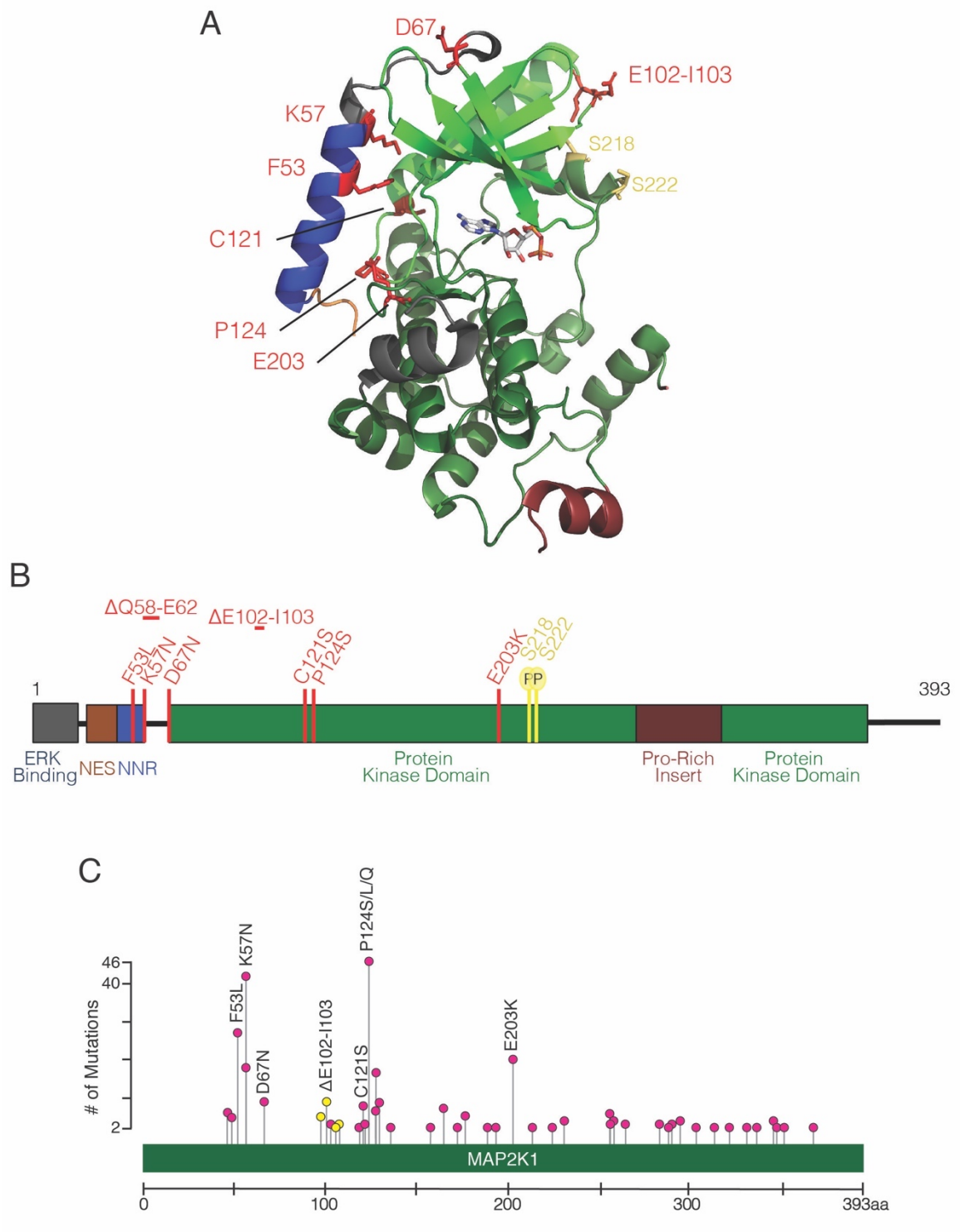

Figure 4.1 MEK1 Mutations

(A) 3D crystal structure of MEK1. (PDB:3EQI). Selected mutations (red) and activation loop phosphorylation sites (yellow) are shown in stick representation. Bound ADP (white) is shown stick representation.

(B) Linear representation of MEK1 protein. Organization of nuclear export signal (NES), negative regulatory region (NRR), protein kinase domain, proline-rich insert, and ERK docking segment is color coded as indicated. Selected mutations and in-frame deletion are indicated in red.

(C) Frequencies of MEK1 mutations reported in cancers 2 or more times. Data are from the cBioportal curated set of non-redundant studies.

levels of activation support the notion that mutations have different mechanisms of activation. The degree of ERK signaling activation in cells is likely influenced by the signaling context, in addition to structural consequences of the mutations.

4.2.2 MEK1 mutations alter basal activation loop phosphorylation levels

Upon phosphorylation at the activation loop, kinases undergo structural changes to adopt an active conformation. MEK1 is activated by RAF phosphorylation of its activation loop residues Ser218 and Ser222. MEK1 remains active until dephosphorylated at these sites by PP2A or, as we have shown in Chapter 3, PP6. Increased activation loop phosphorylation of MEK mutants may in part explain increased MEK activity. MEK1 mutants were examined for their relative levels of activation loop phosphorylation which we found were not necessarily correlative of their relative increases in activity (Figure 4.3). P124S and D67N mutants have reduced basal activation loop phosphorylation despite having higher activity than wild-type MEK1. The F53L mutant had the same basal phosphorylation levels as wild-type and 4-fold higher activity. The remaining mutants have higher activation loop phosphorylation than wild-type MEK1. The activation loop phosphorylation of the ΔE102-I103 mutant is considerably higher than any other mutant and >40 fold higher than wild-type.

The inconsistency between basal activation loop phosphorylation and kinase activity identifies distinct groups of mutations. P124S and D67N mutants are underphosphorylated, suggesting their modest increases in basal activity is not attributed to increased activation by upstream RAFs. The F53L, K57N, C121S, E203K, and ΔQ58-E62 mutants have more correlative activation loop phosphorylation levels and activity levels. In these cases, activation loop phosphorylation most likely contributes to increased kinase activity. The extremely high levels of activation loop phosphorylation and activity of ΔE102-I103 suggest factors other than activating phosphorylation are involved in its mechanism of action.

4.2.3 MEK1 mutations can disrupt or enhance binding to regulatory binding partners

MEK activity is regulated by key binding partners. BRAF-MEK1 complexes are enriched in wild-type BRAF cells and mutant RAS cells[304]. Pathway activation induces BRAF dimerization and phosphorylation of MEK1 which then dissociates from BRAF to activate ERK. Depending on the genetic background, MEK1 mutations may alter MEK1 interactions with RAFs impacting pathway activation. Additionally, KSR1 scaffolding protein binds MEK1 via the proline-rich region to regulate MEK activation by RAF[279]. In the context of wild-type BRAF (HEK293T cells), most MEK1 mutants immunoprecipitated similar amounts of CRAF, BRAF, and KSR1 (Figure 4.4). Interestingly, the C121S mutation disrupts interaction with CRAF, BRAF, and KSR1. The ΔQ58-E62 and ΔE102-I103 deletion mutants do not bind BRAF as well as wild-type MEK1 but bind similarly to CRAF and KSR1. This is not surprising given these deletion mutants have the highest activation loop phosphorylation levels, which favors dissociation from BRAF. Interestingly, P124S has enhanced interactions with BRAF and CRAF, which is consistent with P124S having the lowest activation loop phosphorylation levels.

MEK1 mutant interactions with other binding partners should be explored for their consequences on MEK1 signaling. Changes in binding to MEK phosphatases and substrates (ERK1/2) directly impact signaling propagation further downstream.

4.3 Discussion

Our work characterizing MEK1 mutations, though limited, provide key insight into MEK1 mutant activation and the genetic contexts they are observed in. The wide range of activation levels observed with MEK1 mutations is surprising because ERK pathway activation promotes cell fitness only when within an optimal range. Low and high pathway activation can be toxic to cells. The extreme ERK activation with the ΔE102-I103 mutation is unlikely to be tolerable in contexts where ERK activation is already elevated. In patient samples, this deletion does not co-occur with mutations in other ERK

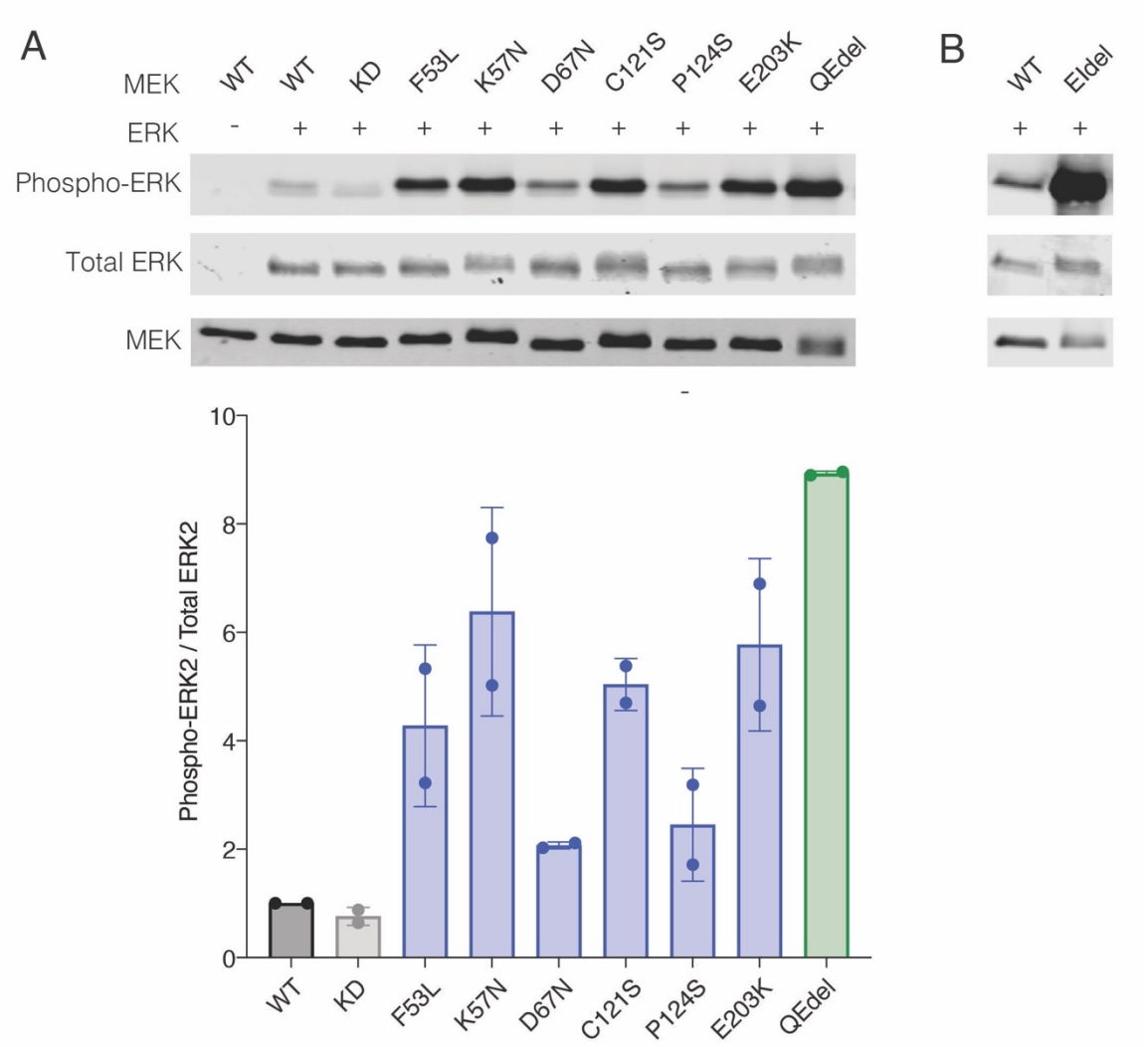

Figure 4.2 MEK1 mutations increase MEK1 kinase activity

(A) MEK1 wild-type (WT), kinase dead (KD), and mutants were purified from HEK293T cells and incubated with ERK2 for 30 minutes. Reactions were evaluated by immunoblot. Quantification of ERK2 phosphorylation levels shown relative to the WT reaction. $n = 2$.

(B) MEK1 wild-type (WT) and ΔE102-I103 deletion mutant (EIdel) kinase reactions run parallel to reactions in (A). Reactions were evaluated separately to avoid signal interference from hyperphosphorylated ERK.

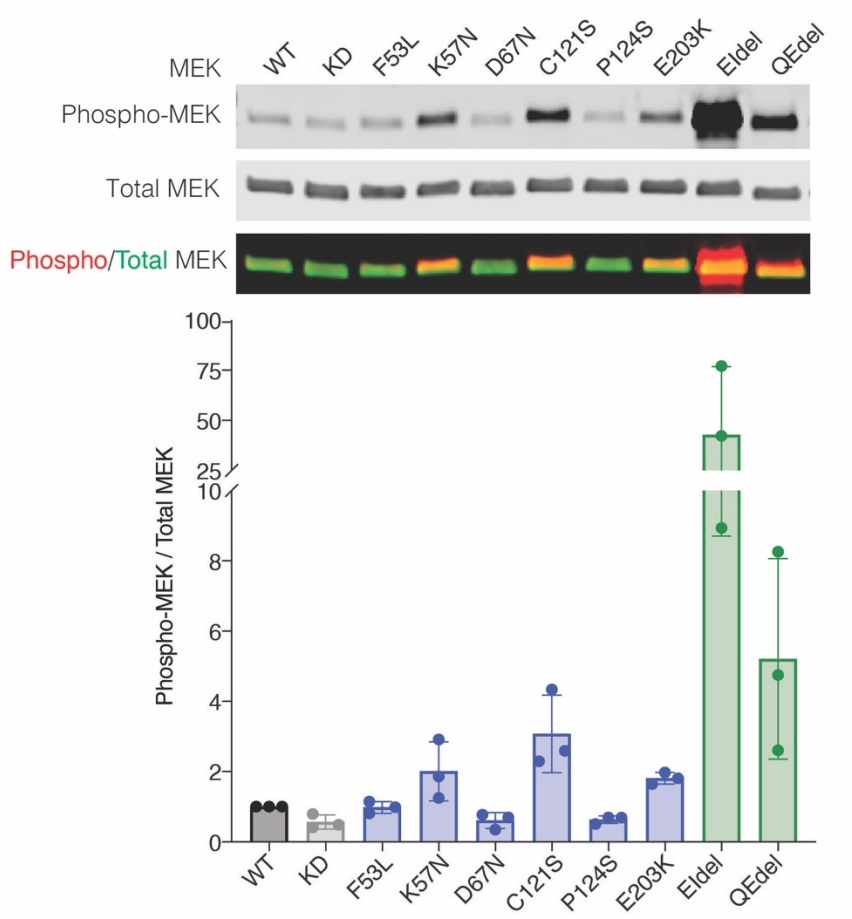

Figure 4.3 MEK1 mutations alter basal activation loop phosphorylation levels

MEK1 wild-type (WT), kinase dead (KD), and mutants were purified from HEK293T cells evaluated by immunoblot for MEK phosphorylation at S218 and S222. Quantification of MEK1 phosphorylation levels shown relative to the WT reaction. $n = 3$.

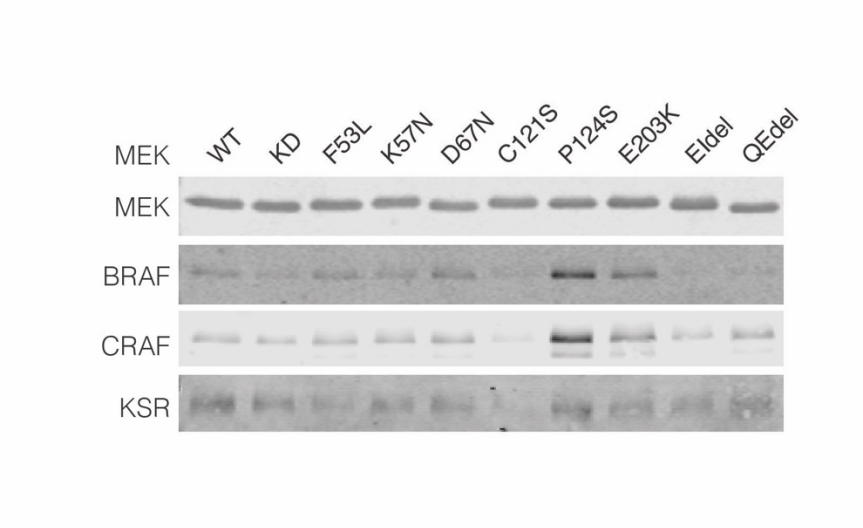

Figure 4.4 MEK1 mutations can disrupt or enhance binding to regulatory binding partners

MEK1 wild-type (WT), kinase dead (KD), and mutants were purified from HEK293T cells evaluated by immunoblot for co-immunoprecipitation of BRAF, CRAF, and KSR1

pathway components and are present only in the triple wild-type genetic subtype of melanoma[77,305]. However, mutations with modest increases in activity, like P124S and D67N, commonly occur with BRAF mutations, NRAS mutations, NF1 mutations, or other MEK1 mutations. Interestingly, MEK1 mutations are generally not present in cancer types with low RAS and RAF mutation rates.

In the context of BRAFi resistance, C121S, E203K, and K57N mutations have been detected in progressive tumors but not in patient-matched MAPKi naïve tumors[101,102,299]. The moderate increases in ERK activity for these mutations contribute to acquired resistance to BRAFi through MAPK reactivation. However, P124 mutations found in progressive tumors were also present in treatment naïve tumors of the same patient[89,300,301]. Pre-existing P124 mutations are associated with poorer response and shorter progression free survival with BRAFi therapy compared to wild-type MEK1. Progressive tumors from patients with pre-existing P124 mutations acquire NRAS mutations or BRAF amplification for BRAFi resistance[91,300]. The modest elevation in MEK1 activity from P124 mutations may contribute to drug resistance but is insufficient to confer resistance alone.

Many MEK1 mutations and deletions map to or spatially near the NRR. Loss or interruption of the helical secondary structure of the NRR results disrupts its stabilization of an inactive conformation and results in elevated MEK1 activation independent of activation loop phosphorylation[306]. ΔQ58-E62, F53L, K57N, and D67N are a part of the NRR helix, (Figure 4.1A). P124S, E203K, and C121D map to regions spatially proximal and potentially interacting with the NRR helix. The disparate activity levels and activation loop phosphorylation levels of these mutants we observed show the activating mechanisms of these mutations are more complex than just the relief of an intramolecular negative regulatory mechanism. ΔE102-I103 is a deletion in the β3-αC loop. Similar activating deletions in the β3-αC loop have been detected in EGFR and BRAF[231,307].

These deletions presumably constrain the αC helix in an active conformation.

Our findings were consistent with the Rosen group's characterizations of these mutants[251]. They identify 3 classes of MEK1 mutations. Class 1 mutants are dependent on the activation loop phosphorylation by RAF for hyperactivation and always co-occur with RAS, RAF, and NF1 mutations in tumors. This class include the D67N and P124S mutants we characterized to have modest increases activation with decreased activation loop phosphorylation compared to wild-type MEK1. The authors demonstrate that additional phosphorylation of these mutants beyond the basal levels result in hyperactivated MEK1. Class 2 mutants have elevated intrinsic activity that is further activated by RAF phosphorylation of the activation loop. These mutations can sometimes co-occur with RAS, RAF, or NF1 mutations in tumors and are associated with acquired BRAFi resistance. The F53L, K57N, C121S, and E203K are class 2 mutations. We found these mutations to have moderate increases activity and activation loop phosphorylation compared to wild-type MEK. Class 3 mutants, which are β3-αC loop region deletions, autophosphorylate and therefore are activation loop phosphorylation independent and intrinsically hyperactive. There is evidence that these deletion mutations promote MEK1 homodimerization and intradimer cross-phosphorylation of activation loops[303]. These mutations, which include the hyperactive and hyperphosphorylated ΔE102-I103 deletion mutant from our studies, do not co-occur with RAS, RAF, or NF1 mutations.

CHAPTER 5: CONCLUDING REMARKS

The ERK signaling pathway is one of the most thoroughly investigated signaling pathways. With increasing activation, ERK signaling proceeds from stimulating cell growth and proliferation to promoting malignant transformation and then to inducing cytotoxicity at extremely high levels of pathway activation. Accordingly, the ERK signaling cascade is central to a broader and more complex signal transduction network. This includes a multitude of regulators and regulatory mechanisms which have been exhaustively studied and described. Mutations or other alterations in the cascade or this extended network shifts signaling levels to initiate tumorigenesis or MAPKi resistance. In this dissertation,

we describe the identification of modulators of MEKi sensitivity in melanoma, discovery of a novel MEK regulator, and the biochemical and cellular characterization of cancer-associated genetic lesions.

Establishing PP6 as a MEK phosphatase provides a mechanistic explanation supporting previous assumptions of PPP6C being a tumor suppressor based on occurrences of PPP6C mutations in melanoma. In terms of potential clinical implications, our work characterizing melanoma-associated PPP6C mutations suggests these loss-of-function mutations may be predictive of poor or limited response to MAPKi therapy. Conversely, activating PPP6C may sensitize cells to MAPKi. The recent development of small molecule PP2A activators that stabilize specific PP2A holoenzymes[263,264] demonstrate the potential for development of PP6 activators for use in combination with other MAPKi to treat $BRAF^{V600E}$ melanoma.

Our characterization of both cancer-associated MEK1 mutations and PPP6C mutations demonstrates how activating mutations in an oncogene and loss-of-function mutations in a tumor suppressor can result in similar signaling consequences These mutations all result in MEK activation which has clear implications for these mutations in tumorigenesis and MAPKi response. However, the levels of MEK activation are highly

variable among all MEK and PPP6C mutants indicating a diversity in the mechanisms of activation and physiological consequences.

Expanding the intricate ERK signaling regulatory network to include PP6 raises new questions related to PP6 involvement in the numerous ERK signaling cellular functions in normal and pathological conditions. These questions, many of which are posed in chapter discussion sections (2.3, 3.3) include determining the specific contexts that govern PP6 regulation of MEK and understanding the functions and distribution of different PP6 holoenzymes. However, in addition to revealing what is not yet understood about PPP6C, the work presented in this dissertation principally contributes to our understanding of ERK signaling regulation.

APPENDIX

Materials

REAGENT or RESOURCE	SOURCE	IDENTIFIER
Antibodies		
PPP6C, rabbit polyclonal	Bethyl Laboratories, Inc	Cat# A300-844A; RRID: AB_2168899
Phospho-MEK1/2 (Ser217/221), rabbit polyclonal	Cell Signaling Technology	Cat# 9121; RRID: AB_331648
Phospho-MEK1/2 (Ser217/221) (41G9), rabbit monoclonal	Cell Signaling Technology	Cat# 3958; RRID: AB_2138014
Phospho-MEK1 (Ser298), rabbit polyclonal	Cell Signaling Technology	Cat# 9128; RRID:AB_330810
Phospho-MEK1 (Thr286), rabbit polyclonal	Cell Signaling Technology	Cat# 9127; RRID: AB_331654
MEK1/2, rabbit polyclonal	Cell Signaling Technology	Cat# 9122; RRID: AB_823567
MEK1/2 (L38C12), mouse monoclonal	Cell Signaling Technology	Cat# 4694; RRID: AB_10695868
P44/42 MAPK (ERK1/2), rabbit polyclonal	Cell Signaling Technology	Cat# 9102; RRID: AB_330744
Phospho-p44/42 MAPK (ERK1/2) (Thr202/Tyr204) (E10), mouse monoclonal	Cell Signaling Technology	Cat# 9106; RRID: AB_331768
RAF-B (F-7), mouse monoclonal	Santa Cruz Biotechnology	Cat# sc-5284; RRID: AB_626760
RAF-1 (C-12), rabbit polyclonal	Santa Cruz Biotechnology	Cat# sc-133; RRID: AB_632305
A-RAF (D2P9P), rabbit monoclonal	Cell Signaling Technology	Cat# 75804; RRID: AB_2799875
Phospho-Aurora A (Thr288) (CD39D8), rabbit monoclonal	Cell Signaling Technology	Cat# 3079; RRID: AB_2061481
Aurora A (1F8), mouse monoclonal	Cell Signaling Technology	Cat# 12100; RRID: AB_2797820
PP2A C Subunit (52F8), rabbit monoclonal	Cell Signaling Technology	Cat# 2259; RRID: AB_561239
Caspase-3, rabbit polyclonal	Cell Signaling Technology	Cat# 9662; RRID: AB_331439
PARP (46D11), rabbit monoclonal	Cell Signaling Technology	Cat# 9532; RRID: AB_659884
ETV4, rabbit polyclonal	Proteintech	Cat# 10684-1-AP; RRID: AB_2100984
DUSP6/MKP3, rabbit polyclonal	Cell Signaling Technology	Cat# 39441; RRID: AB_2799156
SPRY2 (D3G1A), rabbit monoclonal	Cell Signaling Technology	Cat# 14954l RRID: AB_2798658

Phospho-BRAF (Ser445), rabbit polyclonal	Cell Signaling Technology	Cat# 2696; RRID: AB_390721
Phospho-BRAF (Thr401) (JJ08-72), rabbit monoclonal	Invitrogen	Cat# MA5-32430; RRID: AB_2809708
Phospho-BRAF (Thr753), rabbit polyclonal	Invitrogen	Cat# PA5-37498; RRID: AB_2554107
Phospho-MEK1 (Thr292) (D5L3K), rabbit monoclonal	Cell Signaling Technology	Cat# 26975; RRID: AB_2798935
KSR1, rabbit polyclonal	Cell Signaling Technology	Cat# 4640; RRID: AB_ 10544539
Normal mouse IgG	Santa Cruz Biotechnology	Cat# sc-2025; RRID: AB_737182
FLAG M2, mouse monoclonal	Sigma	Cat# F3165; RRID: AB_259529
Penta-HIS, mouse monoclonal	Qiagen	Cat# 34660; RRID: AB_2619735
Goat anti-Rabbit secondary antibody, Alexa Fluor 680	Invitrogen	Cat# A32734; RRID: AB_2633283
Goat anti-Mouse secondary antibody, Alexa Fluor 800	Invitrogen	Cat# A32730; RRID: AB_2633279
Chemicals, Peptides, and Recombinant Proteins		
Selumetinib (AZD6244)	SelleckChem	Cat# S1008
Trametinib (GSK1120212)	SelleckChem	Cat# S2673
Vemurafenib (PLX4032)	SelleckChem	Cat# S1267
Puromycin	Thermo Fisher Scientific	Cat# A1113803
Nocodazole	Sigma	Cat# M1404
Okadaic Acid	Enzo Life Sciences	Cat# ALX-350-063
3xFLAG peptide	Sigma	Cat# F4799
Anti-FLAG M2 affinity gel	Sigma	Cat# A2220
Critical Commercial Assays		
QuikChange II Kit	Agilent	Cat# 200521
Gateway LR Clonase II Enzyme Kit	Thermo Fisher Scientific	Cat# 11791100
Lipofectamine RNAiMAX Reagent	Thermo Fisher Scientific	Cat# 13778100
DNeasy Blood and Tissue Kit	Qiagen	Cat# 69504
Pierce BCA Protein Assay	Thermo Fisher Scientific	Cat# 23250

Experimental Models: Cell Lines		
501mel (human)	Yale SPORE in Skin Cancer Biospecimen Core	
A375 (human)	Laboratory of Harriet Kluger	
YUGEN8 (human)	Yale SPORE in Skin Cancer Biospecimen Core	
YUZEAL (human)	Yale SPORE in Skin Cancer Biospecimen Core	
YUSIK (human)	Yale SPORE in Skin Cancer Biospecimen Core	
YURIF (human)	Yale SPORE in Skin Cancer Biospecimen Core	
YUGASP (human)	Yale SPORE in Skin Cancer Biospecimen Core	
SK-MEL-103 (human)	Laboratory of Narendra Wajapeyee	
SK-MEL-30 (human)	Laboratory of Craig Crews	
M318 (human)	Laboratory of Narendra Wajapeyee	
MEL-ST (human)	Laboratory of Narendra Wajapeyee	
A549 (human)	ATCC	Cat# CCL-185; RRID: CVCL_0023
HCT116 (human)	ATCC	Cat# CCL-247; RRID: CVCL_0291
SW620 (human)	ATCC	Cat# CCL-227; RRID: CVCL_0547
RKO (human)	ATCC	Cat# CRL-2577; RRID: CVCL_0504
U2OS (human)	ATCC	Cat# HTB-96; RRID: CVCL_0042
HEK293T (human)	ATCC	Cat# CRL-11268; RRID: CVCL_1926
Bacterial Strains		
MAX efficiency DH5α	Thermo Fischer Scientific	Cat# 18258012
One Shot Stbl3	Thermo Fischer Scientific	Cat# C737303
Oligonucleotides		
CRISPR PPP6C sgRNA 2a (CACCGTGAGAGTAGACAGATAACAC)		

CRISPR PPP6C sgRNA 2b (AAACGTGTTATCTGTCTACTCTCAC)		
CRISPR PPP6C Sequencing Primer F (CAGATTCTTGTAGATTTCCCTGGAATC)		
CRISPR PPP6C Sequencing Primer R (CTTTGAGGCACAGATCTAGAAAGATG)		
BRAF siRNA (UCUGUAAGGCUUUCACGUUAUA)	Horizon Discovery	
ARAF siRNA (UUUCGUCCCUUGAUGAGUCGGU)	Horizon Discovery	
CRAF siRNA (UCUCUGAAAACAUGUGUUCUGC)	Horizon Discovery	
siGENOME Non-Targeting siRNA #2	Horizon Discovery	Cat# D-001210-02-05
ON-TARGETplus Human PPP2CA (5515) siRNA – SMARTpool	Horizon Discovery	Cat# L-003598-01-0005
ON-TARGETplus Human PPP2CB (5516) siRNA – SMARTpool	Horizon Discovery	Cat# L-003599-00-0005
ON-TARGETplus Human PPP6R1 siRNA (A)	Horizon Discovery	Cat# J-020420-09-0002
ON-TARGETplus Human PPP6R1 siRNA (B)	Horizon Discovery	Cat# J-020420-10-0002
ON-TARGETplus Human PPP6R2 siRNA (A)	Horizon Discovery	Cat# J-021331-09-0002
ON-TARGETplus Human PPP6R2 siRNA (B)	Horizon Discovery	Cat# J-021331-11-0002
ON-TARGETplus Human PPP6R3 siRNA (A)	Horizon Discovery	Cat# J-014646-09-0002
ON-TARGETplus Human PPP6R3 siRNA (B)	Horizon Discovery	Cat# J-014646-10-0002
Recombinant DNA		
pSpCas9(BB)-2A-GFP (PX458)	Addgene	Cat# 48138
pSpCas9(BB)-2A-GFP_hPPP6C-2		
pDONR223_PPP6C_WT	Addgene	Cat# 81811
pLEX_305	Addgene	Cat# 41390
pLEX_305-PPP6C-WT		
pLEX_305-PPP6C-D84N		
pLEX_305-PPP6C-H55Y		
pLEX_305-PPP6C-P186S		
pLEX_305-PPP6C-P259S		

pLEX_305-PPP6C-R264C		
pLEX_305-PPP6C-S270L		
pLEX_305-GFP		
pLKO.1_shPPP6C-1	Sigma	TRCN0000379835
pLKO.1_shPPP6C-2	Sigma	TRCN0000002767
pREP4-MEK1	[308]	
pcDNA3-His6-MEK1	[309]	
pcDNA3-His6-MEK1-K57N		
pcDNA3-His6-MEK1-F53L		
pcDNA3-His6-MEK1-D67N		
pcDNA3-His6-MEK1-C121S		
pcDNA3-His6-MEK1-P124S		
pcDNA3-His6-MEK1-E203K		
pcDNA3-His6-MEK1-ΔQ58-E62		
pcDNA3-His6-MEK1- ΔE102-I103		
pcDNA3-His6-MEK1-K97M		
pcDNA3-His6-MEK2		
pGEX4T3_ERK2	[310]	
pET22b-MEK1	Laboratory of Titus Boggon	
pET22b-MEK1-DE102_I103		
pFLAG-BRAF-V600E		
pFLAG-PPP6C		
psPAX2	Addgene	Cat# 12260
pCMV-VsV-G	Addgene	Cat# 8454
pCMV-dR8.91		

pV1900	[311]	
pV1900-PPP6R3		
pV1900-ANKRD28		
pFLAG-PPP6R1		
pFLAG-PPP6R2		
pFLAG-PPP6R3		
Software and Algorithms		
GENE-E	Broad Institute	https://software.broadinstitute.org/GENE-E/
GraphPad Prism	GraphPad	https://www.graphpad.com
RIGER	Broad Institute	https://software.broadinstitute.org/GENE-E/extensions.html
PYMOL	Schrodinger	https://pymol.org/
Image Studio Lite	LI-COR Biosciences	https://www.licor.com/bio/image-studio-lite/
ImageJ	NIH	https://imagej.nih.gov/ij/
ImageJ plugin ColonyArea		https://b2share.eudat.eu/records/39fa39965b314f658e4a198a78d7f6b5

Cell Lines and Culture Conditions

501mel, YUGEN8, YUZEAL, YUSIK, YURIF, and YUGASP cells were cultured in Opti-MEM medium (Gibco) supplemented with 5% fetal bovine serum (FBS) (Gibco) and 1% penicillin/streptomycin (P/S, Gibco). A375 cells were cultured in Opti-MEM medium supplemented with 10% FBS and 1% P/S. MEL-ST, U2OS, and HEK293T cells were cultured in DMEM medium (Gibco) supplemented with 10% FBS and 1% P/S. SK-MEL-103, SK-MEL-30, HCT116, and M318 cells were cultured in RPMI 1640 medium (Gibco) supplemented with 10% FBS and 1% P/S. RKO were cultured in MEM medium (Gibco) supplemented with 10% FBS and 1% P/S. All cell lines were cultured at 37°C under 5% CO_2.

Methods

Plasmids, Cloning, and Mutagenesis

Plasmids harboring cDNAs of PPP6C, PPP6R1, PPP6R3 and ANKRD28 in pDONR223 were from the human ORFeome collection (v8.1), and the PPP6R2 cDNA was from Transomic. The lentiviral expression vector pLEX_305-PPP6C and the transient expression plasmid pVL1900-ANKRD28 (untagged) were generated by Gateway recombination cloning into their respective destination vectors. The untagged expression vector for PPP6R3 used for preparation of PP6 complexes was generated by Gateway recombination into pV1900 followed by QuikChange mutagenesis to insert a stop codon upstream of the FLAG tag. The transient expression vector for N-terminally FLAG-tagged PPP6C, PPP6R1, PPP6R2 and PPP6R3 were made by PCR amplification of the coding sequence from the source plasmid and inserting into pcDNA3-FLAG by either Gibson assembly (PPP6R3) or restriction enzyme cloning (all others). The mammalian expression vector for N-terminally 6xHis-tagged MEK2 was generated by shuttling the entire coding sequence from pRSET-MEK2 (obtained from the laboratory of Natalie Ahn) and into pcDNA3. All mutants were generated using QuikChange Site Directed Mutagenesis following standard protocols. Constructs were verified by Sanger sequencing through the entire open reading frame.

Recombinant Lentivirus Production and Cell Infection

shRNA lentiviruses were packaged in low passage HEK293T cells by polyethylenimine (PEI) co-transfection with packaging constructs dR8.91 and VsV-G (Addgene, 8454). PPP6C expression lentiviruses were packaged in low passage 293T cells by PEI co-transfection with packaging constructs psPAX2. (Addgene, 12260) and VsV-G (Addgene, 8454). For PEI co-transfection, lentiviral transfer plasmid:packaging plasmid:envelope plasmid ratio was at 10:10:1 with the PEI:DNA ratio at 3:1. Supernatant

media containing virus was collected at 48 hours post transfection. Cells were infected with lentivirus at an MOI of 0.3-0.4 in the presence of 4ug/mL polybrene for 24 hours and selected for >48 hours in fresh media containing (1.5-2.5 ug/mL) puromycin.

shRNA Screening

The shRNA library was custom generated by pooling human MISSION shRNA constructs (Sigma) targeting all annotated protein kinases and phosphatases and packaged into lentiviral particles as described above. To initiate the screen, 501mel cells were transduced for 24 hours with the lentiviral library in 0.4 μg/ml polybrene at an MOI of 0.3 to assure that most cells receive a single viral integration. A sufficient number (8×10^6) of cells were infected to ensure >1,000-fold coverage for each unique shRNA in the library for a reference sequencing sample and for each drug condition. Infected cells were selected with 1.8 μg/mL puromycin for 48 hours, trypsinized, and 8×10^6 cells were reserved for the T_0 reference sample. For the remainder, 8×10^6 cells were plated for each of the 5 conditions: 0.0001% DMSO vehicle control, 1 nM trametinib, 3.3 nM trametinib, 33 nM selumetinib, and 100 nM selumetinib. Every two doublings, cells were counted, and 8×10^6 cells were replated for propagation. The screen was carried out for 10 total population doublings (T_{10}). Genomic DNA from the T_0 and T_{10} samples for each of the drug conditions was extracted using Qiagen DNeasy Blood and Tissue Kit (Qiagen, Cat No. 69504), following the manufacturer's protocol. For each drug condition/time point sample, the shRNA integrants were PCR-amplified from the genomic DNA with barcoded primers and sequenced on an Illumina HiSeq instrument. The RIGER algorithm in GENE-E (www.broadinstitute.org/cancer/software/GENE-E/) was used to rank each gene by their enrichment.

MEKi Dose Response Assays

Cells (750 per well) were seeded in 96-well black/clear bottom plates, allowed to recover overnight, and treated with varying concentrations of trametinib or selumetinib (6 wells/concentration) in fresh media for 72 h. Media aspirated and replaced with fresh media containing 44 μM resazurin (alamarBlue Cell Viability Reagent, Fisher Scientific). Plates were incubated in the dark for 4 hours at 37°C, and fluorescence (excitation 560 nm; emission 590nm) was measured on a plate reader. When MEKi treatment was initiated, starting time reading was obtained on a separate plate containing untreated cells. Starting point readings were subtracted from the 72 h readings to measure overall growth inhibition. Dose response curves were generated with GraphPad Prism.

Clonogenic Growth Assays

Cells (1×10^3) were plated in each well of a six-well plate containing 3 mL of media with or without MEKi and cultured at 37°C under 5% CO_2 undisturbed for 14 days. Media was removed, and cells were gently washed with PBS. The cells were stained with crystal violet staining solution (0.5% crystal violet, 6% formaldehyde, 1% methanol in PBS) for 15 min and washed 3 times with water. Plates were air-dried and imaged. For experiments characterizing PPP6C mutants, cells (2.5×10^3) were plated in 12 well plates containing 1 mL media with or without MEKi.

Cell Lysis and Immunoblot Analysis

Cells were placed on ice, washed twice with cold PBS, and lysed in cold lysis buffer (20 mM Tris [pH 8.0], 137 mM NaCl, 10% glycerol, 1% Igepal CA-630, 1 mM PMSF, 1 mM Na_3VO_4, 10 μg/mL leupeptin, 2 μg/mL pepstatin A, 10 μg/mL aprotinin) for 15 min. Cell lysates were scraped into 1.5 mL tubes and clarified in a 4 °C microcentrifuge at 13,000 rpm for 10 min. Cleared lysates were analyzed by BCA protein assay. 4X SDS-PAGE loading buffer was added to lysates to prepare immunoblot samples. Equal amounts of lysate (15 μg per lane) were fractionated by SDS-PAGE and transferred to polyvinyl

difluoride (PVDF) (Sigma, IPFL85R) membrane. Membranes were blocked in Tris buffered saline (TBS) with 5% non-fat milk for one h and probed overnight at 4 °C with primary antibodies diluted according to manufacturer's recommendations. Membranes were incubated for 1 h in fluorescently-labeled secondary antibodies diluted 1:10,000 in TBS with 5% bovine serum albumin (BSA) and 0.1% Tween20. Western blots were imaged with an Odyssey CLx imaging system (LI-COR Biosciences), and densitometry-based quantification was carried out with Image Studio Lite.

Co-immunoprecipitation

HEK293T cells in 10 cm plates were transiently transfected with equal amounts of pREP-MEK1 (untagged) and FLAG tagged PP6 subunit plasmid precomplexed with polyethyleneimine (PEI) at a 3:1 ratio with DNA. After 48 h, cells were placed on ice and washed twice with cold PBS. On the second PBS wash, cells were scraped into 1.5 mL tubes and pelleted at 1000 rpm for 5 min. Cells were resuspended in 300 μL hypotonic lysis buffer (10 mM Tris-HCl [pH 8.0], 1 mM KCl, 1.5 mM $MgCl_2$, 0.5 mM DTT, 0.05% Igepal CA-630, 1 mM PMSF, 1 mM Na_3VO_4, 10 μg/mL leupeptin, 2 μg/mL pepstatin A, 10 μg/mL aprotinin) and kept on ice for 5 min. Cell lysates were vortexed for 1 minute and run three times through a 25G needle with a syringe. Lysates were spun at 3500 rpm for 10 minutes in a 4°C microcentrifuge. A portion (30 μL) of the supernatant was reserved for analysis of the whole cell lysate sample. The remaining total supernatant was brought to a volume of 500 μL with additional hypotonic lysis buffer, and the [NaCl] was adjusted to 150 mM. Anti-FLAG M2 Affinity Gel beads (Sigma, A2220) were blocked in 5% BSA-TBS solution for 1 h, equilibrated to hypotonic lysis buffer, and 30 μL of the suspension was added to each supernatant. Samples were rotated at 4°C overnight. Beads were pelleted and washed with cold wash buffer 1 (20 mM Tris [pH 7.5], 150 mM NaCl, 1% Triton X-100, 2.5 mM $Na_4P_2O_7$, 1 mM β-glycerophosphate, 3 mM β-

mercaptoethanol, 1 mM PMSF, 1 mM Na_3VO_4, 10 μg/mL leupeptin, 2 μg/mL pepstatin A, 10 μg/mL aprotinin) for 10 minutes, followed by one quick and one 10 min wash with cold wash buffer 2 (50 mM HEPES [pH 7.4], 150 mM NaCl, 3 mM β-mercaptoethanol, 0.1 mM Na_3VO_4, 0.01% Igepal CA-630, 10% glycerol). Beads were resuspended in 30 μL 2X SDS buffer (100mM Tris-Cl [pH 6.8], 4% SDS, 20% glycerol) and boiled for 5 min. Samples were centrifuged in Whatman UNIFILTER 0.45 μm plates (Sigma, WHA77002808) at 4000 rpm for 10 minutes to remove beads, and 4X SDS-PAGE loading buffer was added to filtrates. Samples were analyzed via immunoblot as described above.

Generation of CRISPR/Cas9 Knockout Cell Lines

CRISPR/Cas9 constructs were generated by cloning sgRNA sequences into pSpCas9(BB)-2A-GFP (Addgene, 48138) according to the cloning protocol established by the Zhang lab (https://www.addgene.org/browse/article/7475/). Two sets of sgRNA oligos were used but only one sgRNA targeting exon 4 resulted in PPP6C knockout clones. pSpCas9(BB)-2A-GFP was used to generate negative control clones. 501mel cells were transfected with CRISPR/Cas9 constructs via PEI, and 48 hours post transfection, cells were trypsinized. After centrifugation and removal of media/trypsin, cells were resuspended in PBS and transferred to FACS tubes. Single GFP positive cells were sorted into 96 well plates via a BD FACSAria instrument. 96 well plates were treated with 0, 1, or 2 nM trametinib and incubated for several weeks until colonies were observed. PPP6C knockout 501mel cell colonies only grew out in the presence of trametinib and were maintained in 1-2 nM trametinib but withdrawn from trametinib $\geq$24 h before experiments. PPP6C knockout was confirmed by immunoblot and sanger sequencing of PCR amplified target site.

Protein Purification

MEK1 and MEK1 mutants were expressed in HEK293T cells by PEI transfection with pcDNA3-His-MEK1 alone or in a 4:1 ratio with pFLAG-BRAF-V600E to generate phosphorylated MEK1 (for PP6 phosphatase assays). After 40 h, plates were put on ice and washed once with ice-cold PBS. To lyse cells, 1 mL ice cold lysis buffer (20 mM Tris [pH 7.5], 150 mM NaCl, 1% Triton X-100, 2.5 mM $Na_4P_2O_7$, 1 mM β-glycerophosphate, 1mM Na_3VO_4, 3 mM β-mercaptoethanol, 1 mM PMSF, 10 μg/mL leupeptin, 2 μg/mL pepstatin A, 10 μg/mL aprotinin) was added to each plate. Lysates were scraped into 1.5 mL tubes, incubated on ice for 10 minutes, and clarified in a microcentrifuge at 13,000 rpm for 10 min at 4°C. Supernatants were transferred to fresh tubes, and 50 μL of Talon resin (Takara) was added. Samples were rotated for 2 hours at 4 °C. Beads were pelleted for (2 min, 4000 rpm) at 4°C microcentrifuge, washed twice with lysis buffer containing 10 mM imidazole, and transferred into a column. Beads were washed with 2 mL of wash buffer (50 mM HEPES [pH 7.4], 150 mM NaCl, 3 mM β-mercaptoethanol, 10 mM imidazole, 0.01% Igepal CA-630, 10% glycerol), and MEK1 was eluted in 150 μL fractions with wash buffer + 250 mM imidazole. The two most concentrated fractions as determined by Bradford assay (Bio-Rad, 5000006) were combined and dialyzed overnight at 4°C into 20 mM HEPES [pH 7.4], 150 mM NaCl, 1 mM DTT, 10% glycerol, 0.01% Igepal CA-630. Protein concentration was estimated from Coomassie-stained 10% polyacrylamide gels using a BSA standard curve

To prepare PP6 complexes, HEK293T cells were co-transfected in 15 cm plates with 4 μg pFLAG-PPP6C, 8.6 μg pV1900-PPP6R3 and 8.6 μg pV1900-ANKRD28 pre-complexed with 63.3 μg PEI. Cells were lysed 40 hours post-transfection after washing with cold PBS in 2.25 μL CHAPS lysis buffer (50 mM Tris [pH 7.5], 150 mM NaCl, 0.3% CHAPS, 1 mM PMSF, 10 μg/mL leupeptin, 2 μg/mL pepstatin A, 10 μg/mL aprotinin) per

plate. Lysates were cleared as above, and M2 anti-FLAG affinity gel (33 μL per plate) was added to the supernatant. Samples were rotated at 4 °C for 1 hr, and beads were pelleted, washed three times with lysis buffer (0.3 mL per plate) and once with wash buffer (50 mM HEPES, pH 7.4, 150 mM NaCl, 10% glycerol). Protein was eluted in two rounds with 30 uL wash buffer + 0.5 mg/mL 3xFLAG peptide (Sigma F4799) per plate, snap frozen on dry ice/EtOH and stored at -80 °C. Protein concentration was estimated from Coomassie-stained 10% polyacrylamide gels using a BSA standard curve.

ERK2 was purified in unphosphorylated from bacteria as described in [310]. ERK2 (21 μM) was phosphorylated in vitro by incubation with 0.2 μM bacterially-expressed active His_6-$MEK1^{\Delta E102\text{-}I103}$ in kinase reaction buffer (50 mM Tris [pH 8.0], 50 mM NaCl, 0.5 mM ATP, 1mM DTT, 0.01% Igepal CA-630, 10% glycerol, 10 mM $MgCl_2$) at 30°C for 30 min. MEK1 was removed by adding 20 μL Talon resin, rotating at 4°C for 1 h, and filtered through a chromatography column.

BRAF IP Kinase Assay

Protocol for BRAF IP kinase assays was adapted from [312]. Confluent 10 cm plates of shCTRL, shPPP6C-1, or shPPP6C-2 expressing 501mel cells were washed twice with cold PBS and lysed in RIPA buffer (20 mM Tris [pH 8.0], 137 mM NaCl, 10% glycerol, 1% NP-40, 1 mM PMSF, 1 mM Na_3VO_4, 10 μg/mL leupeptin, 2 μg/mL pepstatin A, 10 μg/mL aprotinin, 0.1% SDS, 0.5% sodium deoxycholate) on ice for 15 min. Cells were scraped into 1.5 mL tubes and lysates were passed through 22G needle with a syringe 3 times. Lysates were clarified in a 4°C microcentrifuge at 13,000 rpm for 10 min. Lysates were analyzed by BCA protein assay and equivalent amounts of protein were pre-cleared for 1 hour at 4°C with nProtein A Sepharose 4 Fast Flow beads (Sigma, GE17-5280-01) pre-equilibrated with lysis buffer. Beads were removed and lysates were

divided into 500 μL aliquots containing 500 μg protein for each assay condition or timepoint. Antibody to BRAF (7.5 μL) was added to each sample, and tubes were rotated 2 h at 4°C. To precipitate immune complexes, 50 μL of a 1:1 suspension of nProtein A Sepharose in lysis buffer was added, and tubes again rotated for 2 h at 4°C. Beads were pelleted, washed three times with lysis buffer, and resuspended in kinase reaction buffer (20 mM Tris [pH 7.4], 20 mM NaCl, 1 mM DTT, 10 mM $MgCl_2$, 1 mM $MnCl_2$). Purified unphosphorylated MEK1 (0.5 μg) and/or vemurafenib (to 1 μM) were added to as indicated. To initiate kinase reactions, ATP was added to a final concentration of 1 mM and volume of 40 μL, and tubes were transferred to 30°C heat block for the indicated times. Reactions were quenched with 4X SDS-PAGE loading buffer and boiled for 5 minutes and then subjected to SDS-PAGE (10% acrylamide) and immunoblotting as described above.

siRNA Transfection

Cells plated in 6-well plates were transfected with siRNA using Lipofectamine RNAiMAX reagent (Thermo Fisher Scientific, 13778100). Equal parts siRNA oligonucleotides (100 nM in 1X siRNA buffer, Horizon Discovery) and Lipofectamine RNAiMAX (diluted 1:100 in Opti-MEM Medium) were combined and incubated for 15 minutes at room temperature. Lipofectamine:siRNA complexes (400 μL) and complete media (600 μL) were added to each well. Cells were incubated for 72 h before being lysed for immunoblot analysis as described above. For cells transfected with two different siRNAs, half the amount of each siRNA was used.

In Vitro Phosphatase Assays

For each reaction, PP6 complex containing 125 ng PPP6C and 500 ng phosphorylated MEK were mixed in 30 μL reaction buffer (50 mM Tris-HCl [pH8.0], 0.5 mM $MnCl_2$, 2 mM

DTT) with or without 100nM okadaic acid as indicated. Reactions were incubated at 30 °C for the indicated time, quenched by the addition of 4X SDS-PAGE loading buffer, and boiled for 5 min. Samples were separated by SDS-PAGE (10% acrylamide) and analyzed by immunoblot.

REFERENCES

1. Yoon, S. & Seger, R. The extracellular signal-regulated kinase: multiple substrates regulate diverse cellular functions. Growth Factors 24, 21–44 (2006).
2. Roskoski, R. ERK1/2 MAP kinases: structure, function, and regulation. Pharmacol Res 66, 105–143 (2012).
3. Roskoski, R. MEK1/2 dual-specificity protein kinases: structure and regulation. Biochem. Biophys. Res. Commun. 417, 5–10 (2012).
4. Zmajkovicova, K. et al. MEK1 is required for PTEN membrane recruitment, AKT regulation, and the maintenance of peripheral tolerance. Mol. Cell 50, 43–55 (2013).
5. Ritt, D. A., Monson, D. M., Specht, S. I. & Morrison, D. K. Impact of feedback phosphorylation and Raf heterodimerization on normal and mutant B-Raf signaling. Mol. Cell. Biol. 30, 806–819 (2010).
6. Dhillon, A. S., Hagan, S., Rath, O. & Kolch, W. MAP kinase signalling pathways in cancer. Oncogene 26, 3279–3290 (2007).
7. Sanchez-Vega, F. et al. Oncogenic Signaling Pathways in The Cancer Genome Atlas. Cell 173, 321–337.e10 (2018).
8. Prior, I. A., Hood, F. E. & Hartley, J. L. The Frequency of Ras Mutations in Cancer. Cancer Res. 80, 2969–2974 (2020).
9. Wooster, R., Futreal, A. P. & Stratton, M. R. Sequencing analysis of BRAF mutations in human cancers. Methods Enzymol 407, 218–224 (2006).
10. Davies, H. et al. Mutations of the BRAF gene in human cancer. Nature 417, 949–954 (2002).
11. Cheng, L., Lopez-Beltran, A., Massari, F., MacLennan, G. T. & Montironi, R. Molecular testing for BRAF mutations to inform melanoma treatment decisions: a move toward precision medicine. Mod Pathol 31, 24–38 (2018).
12. Wan, P. T. C. et al. Mechanism of activation of the RAF-ERK signaling pathway by oncogenic mutations of B-RAF. Cell 116, 855–867 (2004).
13. Dankner, M., Rose, A. A. N., Rajkumar, S., Siegel, P. M. & Watson, I. R. Classifying BRAF alterations in cancer: new rational therapeutic strategies for actionable mutations. Oncogene 37, 3183–3199 (2018).
14. Negrao, M. V. et al. Molecular Landscape of BRAF-Mutant NSCLC Reveals an Association Between Clonality and Driver Mutations and Identifies Targetable Non-V600 Driver Mutations. J Thorac Oncol 15, 1611–1623 (2020).
15. Yao, Z. et al. BRAF Mutants Evade ERK-Dependent Feedback by Different Mechanisms that Determine Their Sensitivity to Pharmacologic Inhibition. Cancer Cell 28, 370–383 (2015).
16. Yao, Z. et al. Tumours with class 3 BRAF mutants are sensitive to the inhibition of activated RAS. Nature 548, 234–238 (2017).
17. Philpott, C., Tovell, H., Frayling, I. M., Cooper, D. N. & Upadhyaya, M. The NF1 somatic mutational landscape in sporadic human cancers. Hum Genomics 11, 13–19 (2017).

18. Krauthammer, M. et al. Exome sequencing identifies recurrent mutations in NF1 and RASopathy genes in sun-exposed melanomas. Nat. Genet. 47, 996–1002 (2015).

19. Cancer Genome Atlas Network. Genomic Classification of Cutaneous Melanoma. Cell 161, 1681–1696 (2015).

20. Hanahan, D. & Weinberg, R. A. Hallmarks of cancer: the next generation. Cell 144, 646–674 (2011).

21. Bugaj, L. J. et al. Cancer mutations and targeted drugs can disrupt dynamic signal encoding by the Ras-Erk pathway. Science 361, eaao3048 (2018).

22. Albeck, J. G., Mills, G. B. & Brugge, J. S. Frequency-modulated pulses of ERK activity transmit quantitative proliferation signals. Mol. Cell 49, 249–261 (2013).

23. Lavoie, H., Gagnon, J. & Therrien, M. ERK signalling: a master regulator of cell behaviour, life and fate. Nat. Rev. Mol. Cell Biol. 263, 5396–26 (2020).

24. Shimamura, A., Ballif, B. A., Richards, S. A. & Blenis, J. Rsk1 mediates a MEK-MAP kinase cell survival signal. Curr. Biol. 10, 127–135 (2000).

25. Boucher, M. J. et al. MEK/ERK signaling pathway regulates the expression of Bcl-2, Bcl-X(L), and Mcl-1 and promotes survival of human pancreatic cancer cells. J Cell Biochem 79, 355–369 (2000).

26. Ewings, K. E. et al. ERK1/2-dependent phosphorylation of BimEL promotes its rapid dissociation from Mcl-1 and Bcl-xL. EMBO J. 26, 2856–2867 (2007).

27. Ley, R., Balmanno, K., Hadfield, K., Weston, C. & Cook, S. J. Activation of the ERK1/2 signaling pathway promotes phosphorylation and proteasome-dependent degradation of the BH3-only protein, Bim. J. Biol. Chem. 278, 18811–18816 (2003).

28. Scott, D. A. et al. Comparative metabolic flux profiling of melanoma cell lines: beyond the Warburg effect. J. Biol. Chem. 286, 42626–42634 (2011).

29. Hall, A. et al. Dysfunctional oxidative phosphorylation makes malignant melanoma cells addicted to glycolysis driven by the (V600E)BRAF oncogene. Oncotarget 4, 584–599 (2013).

30. Thant, A. A. et al. Ras pathway is required for the activation of MMP-2 secretion and for the invasion of src-transformed 3Y1. Oncogene 18, 6555–6563 (1999).

31. Lakka, S. S. et al. Downregulation of MMP-9 in ERK-mutated stable transfectants inhibits glioma invasion in vitro. Oncogene 21, 5601–5608 (2002).

32. Tanimura, S., Asato, K., Fujishiro, S.-H. & Kohno, M. Specific blockade of the ERK pathway inhibits the invasiveness of tumor cells: down-regulation of matrix metalloproteinase-3/-9/-14 and CD44. Biochem. Biophys. Res. Commun. 304, 801–806 (2003).

33. Hodis, E. et al. A landscape of driver mutations in melanoma. Cell 150, 251–263 (2012).

34. Krauthammer, M. et al. Exome sequencing identifies recurrent somatic RAC1 mutations in melanoma. Nat. Genet. 44, 1006–1014 (2012).

35. Hayward, N. K. et al. Whole-genome landscapes of major melanoma subtypes. Nature 545, 175–180 (2017).

36. Berger, M. F. et al. Melanoma genome sequencing reveals frequent PREX2 mutations. Nature 485, 502–506 (2012).

37. Palmieri, G. et al. Molecular Pathways in Melanomagenesis: What We Learned from Next-Generation Sequencing Approaches. Curr Oncol Rep 20, 86–16 (2018).

38. Poynter, J. N. et al. BRAF and NRAS mutations in melanoma and melanocytic nevi. Melanoma Res. 16, 267–273 (2006).

39. Cerami, E. et al. The cBio cancer genomics portal: an open platform for exploring multidimensional cancer genomics data. Cancer Discov 2, 401–404 (2012).

40. Gao, J. et al. Integrative analysis of complex cancer genomics and clinical profiles using the cBioPortal. Sci Signal 6, pl1–pl1 (2013).

41. Hoeflich, K. P. et al. Oncogenic BRAF is required for tumor growth and maintenance in melanoma models. Cancer Res. 66, 999–1006 (2006).

42. Karasarides, M. et al. B-RAF is a therapeutic target in melanoma. Oncogene 23, 6292–6298 (2004).

43. Sala, E. et al. BRAF silencing by short hairpin RNA or chemical blockade by PLX4032 leads to different responses in melanoma and thyroid carcinoma cells. Mol. Cancer Res. 6, 751–759 (2008).

44. Eisen, T. et al. Sorafenib in advanced melanoma: a Phase II randomised discontinuation trial analysis. Br J Cancer 95, 581–586 (2006).

45. Eisen, T. et al. Sorafenib and dacarbazine as first-line therapy for advanced melanoma: phase I and open-label phase II studies. Br J Cancer 105, 353–359 (2011).

46. Ott, P. A. et al. A phase II trial of sorafenib in metastatic melanoma with tissue correlates. PLoS ONE 5, e15588 (2010).

47. McDermott, D. F. et al. Double-blind randomized phase II study of the combination of sorafenib and dacarbazine in patients with advanced melanoma: a report from the 11715 Study Group. J Clin Oncol 26, 2178–2185 (2008).

48. Amaravadi, R. K. et al. Phase II Trial of Temozolomide and Sorafenib in Advanced Melanoma Patients with or without Brain Metastases. Clin. Cancer Res. 15, 7711–7718 (2009).

49. Hauschild, A. et al. Results of a phase III, randomized, placebo-controlled study of sorafenib in combination with carboplatin and paclitaxel as second-line treatment in patients with unresectable stage III or stage IV melanoma. J Clin Oncol 27, 2823–2830 (2009).

50. Tsai, J. et al. Discovery of a selective inhibitor of oncogenic B-Raf kinase with potent antimelanoma activity. Proc. Natl. Acad. Sci. U.S.A. 105, 3041–3046 (2008).

51. Bollag, G. et al. Clinical efficacy of a RAF inhibitor needs broad target blockade in BRAF-mutant melanoma. Nature 467, 596–599 (2010).

52. Joseph, E. W. et al. The RAF inhibitor PLX4032 inhibits ERK signaling and tumor cell proliferation in a V600E BRAF-selective manner. Proc. Natl. Acad. Sci. U.S.A. 107, 14903–14908 (2010).

53. Yang, H. et al. RG7204 (PLX4032), a selective BRAFV600E inhibitor, displays potent antitumor activity in preclinical melanoma models. Cancer Res. 70, 5518–5527 (2010).

54. Flaherty, L. et al. A single-arm, open-label, expanded access study of vemurafenib in patients with metastatic melanoma in the United States. Cancer J 20, 18–24 (2014).

55. Chapman, P. B. et al. Improved survival with vemurafenib in melanoma with BRAF V600E mutation. N. Engl. J. Med. 364, 2507–2516 (2011).

56. Sosman, J. A. et al. Survival in BRAF V600-mutant advanced melanoma treated with vemurafenib. N. Engl. J. Med. 366, 707–714 (2012).

57. Flaherty, K. T. et al. Inhibition of mutated, activated BRAF in metastatic melanoma. N. Engl. J. Med. 363, 809–819 (2010).

58. Koelblinger, P., Thuerigen, O. & Dummer, R. Development of encorafenib for BRAF-mutated advanced melanoma. Curr Opin Oncol 30, 125–133 (2018).

59. Menzies, A. M., Long, G. V. & Murali, R. Dabrafenib and its potential for the treatment of metastatic melanoma. Drug Des Devel Ther 6, 391–405 (2012).

60. Carr, M. J., Sun, J., Eroglu, Z. & Zager, J. S. An evaluation of encorafenib for the treatment of melanoma. Expert Opin Pharmacother 21, 155–161 (2020).

61. Ugurel, S. et al. Survival of patients with advanced metastatic melanoma: the impact of novel therapies-update 2017. Eur. J. Cancer 83, 247–257 (2017).

62. Hatzivassiliou, G. et al. RAF inhibitors prime wild-type RAF to activate the MAPK pathway and enhance growth. Nature 464, 431–435 (2010).

63. Poulikakos, P. I., Zhang, C., Bollag, G., Shokat, K. M. & Rosen, N. RAF inhibitors transactivate RAF dimers and ERK signalling in cells with wild-type BRAF. Nature 464, 427–430 (2010).

64. Heidorn, S. J. et al. Kinase-dead BRAF and oncogenic RAS cooperate to drive tumor progression through CRAF. Cell 140, 209–221 (2010).

65. Oberholzer, P. A. et al. RAS mutations are associated with the development of cutaneous squamous cell tumors in patients treated with RAF inhibitors. J Clin Oncol 30, 316–321 (2012).

66. Su, F. et al. RAS mutations in cutaneous squamous-cell carcinomas in patients treated with BRAF inhibitors. N. Engl. J. Med. 366, 207–215 (2012).

67. Zhang, C. et al. RAF inhibitors that evade paradoxical MAPK pathway activation. Nature 526, 583–586 (2015).

68. Hartsough, E. J. et al. Response and Resistance to Paradox-Breaking BRAF Inhibitor in Melanomas In Vivo and Ex Vivo. Mol. Cancer Ther. 17, 84–95 (2018).

69. Janku, F. et al. Abstract B176: Results of a phase I study of PLX8394, a next-generation BRAF inhibitor, in refractory solid tumors. in B176–B176 (American Association for Cancer Research, 2018). doi:10.1158/1535-7163.TARG-17-B176

70. Favata, M. F. et al. Identification of a novel inhibitor of mitogen-activated protein kinase kinase. J. Biol. Chem. 273, 18623–18632 (1998).

71. Alessi, D. R., Cuenda, A., Cohen, P., Dudley, D. T. & Saltiel, A. R. PD 098059 is a specific inhibitor of the activation of mitogen-activated protein kinase kinase in vitro and in vivo. J. Biol. Chem. 270, 27489–27494 (1995).

72. Grimaldi, A. M. et al. MEK Inhibitors in the Treatment of Metastatic Melanoma and Solid Tumors. Am J Clin Dermatol 18, 745–754 (2017).

73. Zhao, Y. & Adjei, A. A. The clinical development of MEK inhibitors. Nat Rev Clin Oncol 11, 385–400 (2014).

74. Gilmartin, A. G. et al. GSK1120212 (JTP-74057) is an inhibitor of MEK activity and activation with favorable pharmacokinetic properties for sustained in vivo pathway inhibition. Clin. Cancer Res. 17, 989–1000 (2011).

75. Falchook, G. S. et al. Activity of the oral MEK inhibitor trametinib in patients with advanced melanoma: a phase 1 dose-escalation trial. Lancet Oncol 13, 782–789 (2012).

76. Flaherty, K. T. et al. Improved survival with MEK inhibition in BRAF-mutated melanoma. N. Engl. J. Med. 367, 107–114 (2012).

77. Bromberg-White, J. L., Andersen, N. J. & Duesbery, N. S. MEK genomics in development and disease. Brief Funct Genomics 11, 300–310 (2012).

78. Halilovic, E. & Solit, D. B. Therapeutic strategies for inhibiting oncogenic BRAF signaling. Curr Opin Pharmacol 8, 419–426 (2008).

79. Subbiah, V., Baik, C. & Kirkwood, J. M. Clinical Development of BRAF plus MEK Inhibitor Combinations. Trends Cancer 6, 797–810 (2020).

80. Flaherty, K. T. et al. Combined BRAF and MEK inhibition in melanoma with BRAF V600 mutations. N. Engl. J. Med. 367, 1694–1703 (2012).

81. Carlos, G. et al. Cutaneous Toxic Effects of BRAF Inhibitors Alone and in Combination With MEK Inhibitors for Metastatic Melanoma. JAMA Dermatol 151, 1103–1109 (2015).

82. Sanlorenzo, M. et al. Comparative profile of cutaneous adverse events: BRAF/MEK inhibitor combination therapy versus BRAF monotherapy in melanoma. J Am Acad Dermatol 71, 1102–1109.e1 (2014).

83. Ugurel, S. et al. Survival of patients with advanced metastatic melanoma: The impact of MAP kinase pathway inhibition and immune checkpoint inhibition - Update 2019. Eur. J. Cancer 130, 126–138 (2020).

84. Dummer, R. et al. Five-Year Analysis of Adjuvant Dabrafenib plus Trametinib in Stage III Melanoma. N. Engl. J. Med. 383, 1139–1148 (2020).

85. Seth, R. et al. Systemic Therapy for Melanoma: ASCO Guideline. J Clin Oncol 38, 3947–3970 (2020).

86. Pelster, M. S. & Amaria, R. N. Combined targeted therapy and immunotherapy in melanoma: a review of the impact on the tumor microenvironment and outcomes of early clinical trials. Ther Adv Med Oncol 11, 1758835919830826 (2019).

87. Wagle, N. et al. MAP kinase pathway alterations in BRAF-mutant melanoma patients with acquired resistance to combined RAF/MEK inhibition. Cancer Discov 4, 61–68 (2014).

88. Welsh, S. J., Rizos, H., Scolyer, R. A. & Long, G. V. Resistance to combination BRAF and MEK inhibition in metastatic melanoma: Where to next? Eur. J. Cancer 62, 76–85 (2016).

89. Long, G. V. et al. Increased MAPK reactivation in early resistance to dabrafenib/trametinib combination therapy of BRAF-mutant metastatic melanoma. Nat Commun 5, 5694–9 (2014).

90. Wong, D. J. L. et al. Antitumor activity of the ERK inhibitor SCH772984 [corrected] against BRAF mutant, NRAS mutant and wild-type melanoma. Mol Cancer 13, 194–15 (2014).

91. Carlino, M. S. et al. Differential activity of MEK and ERK inhibitors in BRAF inhibitor resistant melanoma. Mol Oncol 8, 544–554 (2014).

92. Morris, E. J. et al. Discovery of a novel ERK inhibitor with activity in models of acquired resistance to BRAF and MEK inhibitors. Cancer Discov 3, 742–750 (2013).

93. Hatzivassiliou, G. et al. ERK inhibition overcomes acquired resistance to MEK inhibitors. Mol. Cancer Ther. 11, 1143–1154 (2012).

94. Germann, U. A. et al. Targeting the MAPK Signaling Pathway in Cancer: Promising Preclinical Activity with the Novel Selective ERK1/2 Inhibitor BVD-523 (Ulixertinib). Mol. Cancer Ther. 16, 2351–2363 (2017).

95. Boga, S. B. et al. MK-8353: Discovery of an Orally Bioavailable Dual Mechanism ERK Inhibitor for Oncology. ACS Med Chem Lett 9, 761–767 (2018).

96. Moschos, S. J. et al. Development of MK-8353, an orally administered ERK1/2 inhibitor, in patients with advanced solid tumors. JCI Insight 3, 184 (2018).

97. Roskoski, R. Targeting ERK1/2 protein-serine/threonine kinases in human cancers. Pharmacol Res 142, 151–168 (2019).

98. Sammons, R. M., Ghose, R., Tsai, K. Y. & Dalby, K. N. Targeting ERK beyond the boundaries of the kinase active site in melanoma. Mol Carcinog 58, 1551–1570 (2019).

99. Sullivan, R. J. et al. First-in-Class ERK1/2 Inhibitor Ulixertinib (BVD-523) in Patients with MAPK Mutant Advanced Solid Tumors: Results of a Phase I Dose-Escalation and Expansion Study. Cancer Discov 8, 184–195 (2018).

100. Varga, A. et al. A First-in-Human Phase I Study to Evaluate the ERK1/2 Inhibitor GDC-0994 in Patients with Advanced Solid Tumors. Clin. Cancer Res. 26, 1229–1236 (2020).

101. Shi, H. et al. Acquired resistance and clonal evolution in melanoma during BRAF inhibitor therapy. Cancer Discov 4, 80–93 (2014).

102. Rizos, H. et al. BRAF inhibitor resistance mechanisms in metastatic melanoma: spectrum and clinical impact. Clin. Cancer Res. 20, 1965–1977 (2014).

103. Van Allen, E. M. et al. The genetic landscape of clinical resistance to RAF inhibition in metastatic melanoma. Cancer Discov 4, 94–109 (2014).

104. Johnson, D. B. et al. Acquired BRAF inhibitor resistance: A multicenter meta-analysis of the spectrum and frequencies, clinical behaviour, and phenotypic associations of resistance mechanisms. Eur. J. Cancer 51, 2792–2799 (2015).

105. Shi, H. et al. Melanoma whole-exome sequencing identifies (V600E)B-RAF amplification-mediated acquired B-RAF inhibitor resistance. Nat Commun 3, 724–8 (2012).

106. Poulikakos, P. I. et al. RAF inhibitor resistance is mediated by dimerization of aberrantly spliced BRAF(V600E). Nature 480, 387–390 (2011).

107. Trunzer, K. et al. Pharmacodynamic effects and mechanisms of resistance to vemurafenib in patients with metastatic melanoma. J Clin Oncol 31, 1767–1774 (2013).

108. Nazarian, R. et al. Melanomas acquire resistance to B-RAF(V600E) inhibition by RTK or N-RAS upregulation. Nature 468, 973–977 (2010).

109. Whittaker, S. R. et al. A genome-scale RNA interference screen implicates NF1 loss in resistance to RAF inhibition. Cancer Discov 3, 350–362 (2013).

110. Goshen-Lago, T., Melamed, D., Admon, A. & Engelberg, D. Isolation and Characterization of Intrinsically Active (MEK-Independent) Mutants of Mpk1/Erk. Methods Mol Biol 1487, 65–88 (2017).

111. Sang, D. et al. Ancestral reconstruction reveals mechanisms of ERK regulatory evolution. Elife 8, 1301 (2019).

112. Goetz, E. M., Ghandi, M., Treacy, D. J., Wagle, N. & Garraway, L. A. ERK mutations confer resistance to mitogen-activated protein kinase pathway inhibitors. Cancer Res. 74, 7079–7089 (2014).

113. Smorodinsky-Atias, K., Soudah, N. & Engelberg, D. Mutations That Confer Drug-Resistance, Oncogenicity and Intrinsic Activity on the ERK MAP Kinases-Current State of the Art. Cells 9, 129 (2020).

114. Brenan, L. et al. Phenotypic Characterization of a Comprehensive Set of MAPK1/ERK2 Missense Mutants. Cell Rep 17, 1171–1183 (2016).

115. Villanueva, J. et al. Acquired resistance to BRAF inhibitors mediated by a RAF kinase switch in melanoma can be overcome by cotargeting MEK and IGF-1R/PI3K. Cancer Cell 18, 683–695 (2010).

116. Fresno Vara, J. A. et al. PI3K/Akt signalling pathway and cancer. Cancer Treat Rev 30, 193–204 (2004).

117. Jiang, N. et al. Role of PI3K/AKT pathway in cancer: the framework of malignant behavior. Mol Biol Rep 47, 4587–4629 (2020).

118. Deng, W. et al. Role and therapeutic potential of PI3K-mTOR signaling in de novo resistance to BRAF inhibition. Pigment Cell Melanoma Res 25, 248–258 (2012).

119. Paraiso, K. H. T. et al. PTEN loss confers BRAF inhibitor resistance to melanoma cells through the suppression of BIM expression. Cancer Res. 71, 2750–2760 (2011).

120. Aguissa-Touré, A.-H. & Li, G. Genetic alterations of PTEN in human melanoma. Cell. Mol. Life Sci. 69, 1475–1491 (2012).

121. Wu, H., Goel, V. & Haluska, F. G. PTEN signaling pathways in melanoma. Oncogene 22, 3113–3122 (2003).

122. Kwong, L. N. & Davies, M. A. Navigating the therapeutic complexity of PI3K pathway inhibition in melanoma. Clin. Cancer Res. 19, 5310–5319 (2013).

123. Irvine, M. et al. Oncogenic PI3K/AKT promotes the step-wise evolution of combination BRAF/MEK inhibitor resistance in melanoma. Oncogenesis 7, 72–11 (2018).

124. Aasen, S. N. et al. Effective Treatment of Metastatic Melanoma by Combining MAPK and PI3K Signaling Pathway Inhibitors. Int J Mol Sci 20, 4235 (2019).

125. Sweetlove, M. et al. Inhibitors of pan-PI3K Signaling Synergize with BRAF or MEK Inhibitors to Prevent BRAF-Mutant Melanoma Cell Growth. Front Oncol 5, 135 (2015).

126. Deuker, M. M., Marsh Durban, V., Phillips, W. A. & McMahon, M. PI3'-kinase inhibition forestalls the onset of MEK1/2 inhibitor resistance in BRAF-mutated melanoma. Cancer Discov 5, 143–153 (2015).

127. Algazi, A. P. et al. A dual pathway inhibition strategy using BKM120 combined with vemurafenib is poorly tolerated in BRAF V600E/K mutant advanced melanoma. Pigment Cell Melanoma Res 32, 603–606 (2019).

128. Bardia, A. et al. Phase Ib Study of Combination Therapy with MEK Inhibitor Binimetinib and Phosphatidylinositol 3-Kinase Inhibitor Buparlisib in Patients with Advanced Solid Tumors with RAS/RAF Alterations. Oncologist 25, e160–e169 (2020).

129. Tolcher, A. W., Peng, W. & Calvo, E. Rational Approaches for Combination Therapy Strategies Targeting the MAP Kinase Pathway in Solid Tumors. Mol. Cancer Ther. 17, 3–16 (2018).

130. Ramanathan, R. K. et al. Phase Ib Trial of the PI3K Inhibitor Copanlisib Combined with the Allosteric MEK Inhibitor Refametinib in Patients with Advanced Cancer. Target Oncol 15, 163–174 (2020).

131. Wake, M. S. & Watson, C. J. STAT3 the oncogene - still eluding therapy? FEBS J 282, 2600–2611 (2015).

132. Bromberg, J. F. et al. Stat3 as an oncogene. Cell 98, 295–303 (1999).

133. Buettner, R., Mora, L. B. & Jove, R. Activated STAT signaling in human tumors provides novel molecular targets for therapeutic intervention. Clin. Cancer Res. 8, 945–954 (2002).

134. Girotti, M. R. et al. Inhibiting EGF receptor or SRC family kinase signaling overcomes BRAF inhibitor resistance in melanoma. Cancer Discov 3, 158–167 (2013).

135. Sos, M. L. et al. Oncogene mimicry as a mechanism of primary resistance to BRAF inhibitors. Cell Rep 8, 1037–1048 (2014).

136. Liu, F. et al. Stat3-targeted therapies overcome the acquired resistance to vemurafenib in melanomas. J Invest Dermatol 133, 2041–2049 (2013).

137. Su, Y. et al. Targeting STAT3 restores BRAF inhibitor sensitivity through miR-759-3p in human cutaneous melanoma cells. Int J Clin Exp Pathol 11, 2550–2560 (2018).

138. Lu, H. et al. PAK signalling drives acquired drug resistance to MAPK inhibitors in BRAF-mutant melanomas. Nature 550, 133–136 (2017).

139. Johannessen, C. M. et al. COT drives resistance to RAF inhibition through MAP kinase pathway reactivation. Nature 468, 968–972 (2010).

140. Perna, D. et al. BRAF inhibitor resistance mediated by the AKT pathway in an oncogenic BRAF mouse melanoma model. Proc. Natl. Acad. Sci. U.S.A. 112, E536–45 (2015).

141. Li, Z. et al. CRISPR Screens Identify Essential Cell Growth Mediators in BRAF Inhibitor-resistant Melanoma. Genomics Proteomics Bioinformatics 18, 26–40 (2020).

142. Julve, M., Clark, J. J. & Lythgoe, M. P. Advances in cyclin-dependent kinase inhibitors for the treatment of melanoma. Expert Opin Pharmacother 2, 1–11 (2020).

143. Hayes, T. K. et al. A Functional Landscape of Resistance to MEK1/2 and CDK4/6 Inhibition in NRAS-Mutant Melanoma. Cancer Res. 79, 2352–2366 (2019).

144. Gupta, R. et al. Loss of BOP1 confers resistance to BRAF kinase inhibitors in melanoma by activating MAP kinase pathway. Proc. Natl. Acad. Sci. U.S.A. 116, 4583–4591 (2019).

145. Bugide, S. et al. Loss of HAT1 expression confers BRAFV600E inhibitor resistance to melanoma cells by activating MAPK signaling via IGF1R. Oncogenesis 9, 44–14 (2020).

146. Vanneste, M. et al. Functional Genomic Screening Independently Identifies CUL3 as a Mediator of Vemurafenib Resistance via Src-Rac1 Signaling Axis. Front Oncol 10, 442 (2020).

147. Shi, Y. Serine/threonine phosphatases: mechanism through structure. Cell 139, 468–484 (2009).

148. Stefansson, B., Ohama, T., Daugherty, A. E. & Brautigan, D. L. Protein phosphatase 6 regulatory subunits composed of ankyrin repeat domains. Biochemistry 47, 1442–1451 (2008).

149. Stefansson, B. & Brautigan, D. L. Protein phosphatase 6 subunit with conserved Sit4-associated protein domain targets IkappaBepsilon. J. Biol. Chem. 281, 22624–22634 (2006).

150. Douglas, P. et al. Polo-like kinase 1 (PLK1) and protein phosphatase 6 (PP6) regulate DNA-dependent protein kinase catalytic subunit (DNA-PKcs) phosphorylation in mitosis. Biosci. Rep. 34, 440 (2014).

151. Rusin, S. F., Adamo, M. E. & Kettenbach, A. N. Identification of Candidate Casein Kinase 2 Substrates in Mitosis by Quantitative Phosphoproteomics. Front Cell Dev Biol 5, 97 (2017).

152. Zeng, K., Bastos, R. N., Barr, F. A. & Gruneberg, U. Protein phosphatase 6 regulates mitotic spindle formation by controlling the T-loop phosphorylation state of Aurora A bound to its activator TPX2. J. Cell Biol. 191, 1315–1332 (2010).

153. Hosing, A. S., Valerie, N. C. K., Dziegielewski, J., Brautigan, D. L. & Larner, J. M. PP6 regulatory subunit R1 is bidentate anchor for targeting protein phosphatase-6 to DNA-dependent protein kinase. J. Biol. Chem. 287, 9230–9239 (2012).

154. Shen, Y. et al. Serine/threonine protein phosphatase 6 modulates the radiation sensitivity of glioblastoma. Cell Death Dis 2, e241–e241 (2011).

155. Zhong, J. et al. Protein phosphatase PP6 is required for homology-directed repair of DNA double-strand breaks. Cell Cycle 10, 1411–1419 (2011).

156. Wengrod, J. et al. Phosphorylation of eIF2α triggered by mTORC1 inhibition and PP6C activation is required for autophagy and is aberrant in PP6C-mutated melanoma. Sci Signal 8, ra27–ra27 (2015).

157. Golden, R. J. et al. An Argonaute phosphorylation cycle promotes microRNA-mediated silencing. Nature 542, 197–202 (2017).

158. Kajino, T. et al. Protein phosphatase 6 down-regulates TAK1 kinase activation in the IL-1 signaling pathway. J. Biol. Chem. 281, 39891–39896 (2006).

159. Ye, J. et al. PP6 controls T cell development and homeostasis by negatively regulating distal TCR signaling. J. Immunol. 194, 1654–1664 (2015).

160. Tan, P. et al. Assembly of the WHIP-TRIM14-PPP6C Mitochondrial Complex Promotes RIG-I-Mediated Antiviral Signaling. Mol. Cell 68, 293–307.e5 (2017).

161. Cho, U. S. & Xu, W. Crystal structure of a protein phosphatase 2A heterotrimeric holoenzyme. Nature 445, 53–57 (2007).

162. Goshima, G., Iwasaki, O., Obuse, C. & Yanagida, M. The role of Ppe1/PP6 phosphatase for equal chromosome segregation in fission yeast kinetochore. EMBO J. 22, 2752–2763 (2003).

163. Afshar, K., Werner, M. E., Tse, Y. C., Glotzer, M. & Gönczy, P. Regulation of cortical contractility and spindle positioning by the protein phosphatase 6 PPH-6 in one-cell stage C. elegans embryos. Development 137, 237–247 (2010).

164. Douglas, P. et al. Protein phosphatase 6 interacts with the DNA-dependent protein kinase catalytic subunit and dephosphorylates gamma-H2AX. Mol. Cell. Biol. 30, 1368–1381 (2010).

165. Rusin, S. F., Schlosser, K. A., Adamo, M. E. & Kettenbach, A. N. Quantitative phosphoproteomics reveals new roles for the protein phosphatase PP6 in mitotic cells. Sci Signal 8, rs12–rs12 (2015).

166. Barbosa, A. D., Pereira, C., Osório, H., Moradas-Ferreira, P. & Costa, V. The ceramide-activated protein phosphatase Sit4p controls lifespan, mitochondrial function and cell cycle progression by regulating hexokinase 2 phosphorylation. Cell Cycle 15, 1620–1630 (2016).

167. Stefansson, B. & Brautigan, D. L. Protein phosphatase PP6 N terminal domain restricts G1 to S phase progression in human cancer cells. Cell Cycle 6, 1386–1392 (2007).

168. Yan, S. et al. NF-κB-induced microRNA-31 promotes epidermal hyperplasia by repressing protein phosphatase 6 in psoriasis. Nat Commun 6, 7652–15 (2015).

169. Chen, F. et al. Multiple protein phosphatases are required for mitosis in Drosophila. Curr. Biol. 17, 293–303 (2007).

170. Lei, W.-L. et al. Protein phosphatase 6 is a key factor regulating spermatogenesis. Cell Death Differ. 27, 1952–1964 (2020).

171. Hu, M.-W. et al. Loss of protein phosphatase 6 in oocytes causes failure of meiosis II exit and impaired female fertility. J. Cell. Sci. 128, 3769–3780 (2015).

172. Garnett, C. T. et al. Sublethal irradiation of human tumor cells modulates phenotype resulting in enhanced killing by cytotoxic T lymphocytes. Cancer Res. 64, 7985–7994 (2004).

173. Mori, M. et al. Effect of ionizing radiation on gene expression in CD4+ T lymphocytes and in Jurkat cells: unraveling novel pathways in radiation response. Cell. Mol. Life Sci. 61, 1955–1964 (2004).

174. Dziegielewski, J. et al. Deletion of the SAPS1 subunit of protein phosphatase 6 in mice increases radiosensitivity and impairs the cellular DNA damage response. DNA Repair (Amst) 85, 102737 (2020).

175. Mi, J., Dziegielewski, J., Bolesta, E., Brautigan, D. L. & Larner, J. M. Activation of DNA-PK by ionizing radiation is mediated by protein phosphatase 6. PLoS ONE 4, e4395 (2009).

176. Ziembik, M. A., Bender, T. P., Larner, J. M. & Brautigan, D. L. Functions of protein phosphatase-6 in NF-κB signaling and in lymphocytes. Biochem Soc Trans 45, 693–701 (2017).

177. Broglie, P., Matsumoto, K., Akira, S., Brautigan, D. L. & Ninomiya-Tsuji, J. Transforming growth factor beta-activated kinase 1 (TAK1) kinase adaptor, TAK1-binding protein 2, plays dual roles in TAK1 signaling by recruiting both an activator and an inhibitor of TAK1 kinase in tumor necrosis factor signaling pathway. J. Biol. Chem. 285, 2333–2339 (2010).

178. Bouwmeester, T. et al. A physical and functional map of the human TNF-alpha/NF-kappa B signal transduction pathway. Nat. Cell Biol. 6, 97–105 (2004).

179. Hayashi, K. et al. Abrogation of protein phosphatase 6 promotes skin carcinogenesis induced by DMBA. Oncogene 34, 4647–4655 (2015).

180. Filali, M., Li, S., Kim, H. W., Wadzinski, B. & Kamoun, M. Identification of a type 6 protein ser/thr phosphatase regulated by interleukin-2 stimulation. J Cell Biochem 73, 153–163 (1999).

181. Zhang, L.-J. et al. Coordinated regulation of transcription factor Bcl11b activity in thymocytes by the mitogen-activated protein kinase (MAPK) pathways and protein sumoylation. J. Biol. Chem. 287, 26971–26988 (2012).

182. Watanabe, K., Umeda, T., Niwa, K., Naguro, I. & Ichijo, H. A PP6-ASK3 Module Coordinates the Bidirectional Cell Volume Regulation under Osmotic Stress. Cell Rep 22, 2809–2817 (2018).

183. Kamoun, M., Filali, M., Murray, M. V., Awasthi, S. & Wadzinski, B. E. Protein phosphatase 2A family members (PP2A and PP6) associate with U1 snRNP and the spliceosome during pre-mRNA splicing. Biochem. Biophys. Res. Commun. 440, 306–311 (2013).

184. Couzens, A. L. et al. Protein interaction network of the mammalian Hippo pathway reveals mechanisms of kinase-phosphatase interactions. Sci Signal 6, rs15–rs15 (2013).

185. Dempster, J. M. et al. Extracting Biological Insights from the Project Achilles Genome-Scale CRISPR Screens in Cancer Cell Lines. bioRxiv 720243 (2019).

186. DepMap, B. DepMap 20Q2 Public. (2020).

187. Meyers, R. M. et al. Computational correction of copy number effect improves specificity of CRISPR-Cas9 essentiality screens in cancer cells. Nat. Genet. 49, 1779–1784 (2017).

188. Malicherova, B. et al. Detection of driver mutations in FFPE samples from patients with verified malignant melanoma. Neoplasma 66, 33–38 (2019).

189. Gold, H. L. et al. PP6C hotspot mutations in melanoma display sensitivity to Aurora kinase inhibition. Mol. Cancer Res. 12, 433–439 (2014).

190. Hammond, D. et al. Melanoma-associated mutations in protein phosphatase 6 cause chromosome instability and DNA damage owing to dysregulated Aurora-A. J. Cell. Sci. 126, 3429–3440 (2013).

191. O'Connor, C. M. et al. Inactivation of PP2A by a recurrent mutation drives resistance to MEK inhibitors. Oncogene 39, 703–717 (2020).

192. Garibyan, L. & Fisher, D. E. How sunlight causes melanoma. Curr Oncol Rep 12, 319–326 (2010).

193. Kurosawa, K. et al. Loss of protein phosphatase 6 in mouse keratinocytes enhances K-rasG12D -driven tumor promotion. Cancer Sci. 109, 2178–2187 (2018).

194. Ma, X. et al. PP6 Disruption Synergizes with Oncogenic Ras to Promote JNK-Dependent Tumor Growth and Invasion. Cell Rep 19, 2657–2664 (2017).

195. Carr, S., Smith, C. & Wernberg, J. Epidemiology and Risk Factors of Melanoma. Surgical Clinics of North America 100, 1–12 (2020).

196. Burotto, M., Chiou, V. L., Lee, J.-M. & Kohn, E. C. The MAPK pathway across different malignancies: a new perspective. Cancer 120, 3446–3456 (2014).

197. Samatar, A. A. & Poulikakos, P. I. Targeting RAS-ERK signalling in cancer: promises and challenges. Nat Rev Drug Discov 13, 928–942 (2014).

198. Lim, S. Y., Menzies, A. M. & Rizos, H. Mechanisms and strategies to overcome resistance to molecularly targeted therapy for melanoma. Cancer 123, 2118–2129 (2017).

199. Gilbert, L. A. et al. Genome-Scale CRISPR-Mediated Control of Gene Repression and Activation. Cell 159, 647–661 (2014).

200. Kim, D. et al. Digenome-seq: genome-wide profiling of CRISPR-Cas9 off-target effects in human cells. Nat Methods 12, 237–43– 1 p following 243 (2015).

201. Evers, B. et al. CRISPR knockout screening outperforms shRNA and CRISPRi in identifying essential genes. Nat Biotechnol 34, 631–633 (2016).

202. Morgens, D. W., Deans, R. M., Li, A. & Bassik, M. C. Systematic comparison of CRISPR/Cas9 and RNAi screens for essential genes. Nat Biotechnol 34, 634–636 (2016).

203. Goldinger, S. M. et al. Upstream mitogen-activated protein kinase (MAPK) pathway inhibition: MEK inhibitor followed by a BRAF inhibitor in advanced melanoma patients. Eur. J. Cancer 50, 406–410 (2014).

204. Šuštić, T. et al. A role for the unfolded protein response stress sensor ERN1 in regulating the response to MEK inhibitors in KRAS mutant colon cancers. Genome Med 10, 90–13 (2018).

205. Nagler, A. et al. A genome-wide CRISPR screen identifies FBXO42 involvement in resistance toward MEK inhibition in NRAS-mutant melanoma. Pigment Cell Melanoma Res 33, 334–344 (2020).

206. Sulahian, R. et al. Synthetic Lethal Interaction of SHOC2 Depletion with MEK Inhibition in RAS-Driven Cancers. Cell Rep 29, 118–134.e8 (2019).

207. Wang, B. et al. ATXN1L, CIC, and ETS Transcription Factors Modulate Sensitivity to MAPK Pathway Inhibition. Cell Rep 18, 1543–1557 (2017).

208. Luo, B. et al. Highly parallel identification of essential genes in cancer cells. Proc. Natl. Acad. Sci. U.S.A. 105, 20380–20385 (2008).

209. Cragg, M. S. et al. Treatment of B-RAF mutant human tumor cells with a MEK inhibitor requires Bim and is enhanced by a BH3 mimetic. J Clin Invest 118, 3651–3659 (2008).

210. Byron, S. A. et al. Sensitivity to the MEK inhibitor E6201 in melanoma cells is associated with mutant BRAF and wildtype PTEN status. Mol Cancer 11, 75–15 (2012).

211. Haass, N. K. et al. The mitogen-activated protein/extracellular signal-regulated kinase kinase inhibitor AZD6244 (ARRY-142886) induces growth arrest in melanoma cells and tumor regression when combined with docetaxel. Clin. Cancer Res. 14, 230–239 (2008).

212. Lugowska, I., Koseła-Paterczyk, H., Kozak, K. & Rutkowski, P. Trametinib: a MEK inhibitor for management of metastatic melanoma. Onco Targets Ther 8, 2251–2259 (2015).

213. Carson, C. C. et al. IL2 Inducible T-cell Kinase, a Novel Therapeutic Target in Melanoma. Clin. Cancer Res. 21, 2167–2176 (2015).

214. Zhu, L., Yu, X., Akatsuka, Y., Cooper, J. A. & Anasetti, C. Role of mitogen-activated protein kinases in activation-induced apoptosis of T cells. Immunology 97, 26–35 (1999).

215. Miller, A. T. & Berg, L. J. Defective Fas ligand expression and activation-induced cell death in the absence of IL-2-inducible T cell kinase. J. Immunol. 168, 2163–2172 (2002).

216. Mamand, S., Allchin, R. L., Ahearne, M. J. & Wagner, S. D. Comparison of interleukin-2-inducible kinase (ITK) inhibitors and potential for combination therapies for T-cell lymphoma. Sci Rep 8, 14216–13 (2018).

217. Yu, W., Fantl, W. J., Harrowe, G. & Williams, L. T. Regulation of the MAP kinase pathway by mammalian Ksr through direct interaction with MEK and ERK. Curr. Biol. 8, 56–64 (1998).

218. Khan, Z. M. et al. Structural basis for the action of the drug trametinib at KSR-bound MEK. Nature 588, 509–514 (2020).

219. Tang, G., Yang, Y., Shang, L., Jun, F. & Liu, Q. A DSTYK mutation activates ERK1/2 signaling to promote intraspinal dissemination in a case of solitary fibrous tumor/hemangiopericytoma. Lab Invest 99, 1501–1514 (2019).

220. Miao, W. et al. A Targeted Quantitative Proteomic Method Revealed a Substantial Reprogramming of Kinome during Melanoma Metastasis. Sci Rep 10, 2485–10 (2020).

221. Zhang, J. et al. DSTYK Promotes Metastasis and Chemoresistance via EMT in Colorectal Cancer. Front Pharmacol 11, 1250 (2020).

222. Sanna-Cherchi, S. et al. Mutations in DSTYK and dominant urinary tract malformations. N. Engl. J. Med. 369, 621–629 (2013).

223. Gewinner, C. et al. Evidence that inositol polyphosphate 4-phosphatase type II is a tumor suppressor that inhibits PI3K signaling. Cancer Cell 16, 115–125 (2009).

224. Fedele, C. G. et al. Inositol polyphosphate 4-phosphatase II regulates PI3K/Akt signaling and is lost in human basal-like breast cancers. Proc. Natl. Acad. Sci. U.S.A. 107, 22231–22236 (2010).

225. Perez-Lorenzo, R. et al. A tumor suppressor function for the lipid phosphatase INPP4B in melanocytic neoplasms. J Invest Dermatol 134, 1359–1368 (2014).

226. Bermudez, O., Pagès, G. & Gimond, C. The dual-specificity MAP kinase phosphatases: critical roles in development and cancer. Am. J. Physiol., Cell Physiol. 299, C189–202 (2010).

227. Cai, C. et al. Down-regulation of dual-specificity phosphatase 5 predicts poor prognosis of patients with prostate cancer. Int J Clin Exp Med 8, 4186–4194 (2015).

228. Okudela, K. et al. Down-regulation of DUSP6 expression in lung cancer: its mechanism and potential role in carcinogenesis. Am. J. Pathol. 175, 867–881 (2009).

229. Shin, S.-H., Park, S.-Y. & Kang, G. H. Down-regulation of dual-specificity phosphatase 5 in gastric cancer by promoter CpG island hypermethylation and its potential role in carcinogenesis. Am. J. Pathol. 182, 1275–1285 (2013).

230. Xu, S., Furukawa, T., Kanai, N., Sunamura, M. & Horii, A. Abrogation of DUSP6 by hypermethylation in human pancreatic cancer. J. Hum. Genet. 50, 159–167 (2005).

231. Chen, Y.-N. P. et al. Allosteric inhibition of SHP2 phosphatase inhibits cancers driven by receptor tyrosine kinases. Nature 535, 148–152 (2016).

232. Jones, G. G. et al. SHOC2 phosphatase-dependent RAF dimerization mediates resistance to MEK inhibition in RAS-mutant cancers. Nat Commun 10, 2532–16 (2019).

233. Young, L. C. et al. SHOC2-MRAS-PP1 complex positively regulates RAF activity and contributes to Noonan syndrome pathogenesis. Proc. Natl. Acad. Sci. U.S.A. 115, E10576–E10585 (2018).

234. Ory, S., Zhou, M., Conrads, T. P., Veenstra, T. D. & Morrison, D. K. Protein phosphatase 2A positively regulates Ras signaling by dephosphorylating KSR1 and Raf-1 on critical 14-3-3 binding sites. Curr. Biol. 13, 1356–1364 (2003).

235. Gómez, N. & Cohen, P. Dissection of the protein kinase cascade by which nerve growth factor activates MAP kinases. Nature 353, 170–173 (1991).

236. Sontag, E. et al. The interaction of SV40 small tumor antigen with protein phosphatase 2A stimulates the map kinase pathway and induces cell proliferation. Cell 75, 887–897 (1993).

237. Letourneux, C., Rocher, G. & Porteu, F. B56-containing PP2A dephosphorylate ERK and their activity is controlled by the early gene IEX-1 and ERK. EMBO J. 25, 727–738 (2006).

238. Hong, A. et al. Exploiting Drug Addiction Mechanisms to Select against MAPKi-Resistant Melanoma. Cancer Discov 8, 74–93 (2018).

239. Moriceau, G. et al. Tunable-combinatorial mechanisms of acquired resistance limit the efficacy of BRAF/MEK cotargeting but result in melanoma drug addiction. Cancer Cell 27, 240–256 (2015).

240. Boyle, E. A., Pritchard, J. K. & Greenleaf, W. J. High-resolution mapping of cancer cell networks using co-functional interactions. Mol. Syst. Biol. 14, e8594 (2018).

241. Kim, E. et al. A network of human functional gene interactions from knockout fitness screens in cancer cells. Life Sci Alliance 2, e201800278 (2019).

242. Montagut, C. et al. Elevated CRAF as a potential mechanism of acquired resistance to BRAF inhibition in melanoma. Cancer Res. 68, 4853–4861 (2008).

243. Shi, H., Kong, X., Ribas, A. & Lo, R. S. Combinatorial treatments that overcome PDGFRβ-driven resistance of melanoma cells to V600EB-RAF inhibition. Cancer Res. 71, 5067–5074 (2011).

244. Lake, D., Corrêa, S. A. L. & Müller, J. Negative feedback regulation of the ERK1/2 MAPK pathway. Cell. Mol. Life Sci. 73, 4397–4413 (2016).

245. Coles, L. C. & Shaw, P. E. PAK1 primes MEK1 for phosphorylation by Raf-1 kinase during cross-cascade activation of the ERK pathway. Oncogene 21, 2236–2244 (2002).

246. Rossomando, A. J., Dent, P., Sturgill, T. W. & Marshak, D. R. Mitogen-activated protein kinase kinase 1 (MKK1) is negatively regulated by threonine phosphorylation. Mol. Cell. Biol. 14, 1594–1602 (1994).

247. Sharma, P. et al. Phosphorylation of MEK1 by cdk5/p35 down-regulates the mitogen-activated protein kinase pathway. J. Biol. Chem. 277, 528–534 (2002).

248. Brautigan, D. L. & Shenolikar, S. Protein Serine/Threonine Phosphatases: Keys to Unlocking Regulators and Substrates. Annu. Rev. Biochem. 87, 921–964 (2018).

249. Heo, J., Larner, J. M. & Brautigan, D. L. Protein kinase CK2 phosphorylation of SAPS3 subunit increases PP6 phosphatase activity with Aurora A kinase. Biochem. J. 477, 431–444 (2020).

250. Oberoi, J. et al. Structural and functional basis of protein phosphatase 5 substrate specificity. Proc. Natl. Acad. Sci. U.S.A. 113, 9009–9014 (2016).

251. Gao, Y. et al. Allele-Specific Mechanisms of Activation of MEK1 Mutants Determine Their Properties. Cancer Discov 8, 648–661 (2018).

252. Puig-Butille, J. A. et al. AURKA Overexpression Is Driven by FOXM1 and MAPK/ERK Activation in Melanoma Cells Harboring BRAF or NRAS Mutations: Impact on Melanoma Prognosis and Therapy. J Invest Dermatol 137, 1297–1310 (2017).

253. Kong, X. et al. Cancer drug addiction is relayed by an ERK2-dependent phenotype switch. Nature 550, 270–274 (2017).

254. Leung, G. P. et al. Hyperactivation of MAPK Signaling Is Deleterious to RAS/RAF-mutant Melanoma. Mol. Cancer Res. 17, 199–211 (2019).

255. Rogiers, A., Wolter, P. & Bechter, O. Dabrafenib plus trametinib rechallenge in four melanoma patients who previously progressed on this combination. Melanoma Res. 27, 164–167 (2017).

256. Seghers, A. C., Wilgenhof, S., Lebbé, C. & Neyns, B. Successful rechallenge in two patients with BRAF-V600-mutant melanoma who experienced previous progression during treatment with a selective BRAF inhibitor. Melanoma Res. 22, 466–472 (2012).

257. Dompe, N. et al. A CRISPR screen identifies MAPK7 as a target for combination with MEK inhibition in KRAS mutant NSCLC. PLoS ONE 13, e0199264 (2018).

258. Unni, A. M. et al. Hyperactivation of ERK by multiple mechanisms is toxic to RTK-RAS mutation-driven lung adenocarcinoma cells. Elife 7, 3887 (2018).

259. Wittig-Blaich, S. et al. Systematic screening of isogenic cancer cells identifies DUSP6 as context-specific synthetic lethal target in melanoma. Oncotarget 8, 23760–23774 (2017).

260. Kettenbach, A. N. et al. Global assessment of its network dynamics reveals that the kinase Plk1 inhibits the phosphatase PP6 to promote Aurora A activity. Sci Signal 11, eaaq1441 (2018).

261. Xu, Y. et al. Structure of the protein phosphatase 2A holoenzyme. Cell 127, 1239–1251 (2006).

262. Wlodarchak, N. et al. Structure of the Ca2+-dependent PP2A heterotrimer and insights into Cdc6 dephosphorylation. Cell Res. 23, 931–946 (2013).

263. Leonard, D. et al. Selective PP2A Enhancement through Biased Heterotrimer Stabilization. Cell 181, 688–701.e16 (2020).

264. Morita, K. et al. Allosteric Activators of Protein Phosphatase 2A Display Broad Antitumor Activity Mediated by Dephosphorylation of MYBL2. Cell 181, 702–715.e20 (2020).

265. Kauko, O. et al. PP2A inhibition is a druggable MEK inhibitor resistance mechanism in KRAS-mutant lung cancer cells. Sci Transl Med 10, eaaq1093 (2018).

266. Sablina, A. A., Hector, M., Colpaert, N. & Hahn, W. C. Identification of PP2A complexes and pathways involved in cell transformation. Cancer Res. 70, 10474–10484 (2010).

267. Yeh, E. et al. A signalling pathway controlling c-Myc degradation that impacts oncogenic transformation of human cells. Nat. Cell Biol. 6, 308–318 (2004).

268. Khanna, A., Pimanda, J. E. & Westermarck, J. Cancerous inhibitor of protein phosphatase 2A, an emerging human oncoprotein and a potential cancer therapy target. Cancer Res. 73, 6548–6553 (2013).

269. Mannava, S. et al. PP2A-B56α controls oncogene-induced senescence in normal and tumor human melanocytic cells. Oncogene 31, 1484–1492 (2012).

270. Giroux, S. et al. Embryonic death of Mek1-deficient mice reveals a role for this kinase in angiogenesis in the labyrinthine region of the placenta. Curr. Biol. 9, 369–372 (1999).

271. Bélanger, L.-F. et al. Mek2 is dispensable for mouse growth and development. Mol. Cell. Biol. 23, 4778–4787 (2003).

272. Fischmann, T. O. et al. Crystal structures of MEK1 binary and ternary complexes with nucleotides and inhibitors. Biochemistry 48, 2661–2674 (2009).

273. Gopalbhai, K. et al. Negative regulation of MAPKK by phosphorylation of a conserved serine residue equivalent to Ser212 of MEK1. J. Biol. Chem. 278, 8118–8125 (2003).

274. Park, E. R., Eblen, S. T. & Catling, A. D. MEK1 activation by PAK: a novel mechanism. Cell Signal 19, 1488–1496 (2007).

275. Eblen, S. T. et al. Mitogen-activated protein kinase feedback phosphorylation regulates MEK1 complex formation and activation during cellular adhesion. Mol. Cell. Biol. 24, 2308–2317 (2004).

276. Meister, M., Tomasovic, A., Banning, A. & Tikkanen, R. Mitogen-Activated Protein (MAP) Kinase Scaffolding Proteins: A Recount. Int J Mol Sci 14, 4854–4884 (2013).

277. Roy, M., Li, Z. & Sacks, D. B. IQGAP1 is a scaffold for mitogen-activated protein kinase signaling. Mol. Cell. Biol. 25, 7940–7952 (2005).

278. Cacace, A. M. et al. Identification of constitutive and ras-inducible phosphorylation sites of KSR: implications for 14-3-3 binding, mitogen-activated protein kinase binding, and KSR overexpression. Mol. Cell. Biol. 19, 229–240 (1999).

279. McKay, M. M., Ritt, D. A. & Morrison, D. K. Signaling dynamics of the KSR1 scaffold complex. Proc. Natl. Acad. Sci. U.S.A. 106, 11022–11027 (2009).

280. Rodriguez-Viciana, P. et al. Germline mutations in genes within the MAPK pathway cause cardio-facio-cutaneous syndrome. Science 311, 1287–1290 (2006).

281. Estep, A. L., Palmer, C., McCormick, F. & Rauen, K. A. Mutation analysis of BRAF, MEK1 and MEK2 in 15 ovarian cancer cell lines: implications for therapy. PLoS ONE 2, e1279 (2007).

282. Scheffler, M. et al. Co-occurrence of targetable mutations in Non-small cell lung cancer (NSCLC) patients harboring MAP2K1 mutations. Lung Cancer 144, 40–48 (2020).

283. Arcila, M. E. et al. MAP2K1 (MEK1) Mutations Define a Distinct Subset of Lung Adenocarcinoma Associated with Smoking. Clin. Cancer Res. 21, 1935–1943 (2015).

284. Marks, J. L. et al. Novel MEK1 mutation identified by mutational analysis of epidermal growth factor receptor signaling pathway genes in lung adenocarcinoma. Cancer Res. 68, 5524–5528 (2008).

285. Landau, D. A. et al. Mutations driving CLL and their evolution in progression and relapse. Nature 526, 525–530 (2015).

286. Bentivegna, S. et al. Rapid identification of somatic mutations in colorectal and breast cancer tissues using mismatch repair detection (MRD). Hum Mutat 29, 441–450 (2008).

287. Murugan, A. K., Dong, J., Xie, J. & Xing, M. MEK1 mutations, but not ERK2 mutations, occur in melanomas and colon carcinomas, but none in thyroid carcinomas. Cell Cycle 8, 2122–2124 (2009).

288. Wang, C., Sandhu, J. & Fakih, M. A case of class 3 MEK1 mutated metastatic colorectal cancer with a non-durable tumor marker response to MEK and ERK inhibitors. J Gastrointest Oncol 10, 1140–1143 (2019).

289. Chuang, J. et al. MAP2K1 Mutations in Advanced Colorectal Cancer Predict Poor Response to Anti-EGFR Therapy and to Vertical Targeting of MAPK Pathway. Clin Colorectal Cancer 26, 5705 (2020).

290. Choi, Y. L. et al. Oncogenic MAP2K1 mutations in human epithelial tumors. Carcinogenesis 33, 956–961 (2012).

291. Sogabe, S. et al. MEK inhibitor for gastric cancer with MEK1 gene mutations. Mol. Cancer Ther. 13, 3098–3106 (2014).

292. Zeng, K. et al. BRAFV600E and MAP2K1 mutations in Langerhans cell histiocytosis occur predominantly in children. Hematol Oncol 35, 845–851 (2017).

293. McGinnis, L. M., Nybakken, G., Ma, L. & Arber, D. A. Frequency of MAP2K1, TP53, and U2AF1 Mutations in BRAF-mutated Langerhans Cell Histiocytosis: Further Characterizing the Genomic Landscape of LCH. Am J Surg Pathol 42, 885–890 (2018).

294. Nelson, D. S. et al. MAP2K1 and MAP3K1 mutations in Langerhans cell histiocytosis. Genes Chromosomes Cancer 54, 361–368 (2015).

295. Brown, N. A. et al. High prevalence of somatic MAP2K1 mutations in BRAF V600E-negative Langerhans cell histiocytosis. Blood 124, 1655–1658 (2014).

296. Waterfall, J. J. et al. High prevalence of MAP2K1 mutations in variant and IGHV4-34-expressing hairy-cell leukemias. Nat. Genet. 46, 8–10 (2014).

297. Nikolaev, S. I. et al. Exome sequencing identifies recurrent somatic MAP2K1 and MAP2K2 mutations in melanoma. Nat. Genet. 44, 133–139 (2011).

298. Emery, C. M. et al. BRAF-inhibitor Associated MEK Mutations Increase RAF-Dependent and -Independent Enzymatic Activity. Mol. Cancer Res. 15, 1431–1444 (2017).

299. Wagle, N. et al. Dissecting therapeutic resistance to RAF inhibition in melanoma by tumor genomic profiling. J Clin Oncol 29, 3085–3096 (2011).

300. Carlino, M. S. et al. Preexisting MEK1P124 mutations diminish response to BRAF inhibitors in metastatic melanoma patients. Clin. Cancer Res. 21, 98–105 (2015).

301. Shi, H. et al. Preexisting MEK1 exon 3 mutations in V600E/KBRAF melanomas do not confer resistance to BRAF inhibitors. Cancer Discov 2, 414–424 (2012).

302. Emery, C. M. et al. MEK1 mutations confer resistance to MEK and B-RAF inhibition. Proc. Natl. Acad. Sci. U.S.A. 106, 20411–20416 (2009).

303. Yuan, J. et al. Activating mutations in MEK1 enhance homodimerization and promote tumorigenesis. Sci Signal 11, eaar6795 (2018).

304. Haling, J. R. et al. Structure of the BRAF-MEK complex reveals a kinase activity independent role for BRAF in MAPK signaling. Cancer Cell 26, 402–413 (2014).

305. Williams, E. A. et al. Melanoma with in-frame deletion of MAP2K1: a distinct molecular subtype of cutaneous melanoma mutually exclusive from BRAF, NRAS, and NF1 mutations. Mod Pathol 33, 2397–2406 (2020).

306. Mansour, S. J., Candia, J. M., Matsuura, J. E., Manning, M. C. & Ahn, N. G. Interdependent domains controlling the enzymatic activity of mitogen-activated protein kinase kinase 1. Biochemistry 35, 15529–15536 (1996).

307. Eck, M. J. & Yun, C.-H. Structural and mechanistic underpinnings of the differential drug sensitivity of EGFR mutations in non-small cell lung cancer. Biochim Biophys Acta 1804, 559–566 (2010).

308. Abbott, D. W. & Holt, J. T. Mitogen-activated protein kinase kinase 2 activation is essential for progression through the G2/M checkpoint arrest in cells exposed to ionizing radiation. J. Biol. Chem. 274, 2732–2742 (1999).

309. Goldberg, A. B., Cho, E., Miller, C. J., Lou, H. J. & Turk, B. E. Identification of a Substrate-selective Exosite within the Metalloproteinase Anthrax Lethal Factor. J. Biol. Chem. 292, 814–825 (2017).

310. Sheridan, D. L., Kong, Y., Parker, S. A., Dalby, K. N. & Turk, B. E. Substrate discrimination among mitogen-activated protein kinases through distinct docking sequence motifs. J. Biol. Chem. 283, 19511–19520 (2008).

311. Miller, C. J. et al. Comprehensive profiling of the STE20 kinase family defines features essential for selective substrate targeting and signaling output. PLoS Biol. 17, e2006540 (2019).

312. Bondzi, C., Grant, S. & Krystal, G. W. A novel assay for the measurement of Raf-1 kinase activity. Oncogene 19, 5030–5033 (2000).